(2)

AD_____

ARMY PROJECT ORDER NO: 87PP7853

TITLE: MICROVASCULAR PHYSIOLOGIC AND ANATOMIC RESPONSES OF THE GUINEA PIG TO EXPERIMENTAL ARENAVIRUS INFECTION

PRINCIPAL INVESTIGATOR: Murray A. Katz, M.D.

CONTRACTING ORGANIZATION: Tucson Veterans Administation
Medical Center
Research Service (151)
Tucson, Arizona 85723

REPORT DATE: March 31, 1991

TYPE OF REPORT: Final Report

PREPARED FOR: U.S. ARMY MEDICAL RESEARCH AND DEVELOPMENT COMMAND
Fort Detrick, Frederick, Maryland 21702-5012

The findings in this report are not to be construed as an official Department of the Army position unless so designated by other authorized documents.

SECURITY CLASSIFICATION OF THIS PAGE

REPORT DOCUMENTATION PAGE

Form Approved OMB No. 0704-0188

1a. REPORT SECURITY CLASSIFICATION: Unclassified	1b. RESTRICTIVE MARKINGS
2a. SECURITY CLASSIFICATION AUTHORITY	3. DISTRIBUTION/AVAILABILITY OF REPORT: Approved for public release; distribution unlimited
2b. DECLASSIFICATION/DOWNGRADING SCHEDULE	
4. PERFORMING ORGANIZATION REPORT NUMBER(S)	5. MONITORING ORGANIZATION REPORT NUMBER(S)
6a. NAME OF PERFORMING ORGANIZATION: Tucson Veterans Administration Medical Center; 6b. OFFICE SYMBOL (If applicable)	7a. NAME OF MONITORING ORGANIZATION
6c. ADDRESS (City, State, and ZIP Code): Research Service (151) Tucson, Arizona 85723	7b. ADDRESS (City, State, and ZIP Code)
8a. NAME OF FUNDING/SPONSORING ORGANIZATION: U.S. Army Medical Research & Development Command; 8b. OFFICE SYMBOL (If applicable)	9. PROCUREMENT INSTRUMENT IDENTIFICATION NUMBER: Army Project Order No. 87PP7853
8c. ADDRESS (City, State, and ZIP Code): Fort Detrick Frederick, Maryland 21702-5012	10. SOURCE OF FUNDING NUMBERS

PROGRAM ELEMENT NO.	PROJECT NO.	TASK NO.	WORK UNIT ACCESSION NO.
62787A	3M1- 62787A871	AB	WUDA313197

11. TITLE (Include Security Classification): Microvascular Physiologic and Anatomic Responses of the Guinea Pig to Experimental Arenavirus Infection

12. PERSONAL AUTHOR(S): Murray A. Katz, M.D.

13a. TYPE OF REPORT	13b. TIME COVERED	14. DATE OF REPORT (Year, Month, Day)	15. PAGE COUNT
Final Report	FROM 7/1/87 TO 3/31/91	1991 March 31	99

16. SUPPLEMENTARY NOTATION

17. COSATI CODES			18. SUBJECT TERMS (Continue on reverse if necessary and identify by block number)
FIELD	GROUP	SUB-GROUP	
06	04		Pichinde Virus (Unc) Protein Transport (Unc); Microcirculation (Unc); Water Transport (Unc); Guinea pigs; Arenaviruses RAI; Microvascular; Hemorrhage; Lab Animals; BD
06	13		

19. ABSTRACT (Continue on reverse if necessary and identify by block number)

These studies complete the physiologic inquiry into the course of Pinchindé virus infection in strain 13 guinea pigs. Findings are categorized into four major groups and include:

1) Jejunal capillary protein reflection coefficient was reduced from .75 ± .02 SEM to .52 ± .03. This leak was well compensated since major edema accumulation was lacking; however, some was present in lung, liver, and kidney. The leak was not promoted by inanition in the ill animals, and it was reversed in some by a 2% crystalloid volume expansion.

2) In contrast to the lymph flux studies showing subtle leak in jejunal capillaries, intravital microscopic and electron microscopic examination of mesenteric and villous capillaries showed no leak of 170 kD dextran as well as intact intercellular junctions. There was, however, leukocyte adherence to hepatic vascular endothelial cells, reduced phagocytic ability of the Kupffer cells, reduced microvillous projections (Continued)

20. DISTRIBUTION/AVAILABILITY OF ABSTRACT	21. ABSTRACT SECURITY CLASSIFICATION	
☐ UNCLASSIFIED/UNLIMITED ☐ SAME AS RPT. ☐ DTIC USERS	Unclassified	
22a. NAME OF RESPONSIBLE INDIVIDUAL: Mrs. Virginia M. Miller	22b. TELEPHONE (Include Area Code): 301-663-7325	22c. OFFICE SYMBOL: SGRD-RMI-S

DD Form 1473, JUN 86 — Previous editions are obsolete. — SECURITY CLASSIFICATION OF THIS PAGE

(19. Abstract, continued)

from hepatocytes, and reduced endothelial fenestrae in the hepatic sinusoidal endothelial cells. Material resembling viral ribonucleocapsids was seen in Kupffer cells and in intestinal macrophages. All these anatomic features are characteristic of endotoxin exposure and/or TNF. The former was undetectable in these studies, and some authors have reported that TNF is increased in Pichinde infected GP13.

3) The cause of death from this disease depended on animal size or age. Large animals (> 700g) died in 12-14 days with a severe anion gap metabolic acidosis which may have been ketoacidosis from pancreatic failure. Small animals (< 400g) died in 19-23 days of acute hypoxia. Many aspects of the disease were noteworthy before death including increased lung and heart protein permeability, increased lung wet-to-dry ratios, and the presence of viral antigen in pulmonary epithelial and mononuclear cells with virus-like particles also seen in the endothelial cells of the aorta. Aortic endothelial cells appeared to have normal calcium transients to standard agonist stimulation, but when virus was added in vitro to guinea pig aortic endothelial cell monolayers, they had a reduced tritiated thymidine uptake. Not only do these studies support previously noted participation of mononuclear cells in the disease process, but they show a direct role for abnormal endothelial cell function as well.

4) As a marker of toxic oxygen free radical production, it was noted that ethane production which was first developed as a useable monitor in these studies is elevated nearly to threefold over the course of the viremia. Inhibition of this rise by scavenging it through various treatment regimens using butylated hydroxy toluene or vitamin C was not generally successful. The weight decrement in animals with illness was clearly separable from the elevated ethane output. The bronchoalveolar lavage fluid harvested from infected animals showed a rise in percent lymphocytes. As the disease progressed, the macrophages present in this fluid individually showed elevated unstimulated superoxide anion production to such an extent, that the reserves of such cells were exhausted to further stimulation with phorbol myristate.

The Pichinde model in strain 13 guinea pigs has features of a mild capillary leak syndrome in the nonvillous portions of the gut as well as in heart, lung, and probably kidney, but this does not seem to be a significant cause of death which in young animals appears to be from acute hypoxia and in older animals from a severe, and as yet incompletely characterized, metabolic acidosis with some degree of azotemia. The virus is probably present not only in the RE system but in endothelial cells as well, and certainly their function was markedly aberrant with decreased DNA synthesis. Some of these effects may be due to elevated levels of TNF.

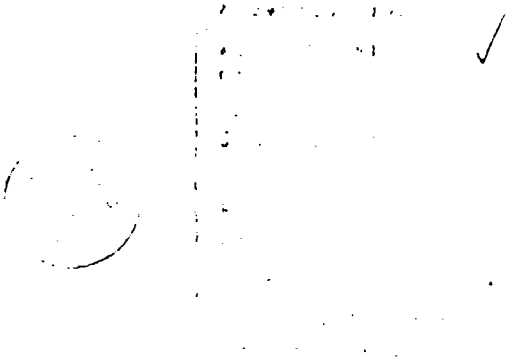

FOREWORD

Opinions, interpretations, conclusions and recommendations are those of the author and are not necessarily endorsed by the U.S. Army.

_____ Where copyrighted material is quoted, permission has been obtained to use such material.

_____ Where material from documents designated for limited distribution is quoted, permission has been obtained to use the material.

MK Citations of commercial organizations and trade names in this report do not constitute an official Department of the Army endorsement or approval of the products or services of these organizations.

MK In conducting research using animals, the investigator(s) adhered to the "Guide for the Care and Use of Laboratory Animals," prepared by the Committee on Care and Use of Laboratory Animals of the Institute of Laboratory Animal Resources, National Research Council (NIH Publication No. 86-23, Revised 1985).

_____ For the protection of human subjects, the investigator(s) have adhered to policies of applicable Federal Law 45CFR46.

M. Murray, Ci K.

PI Signature Date

Table of Contents

Abstract

These studies complete the physiologic inquiry into the course of Pinchindé virus infection in strain 13 guinea pigs. Findings are categorized into four major groups and include:

1) Jejunal capillary protein reflection coefficient was reduced from .75 ± .02 SEM to .52 ± .03. This leak was well compensated since major edema accumulation was lacking; however, some was present in lung, liver, and kidney. The leak was not promoted by inanition in the ill animals, and it was reversed in some by a 2% crystalloid volume expansion.

2) In contrast to the lymph flux studies showing subtle leak in jejunal capillaries, intravital microscopic and electron microscopic examination of mesenteric and villous capillaries showed no leak of 170 kD dextran as well as intact intercellular junctions. There was, however, leukocyte adherence to hepatic vascular endothelial cells, reduced phagocytic ability of the Kupffer cells, reduced microvillous projections from hepatocytes, and reduced endothelial fenestrae in the hepatic sinusoidal endothelial cells. Material resembling viral ribonucleocapsids was seen in Kupffer cells and in intestinal macrophages. All these anatomic features are characteristic of endotoxin exposure and/or TNF. The former was undetectable in these studies, and some authors have reported that TNF is increased in Pichindé infected GP13.

3) The cause of death from this disease depended on animal size or age. Large animals (> 700g) died in 12-14 days with a severe anion gap metabolic acidosis which may have been ketoacidosis from pancreatic failure. Small animals (< 400g) died in 19-23 days of acute hypoxia. Many aspects of the disease were noteworthy before death including increased lung and heart protein permeability, increased lung wet-to-dry ratios, and the presence of viral antigen in pulmonary epithelial and mononuclear cells with virus-like particles also seen in the endothelial cells of the aorta. Aortic endothelial cells appeared to have normal calcium transients to standard agonist stimulation, but when virus was added *in vitro* to guinea pig aortic endothelial cell monolayers, they had a reduced tritiated thymidine uptake. Not only do these studies support previously noted participation of mononuclear cells in the disease process, but they show a direct role for abnormal endothelial cell function as well.

4) As a marker of toxic oxygen free radical production, it was noted that ethane production which was first developed as a useable monitor in these studies is elevated nearly to threefold over the course of the viremia. Inhibition of this rise by scavenging it through various treatment regimens using butylated hydroxy toluene or vitamin C was not generally successful. The weight decrement in animals with illness was clearly separable from the elevated ethane output. The bronchoalveolar lavage fluid harvested from infected animals showed a rise in percent lymphocytes. As the disease progressed, the macrophages present in this fluid individually showed elevated unstimulated superoxide anion production to such an extent, that the reserves of such cells were exhausted to further stimulation with phorbol myristate.

The Pichinde model in strain 13 guinea pigs has features of a mild capillary leak syndrome in the nonvillous portions of the gut as well as in heart, lung, and probably kidney, but this does not seem to be a significant cause of death which in young animals appears to be from acute hypoxia and in older animals from a severe, and as yet incompletely characterized, metabolic acidosis with some degree of azotemia. The virus is probably present not only in the RE system but in endothelial cells as well, and certainly their function was markedly aberrant with decreased DNA synthesis. Some of these effects may be due to elevated levels of TNF.

I. Study (a) Characterization of permeability-surface area product (PS) and reflection coefficient (σ) of intestinal microcirculation.

A. Introduction

Capillary disruption accounting for hemorrhage and pulmonary involvement in Lassa fever; conjunctival, mucosal, and upper cutaneous bleeding and flushing in Argentine hemorrhagic fever; and proteinuria and hemoconcentration in Bolivian hemorrhagic fever has been the putative etiology of such phenomena in Arenavirus infection, as well as in Hanta virus infections in hemorrhagic fever with renal syndrome and nephropathia epidemica (1-4). Although this may seem obvious, few measurements of capillary transport descriptors in such diseases have been carried out; and recent studies by Liu and colleagues (5-6) have called the capillary disruption thesis into question in Pichindé virus (PV) infection in strain 13 guinea pigs (GP13), and suggest that perhaps interstitial accumulation may result from failure of lymphatic uptake of macromolecules. In our midterm report we established the methods for measurement of capillary descriptors in the jejunal microcirculation (7), and in this report demonstrate the validity of the capillary disruption thesis and other features of the capillary abnormality including potential reversibility with volume expansion.

B. Methods

Lymphatic cannulation of prenodal lymphatics is a well described method utilized to assess permeability-surface area products (PS) and reflection coefficients (σ) of a tissue in which there is net filtration by capillaries either in a normal state or induced by partial venous occlusion (for reviews and methods, see 8,9,10). An abbreviated description for the GP13 study is as follows:

Healthy GP13s of either sex obtained from either ARI (East Bridgewater, Massachusetts) or Crest Caviary (Raymond, California) were anesthetized with 40 mg/kg sodium pentobarbital and tracheotomized. Femoral arterial and venous catheters were placed following which a 200 u/kg bolus of heparin sodium was administered iv following which a sustaining infusion rate of 1.0 ml $\cdot$ hr^{-1} $\cdot$ $(100g)^{-1}$ of iv solution of Na 138 mEq/l, K 8mEq/l, HCO_3 28 mEq/l, Cl 118 mEq/l was delivered at 40°C throughout the study. Heparin was added to the infusate to infuse 1 u/kg/minute. The animal's rectal temperature was maintained at 37.5°C on a heating board. Mean arterial pressure was continuously monitored with a P23Db Statham pressure probe and 2200 monitor (Oxnard, CA). A laparotomy was performed, and a polyethylene cannula 8.5 cm long with an id of .38 mm was tied into the main mesenteric lymphatic in the distribution of the superior mesenteric artery. When lymph was seen to flow, the cannula was connected to larger bore PE tubing and the end placed into tared microcentrifuge tubes coated with heparin and layered with water equilibrated mineral oil. Lymph flow rates were computed every half hour with midpoint arterial sampling. Proteins were measured on an autoanalyzer using the biuret method, and for future studies, a limited number of samples were subjected to protein electrophoresis. (These showed a fairly uniform lymph protein distribution for albumin 52-54%, α1 10-11%, α2 18-26%, β 9-13%, γ 3-4%).

Moist umbilical tape was looped around the portal vein and through a segment of Tygon tubing to allow for gentle partial and graded ligation of the portal vein.

Analysis was carried out by the nonlinear crosspoint method described and analyzed previously in our laboratory (10). In brief, if two different lymp flows (J_{v1},J_{v2}) are associated with two different lymph/plasma protein concentration ratios (R_1,R_2), we may write

$$PS = \frac{J_{v1}\,(1-\sigma)}{\ln\left[\frac{R_1\sigma}{R_1-(1-\sigma)}\right]} = \frac{J_{v2}\,(1-\sigma)}{\ln\left[\frac{R_2\sigma}{R_2-(1-\sigma)}\right]} \qquad \text{Eq 1]}$$

Since the middle and right hand terms are equal, σ may be quickly solved by an iterative root finding routine such as "Quickdraw McGraph" on SuperCalc 4.0 Software. Once σ is known, then PS is explicitly calculated. As described in reference the percent of successful solutions can be quite small owing to random error. Perfect data with random error superimposed can have successful crosspoints in as little as 25% of paired samples (10). Discussion of errors in this method which has been referred to as a "quasi-steady state" method reveals it to be at least as good as most other methods of data analysis (10,11).

Five groups of GP13 were studied over two different time periods. Numbering systems were established after the second study was completed. Group IV consisted of seven GP13 injected ip with 10^4 PFU Jahrling adapted Pichindé virus (12) (obtained from Ft. Detrick Virology Laboratories, Frederick, MD). Since at this time the question was the comparison of infected to control GP, we compared Group IV to Group V which consisted of 38 uninfected GP13 otherwise treated identically to Group IV. All studies of infected GP were conducted on day 12-13 because it had previously been determined that death in this weight range (≥600g) typically occurred on day 14.

After Groups IV and V were compared, it was found, as fully described in the Results section, that jejunal capillary protein reflection coefficient, σ, was significantly decreased in the viral Group IV. It was tempting to conclude that the virus was responsible, but Groups IV and V differed also in weight and in nutritional status, since infected GP lost 20.3% ± 2.4% SEM of their body weight related largely to reduced food intake in infected GP13. Thus, differences between Groups IV and V might be attributable to inanition. Moreover, since it could be argued that animals studied under conditions of hydropenia, as Groups IV and V were, might behave differently under conditions of volume expansion of the extracelllular fluid. For example, Liu and his colleagues noted that for both infected and uninfected GP13, cardiac output is not maximal until a 1.6% to 2.4% volume expansion is administered (13). Perhaps examination of σ with volume expansion would show different results, namely, a reversal of reduced σ in infected GP13 due to radial stretching of capillaries with consequent "ellipticization" of small pores and consequent rise of σ—a phenomenon we have suggested may account for the well-described increase in σ as capillary pressure increases (11,14-20).

In order to test these notions we tested with the same methods three groups of GP13 with smaller starting weights in order to attempt to achieve more homogeneity than seen in Groups IV and V. These new groups were named after completion of the studies, since it was unknown at the start that Groups I and II would be different: Groups I and II consisted of PV injected GP studies on day 13 as was Group IV, except that these new groups underwent a 2% volume expansion at the start of the studies followed by equilibration of thirty minutes before taking samples under sustaining infusion rates as noted above for Group IV. Group I consisted of those GP (n=4) which were indistinguishable in their capillary descriptors (σ,PS) from the hydropenic, infected Group IV. Group II consisted of three GPs which showed a normalization of σ with volume expansion. Group III consisted of five control GP13 which were restricted to about 60% of normal caloric intake (~ 20g per day) for twelve or more days prior to surgery.

In summary the groups were:

I (n=4)	PV injected, volume expanded, unresponsive σ (low)
II (n=3)	PV injected, volume expanded, responsive σ (high)
III (n=5)	Control, caloric restricted, volume expanded
IV (N=7)	PV injected, hydropenic
V (n=38)	Control, ad lib diet, hydropenic

All animals in Groups I-III were dissected at the completion of the studies. Whole hearts, lungs, spleens, stomachs, livers, kidneys, and brains were quickly removed, blotted, and weighed as percentages of body weights. All protocols for Study (a) as well as the entire project were approved by the Tucson Veterans Affairs Medical Center Institutional Animal Care and Use Committee and the Research and Development Committee.

Other computations (described previously) included the Peclet number expressing the relative magnitude of convective vs permeative coefficients contributing to transport:

$$\text{Peclet No.} = \frac{J_V(1-\sigma)}{PS} \qquad \text{Eq 3]}$$

where J_V is lymph flux rate, and the percent of total protein transport carried by permeative or diffusive processes:

$$\%\ \text{Fr D} = \frac{PS\ (1-R)}{J_V R} \times 100 \qquad \text{Eq 4]}$$

where R is the lymph/plasma protein concentration ratio.

C. Statistical Analysis

Groups IV and V results were published first (21) and compared for homogeneity of variations using the F test. If variances could not be demonstrated different ($P > .05$) then a non paired two-tailed Student t test was used

to compare means for differences with $2P < .05$ taken as a significant difference. If the F test showed differences between variances, the more conservative Behrens-Fisher t' test was utilized (22).

Within the volume expanded groups (I-III), three possible variances for each variable were compared by the Hartley Fmax test. If the high and low variance were indistinguishable ($P > .05$), then the very conservative Scheffé contrast test was used to compare I vs II, I vs III, II vs III, and I and II vs III with significant differences taken at the $2P < .05$ level. The Scheffe test was selected because in these small groups we wished to underestimate the significance of differences (22). In the event that the Hartley Fmax test showed critical differences among variances, the Mann-Whitney U test was used to compare differences between the distributions of Groups I, II and III. This was done by the Z-transformation of U corrected for tied ranks (23) on a program designed by us for use on Super Calc 5.0 software (Computer Associates International, Inc., San Jose, CA).

To determine whether volume expansion and calorie restriction have effects on the variables measured, Groups I and IV and Groups III and V were compared using the Hartley determined nonpaired Student t or the Behrens-Fisher t' test.

D. Results

The clinical observations made on the infected GPs in Group IV were that they lost 120 ± 17 SEM grams or 20.3 ± 2.4 % of their body weight. Their final weights were 476 ± 47 g which was substantially less than the control group Figure (a)1 (643 ± 21 g, $2P < .001$). Figure (a)1 shows the weight, mean arterial
F. (a)1 pressure, hematocrit, and serum protein concentration comparisons between groups.

When the endotracheal tube was placed, no fluid was aspirated from either lung in control or infected groups. On laparotomy, no ascites nor fluid collections around the psoas muscles were seen. At autopsy the lungs were pink and without hemorrhagic foci, and the pericardial sac was free of fluid as were the pleural spaces. No gross hemorrhages were found in the lung, heart, brain, kidneys, or gastrointestinal tract. A uniform finding in the infected guinea pigs was a remarkable decrease in fat stores around the heart, muscles of the neck and pelvic girdle, skin and intestine. Detailed histologic information is being established as a part of a large and separate study. However, gross findings were minimal.

The pattern of death at day 13 without gross findings has been our fairly uniform experience with GP13s in this weight range. For smaller GP13s in the range of 200-250 g, survival is prolonged to day 19 or 20 post inoculation at which time pulmonary hemorrhage in various degrees from focal to pulmonary hepatization is regularly seen. At this time obvious fluid can be aspirated from the bronchi during life, and the cut surface of the lung weeps.

F. (a)2 The prenodal lymph flux data are shown in Figure (a)2. Mean lymph flux, J_y, was decreased some 11 % in the infected Group, but the wide variance in this group contributed to obscuring any possible differences between groups. All

lymph flux values were corrected for body weight at the time of the study. The lymph to plasma protein concentration ratio, R, was .55 ± .02 in the normal Group V and .70 ± .05 in the infected Group IV ($2P < .01$). The combination of wide variations in J_v and a significant rise in R with infection resulted in an insignificantly elevated protein clearance rate, J_vR, of 3.14 ± .62 $\mu l \cdot min^{-1} \cdot (100\ g)^{-1}$ in the infected Group IV compared to 2.86 ± .21 for the normal GPs Group V.

F. (a)3 Figure (a)3 shows the membrane transport descriptors for reflection coefficient (σ) and permeability-surface area product (PS) for protein in Groups IV and V. The crosspoint method does not always yield unique values for σ and PS as described previously [10,11]. In fact, only 23 of the 38 normal GPs had successful runs, but in their demographic characteristics, these 23 were not different from the other 15 in the normal group. The absence of crosspoints appears to be a problem with convergence of Equation 1 which is dependent on absolute values of J_{v1}, J_{v2}, R_1, R_2 and their differences [10]. All the infected guinea pigs had successful crosspoint determinations. The reflection coefficient was .75 ± .018 for normal GPs in Group IV and .52 ± .032 for the infected Group IV ($2P < .001$). PS was not different between the groups, although the mean for the infected group, 2.48 ± .30, was lower than that of the normals, 3.21 ± .29.

The Peclet number of a system composed of a barrier which passively allows convective and diffusive transport across it is the ratio of convective to permeative coefficients $(J_v(1-\sigma)/(PS))$. The balance of these factors is about equal for both groups, being .97 ± .10 for the normal group and 1.20 ± .19 for the infected group. Even though the coefficients are balanced, as seen in
F. (a)4 Figure (a)4, the large lymph/plasma protein concentration ratio in the infected group indicates that the driving force for diffusion (1-R) is less for the infected Group IV which yields a transport of protein by diffusion or permeation a significantly smaller fraction of the total than in the normal Group V. Although splitting the total transport of protein into diffusive and convective components is inexact [11]; in general, the normal GPs transport about 52.4 ± 2.7 % of protein carried across jejunal capillaries by diffusion while the infected GPs transport only 32.2 ± 3.5 % by this dissipative process ($2P < .001$).

T. (a)1 In Table a(1) we compare the results of four PV-infected GP13 which did not respond to volume expansion by demonstrating a depressed jejunal capillary σ (Group I), three PV infected GP13 who did respond to volume expansion (Group II), and five control volume expanded GP13 which had been on 60% ad lib calories for two weeks. The initial conditions of weight, mean arteriolar pressure, hematocrit, serum protein concentration, jejunal lymph flow and protein clearance were not different among the groups. However, there is a clue to differences in that the lymph/plasma protein concentration ratio (R) in the infected groups (I,II) is significantly above that of control animals (III) ($2P<.05$). Among the nonresponders, the R = .56 ± .04 SEM was significantly different from normal R = .33 ± .03, but the spread of values for R among Group II shows no significant differences between II and III.

T. (a)2 Table a(2) shows the results and comparisons among the groups for the lymph flux variables. The most striking feature is that σ in Group I (.54 ± .05) was considerably less than Group II (.86 ± .02) resulting from classification of the PV infected animals into two groups, but the Group II animals had a σ which was

indistinguishable from control animals (.86 ± .02 vs .83 ± .02, 2P = NS). As in our previously published non-volume expanded studies, the PS values were not different. Protein fluxes during the analytic studies were the same for all three groups, and this was accounted for by a high R in the nonresponding Group I with a lower than normal lymph flux (Jv). Animals which are normal (Group III) or those infected animals responding to volume expansion (Group II) carry about 60% of their transported protein by diffusion while the nonresponders carry only 28% by diffusion.

T. (a)3 Table a(3) shows the possible anatomic predictors of the various responses of the animal groups to volume expansion and virus injection. Whole weights of heart, spleen, stomach, and brain as a percentage of bodyweight were not different among groups. However, all infected GPs showed increased relative weights of lung, liver, and kidney compatible with a congested state discussed in previous studies from our laboratories.

T. (a)4 In Table a(4) we compare the nonresponsive virus infected Group I and the calorie restricted Group III, both of which were volume expanded, to the previously reported nonvolume expanded infected and uninfected groups (IV and V respectively). Groups I and IV are indistinguishable. Although a number of interesting differences exist between Groups III and V, it is clear that calorie restriction in Group III cannot account for reduced σ seen in virus infected groups, because Group III had a higher σ than the nonvolume expanded and ad lib fed Group V.

E. Discussion

In the absence of obvious edema or effusions, Pichindé infected strain 13 guinea pigs show a rise in jejunal lymph/plasma protein concentration ratio without altered lymph flux or lymph protein clearance. This change is brought about by a reduced reflection coefficient which is also responsible for changing the transcapillary protein transport from one which is equally divided between convection and diffusion to one dominated by convection. It remains unexplained why gross edema is not present.

Edema preventing safety factors [24, 25, 26] must be operative in this model. Some of the well known factors are unlikely. For example, it is unlikely that interstitial compliance is decreased or that interstitial hydrostatic pressure is increased, because each of these would lead to increased lymph flow, and this was not seen.

A shift in post- to precapillary resistance ratios is possible such that microvascular pressures in the jejunum were decreased. Capillary flow stasis might have also contributed to the lack of edema, but this would imply that the data contain a type II error in which PS was actually decreased, but was undetected by statistical analysis. This is certainly possible. The end result in this weight range of GPI3 is that gross edema is prevented, despite the decreased reflection coefficient. The possibility that PS was in fact decreased is brought into focus when one considers how the PS was computed. The PS was computed from J_v which was corrected for animal weight at the time of the study. It might be argued that if the loss of animal weight was due largely to a decrement in adipose tissue which is poorly vascularized, then one should correct

J_v and hence PS values to the original rather than the final guinea pig weight. This would have no effect on the reflection coefficient, the Peclet number, or the % permeative transport; however, the lymph flux and PS values would be reduced some 20% below their currently computed values. Capillary flow stasis would then be a more likely mechanism leading to prevention of edema than the current method of computation would indicate. Indeed, intravital microscopy of livers (as seen elsewhere in this report) and mesenteries of these guinea pigs in our laboratories by Dr. Robert McCuskey shows that these splanchnic beds have poor circulation with evident granulocyte adherence to the endothelium of sinusoids and venules, a phenomenon which decreases the effective size of vessels thereby greatly increasing vascular resistance.

Whether the capillary changes might be related to calorie deprivation of the infected group owing to their anorexia rather than the virus infection itself seems unlikely, but was a possible explanation of the findings, and the reason for inclusion of Group III. Groups I, II and III were included to judge the effects of volume expansion.

The combined studies lead to a number of conclusions: a) Pichindé virus infection in GP13 produces a compensated compillary leak in the jejunal microcirculation with a reduced σ for protein that is reversible in some guinea pigs by 2% volume expansion; b) Those infected GPs whose capillary leak cannot be reversed by volume expansion are characterized by a very high lymph/plasma protein concentration ratio ($R \geq .56$), perhaps indicating a more severe reduction in capillary barrier function than in those animals showing reversal with volume expansion, c) the reduced σ in Pichindé virus infected GP13 is not due to inanition, since calorie restricted normal GP13 do not have a reduced σ, and d) the capillary defect in Pichindé virus infection may not produce much clinical edema, but does produce pulmonary, hepatic, and renal congestion. The first of these can procede to severe hepatization, and, as shall be subsequently seen, to pulmonary edema, severe hypoxemia, and death.

II. Studies (b) and (e) Characterization of GP13 mesenteric microcirculatory module with measurement of microvascular blood flow, granulocyte adherence, and mesenteric local hemorrhage in Pichinde infection and Morphometric and intravital assessment of hepatic microcirculation and Kupffer cell function

A. Introduction

Arenaviruses form an important source of human disease carried by rodents in South America and Africa (1,2). Hemorrhagic fevers due to these agents may be severe to lethal in humans. Human-to-human transmission of lethal disease is known to exist. Since these viruses commonly produce shock-like symptoms, involvement of the microvasculature is not surprising; and capillary congestion, diapedesis of erythrocytes, microscopic hemorrhages, edema and organ swelling are seen in major organs. To date, however, the pathophysiology of microvascular injury remains to be elucidated.

Hepatic microvascular failure is implicated in the pathophysiology of septic and endotoxic shock; and, Kupffer cells which comprise one of the hepatic sinusoidal lining cells are not only phagocytes but also the source of a variety of toxic and beneficial mediators such as prostaglandins, leukotrienes,

thromboxanes, free radicals, interleukin-1, tumor necrosis factor, interferon, lysosomal enzymes, procoagulants, etc. (reviewed in references 3 and 4). As a result, these cells have been implicated as playing a major role in septic and endotoxic shock since bacterial endotoxin which is principally cleared by Kupffer cells also modulates the release of these substances (reviewed in 3 and 4). This is of particular interest since macrophages are reported to a major target for arenavirus infection; and, Kupffer cell hyperplasia and hepatic necrosis are frequently observed (1,2,5-7). This suggests that involvement of the hepatic microvasculature and Kupffer cells in the pathophysiology of arenaviral infections may contribute significantly to the lethality of these diseases.

Given the above, the purpose of the current investigation was to elucidate the dynamic events that occur in the hepatic microvasculature during the lethal course of an animal model of human arenavirus infection which employs Pichindé viral infection of strain 13 guinea pigs (5,7). This model poses minimal danger to laboratory workers when treated as a Class II Biohazard. In addition, the mesenteric and intestinal microvasculature also were studied and the responses compared and contrasted to those in the hepatic microvasculature. The mesentery provides a convenient site to evaluate the effects of arenaviral infection in a relatively simple microvascular bed containing arterioles, capillaries having continuous endothelium and basal lamina, and venules. The intestinal villi provide a somewhat more complex microvasculature at a location where high concentrations of virus were detected by immuno-cytochemistry (Jensen, personal communication). In contrast, the highly metabolic liver has a highly complex microvasculature containing sinusoids having a dual afferent blood supply from the portal venule and hepatic arteriole. The sinusoids have fenestrated endothelial walls and are not surrounded by a continuous basal lamina; they also contain the phagocytic Kupffer cells on their luminal surfaces. Such microcirculatory studies are best done using a high resolution *in vivo* microscopic methods so that the direction and magnitude of dynamic microvascular events can be assessed in life as a function of time. Subsequent electron microscopic evaluation permits ultrastructural evaluation of cellular damage.

As a result, the specific aims of this project were to determine qualitatively and quantitatively what alterations occur as a function of time in the hepatic, mesenteric and intestinal microvasculature of strain 13 guinea pigs following infection with Pichindé virus. Changes in the patterns, pathways, rates and volumes of blood flow through the hepatic microvasculature were assessed by high resolution light microscopy of the liver, mesentery and intestinal villi *in situ* in anesthetized animals. The causes of these changes, e.g., vasodilation or constriction, endothelial adhesion of leukocyte and platelets and/or intravascular aggregation, sinusoidal lining cell swelling and/or rupture, etc., were determined. Alterations in phagocytic Kupffer cell function in the liver also were quantitatively assessed. Subsequently, the ultrastructural alterations in the microvascular wall were evaluated by transmission and scanning electron microscopy.

B. Experimental Design and Methods

Strain 13 guinea pigs (225-515g) inoculated with 10^4 plaque forming units of Pichindé virus adapted by USAMRIID (5,7) served as the experimental model of

arenavirus infection. Twenty-four animals were successfully studied on days 11-18 days after infection. An additional 10 uninfected animals served as controls.

The livers, mesenteries, and intestinal villi were studied by established high resolution, in vivo microscopic methods (8). To accomplish this, a lobe of the liver or a loop of small intestine was gently exteriorized through an incision in the abdominal wall, and transilluminated or epi-illuminated with monochromatic light. Homeostasis was maintained by suffusion of the exposed liver with Ringer's solution warmed to body temperature. Optical images were secured using 40 x or 80 x water immersion objectives and appropriate oculars. The resulting microscopic images were televised using a high sensitivity, high resolution silicon vidicon camera or a silicon-intensified target vidicon camera. The televised images then were recorded on video tape for subsequent analysis.

The function of Kupffer cells was assessed by evaluating the phagocytosis of FITC-latex particles (1.0 μm in diameter) injected intraportally (ileocecal vein). To do this the distribution and relative number of phagocytic Kupffer cells was measured by counting the number of cells that phagocytosed latex (3,4,9,10,11). This is done 15 minutes after infusing a standardized concentration of latex particles. To assess regional distribution, the number of phagocytic Kupffer cells per standardized microscopic filed was counted in 10 periportal (Zone 1), and 10 centrilobular (Zone 3) regions. For these measurements the livers were imaged by incident fluorescence microscopy (3,4,9,10,11). This permitted the use of lower magnifications (40 x objective) and subsequently larger fields of measurement. While 1.0 μm latex particles were easily visualized with an 80 x objective, they are difficult to see with the 40 x objective unless fluorescence microscopy is used. However, the field of measurement with the 80 x objective is quite restricted and best used to evaluate phagocytosis of single particles by individual Kupffer cells.

In addition to the above evaluation of Kupffer cell (KC) function, the following hepatic microvascular parameters were assessed: (a) patterns of blood flow within the lobules and velocities of blood flow in the sinusoids; (b) aggregation and/or adhesion of formed elements in the blood to each other or to the sinusoid walls; and (c) dimensional changes in the microvasculature due to constriction, dilation and/or swelling of sinusoidal lining cells. The relative adequacy of blood perfusion through the sinusoids was evaluated by counting the number of sinusoids containing flow in the same microscopic fields where the number of phagocytic KC was determined. Similar variables are evaluated for the mesenteric and intestinal microvasculature.

For the liver, mesentery and intestinal villi, epi-fluorescence of FITC-dextrans of different molecular weights (20,000-170,000 kD) infected intravenously were used to identify changes in microvascular permeability elicited by arenaviral infection.

The ultrastructural changes that occurred in the liver, mesentery and intestinal villi during the course of the disease were evaluated by routine transmission and scanning electron microscopic methods (8,12,15). For these studies, 8 animals were sacrificed between days 13 and 17 following inoculation. The observed ultrastructural changes were correlated with those recorded by in vivo light microscopy. Particular attention was paid to damage to the hepatic

sinusoid wall including endothelial cells and their fenestrae, Kupffer cells and perisinusoidal fat-storing cells of Ito. In the mesentery and intestinal villi, attention was paid to alteration of the integrity of capillaries and venules, particulary their endothelial junctions and basal laminae.

The plasma from 10 of the above infected animals was tested for the presence of endotoxin using a highly sensitive, kinetic, densimetric Limulus Amoebocyte Lysate assay (10).

The quantitative data obtained from the various experiments was evaluated by calculating the mean values for each animal, means ± SEM for each group and subsequently testing for significance between the groups using the Student t-test. Analysis of variance was used when comparing two groups to control. $P < .05$ was considered to be significant.

C. Results

Until 18 months ago it was not possible for us to study the effects of arenavirus on the microcirculation due, first, to a lack of appropriate containment facilities; and, second to a shortage of strain 13 guinea pigs. As a result, during the first half of this project efforts were directed toward establishing reproducible methodologies to study the guinea pig mesenteric, intestinal and hepatic microvasculature by high resolution in vivo microscopy. It was found that a number of modifications in our instrumentation were required to accomodate guinea pigs; the equipment in the past was designed for use primarily with mice and small rats. These were reported in detail in the midterm report, and, as a result a number of protocols and procedures related to the animal size, surgery, anesthetic administration, FITC-dextran concentration, and drug doses were established to permit study of liver, intestine and mesentery in control guinea pigs as well as animals infected with arenavirus during the past 18 months.

The livers, mesenteries and intestinal villi of guinea pigs studied by in vivo microscopy 12-18 days after infection of the animals with Pichinde virus (10^4 PFU/animal) demonstrated the following alterations in the microvasculature. No basic differences were noted between animals 12-18 days post infection.

The circulation of blood through the hepatic microvasculature was slow with profiles of individual RBCs and WBCs frequently seen as were aggregates of platelets and WBCs. Blood flow in many sinusoids was stagnant and appeared blocked by WBCs adherent to the endothelium as well as by platelet aggregates (Figure (b-e)1). Numerous WBCs also were adherent to the endothelium of central venules (Figures (b-e)2 and 3). In the sinusoids that contained blood flow, only a few scattered latex particles appeared to have been phagocytosed by Kupffer cells. Kupffer cell phagocytic function (# phagocytic Kupffer cells/ microscopic field) between 12 and 18 days post-infection was depressed by 50% compared to uninfected animals: Control 23.01 ± 1.40 SEM; Infected 11.4 ± 1.42 SEM. Hepatic parenchymal cell injury also was very apparent with many cells appearing highly vacuolated.

F.(b-e)1
F.(b-e)3

Subsequent to examination of the liver, the mesenteric microcirculation was studied. As in the liver, the circulation in major mesenteric vessels was slow; many of the smaller arterioles, capillaries and venules contained stagnant

blood. During a 30 minute period following the injection of 1 ml of 10% FITC-170kD dextran, no significant leakage of this substance was seen from capillaries or post-capillary venules that contained blood flow (Figure (b-e)4). F.(b-e)4

While the mesenteric microcirculation was poor (except for main vessels supplying the gut), the circulation in the tips of the intestinal villi surprisingly appeared to be relatively normal (Figure (b-e)5A). As in the mesentery, there was no leakage of FITC-170kD dextran (Figure (b-e)5B). F.(b-e)5A F.(b-e)5B

Electron microscopic (TEM and SEM) examination of the livers from the above animals which were perfused-fixed suggest the depressed Kupffer function as indicated by few pseudopodia and filopodia on the surface and limited phagocytosed latex particles (Figure (b-e)6). Kupffer cells were filled with cellular debris and vacuoles containing material suggestive of viral ribosomes and ribonucleocapsids (15) (Figure (b-e)7) as were macrophages which had infiltrated the parenchyma. There also was a suggestion that there may be a reduction in the number of endothelial fenestrae in the hepatic sinusoids (Figures (b-e)8, 9). The space of Disse, and bile cannaliculi frequenty were dilated and contained few microvilli projecting from surrounding hepatic parenchymal cells (Figure (b-e) 10). It should be noted that perfusion-fixation of the livers sometimes was difficult due to plugging of many sinusoids as indicated above. F.(b-e)6 F.(b-e)7 F.(b-e)8 F.(b-e)10

Transmission EM of the villi from the small intestine of a terminal infected guinea pig revealed similar findings to the above for the liver. The tips of the intestinal villi were packed with numerous infiltrated cells, presumably macrophages derived from monocytes, which contained considerable numbers of phagolysosomes and materials suggestive of viral ribonucleocapsides (Figure (b-e)11). These cells are in the same location as those containing high concentrations of virus (per Dr. B. Jensen). There was no evidence of disruption of the endothelial walls of vessels in this area (Figure (b-e)12); all intercellular junctions appeared to be intact. The epithelial barrier was also histologically intact (Figure (b-e)13). Finally, there was no detectible endotoxin circulating in the blood of the infected animals further supporting the view that the intestinal barrier remained reasonably intact during the terminal stages of the infection. F.(b-e)11 F.(b-e)12 F.(b-e)13

D. Discussion

The results of this study demonstrated that, during the terminal stages of Pichindé viral infection (days 12-18) in strain 13 guinea pigs, there was no major increase in microvascular permeability in the intestine or mesentery. No extravascular fluorescence of 40-170kD FITC-dextran was detected around capillaries and post capillary venules in mesentery or in intestinal villi where considerable viral infection could be demonstrated (Jensen, personal communication). Consistant with this *in vivo* microscopic observation was the lack of any ultrastructural evidence suggestive of damage to the integrity of the endothelial lining in the vessels in intestinal villi.

The microvascular alterations seen in the liver, e.g., leukocyte adhesion to the endothelium resulting in obstruction of blood flow in sinusoids, platelet aggregation, swollen endothelium, depressed phagocytic function of Kupffer cells, etc. were all similiar to responses elicited with endotoxin and/or tumor necrosis

factor (TNF) (3,4,18). It is suspected that TNF but not endotoxin plays a major role in the hepatic pathophysiology of arenaviral infection since increased levels of circulating TNF have been detected in Pichindé virus infected guinea pigs (Aronson, personal communication), endotoxin was not detected by us in the plasma, and the intestinal epithelial barrier appeared ultrastructurally intact. It is hypothesized that Kupffer cells and other macrophages are the source of the TNF since they not only are the principal cellular site for the viral infection (5-7) but also are the principal source of TNF production (3,4,19). The dilation of bile cannaliculi and the reduction in size and numbers of microvilli from the surfaces of hepatocytes also is consistant with this hypothesis.

In summary, the results of this study demonstrated no significant changes in microvascular permeability in the mesentery or intestinal mucosa due to Pichindé viral infection in strain 13 guinea pigs. Hepatic microvascular and parenchymal alterations were consistant with TNF release from viral infected Kupffer cells.

III. Study (c) Quantitative assessment of organ involvement by plasma leak and hemorrhage by 51Cr-red blood cells and 125I-human serum albumin leak

A. Introduction

The initial purpose of study (c) was to define the presumed plasma leak and hemorrhage following severe P. virus infection in GP13s. Our data did not show these effects and this original hypothesis was rejected. We observed, however, that P. virus appeared to produce distinctly different disease processes in small (young) (initial body weight, IBW <400 g) vs large (old) (IBW >700 g) GP13. This view was supported by the unique survival times (>18 days vs <14 days) with each group, respectively. These data generated the following additional questions:

1. What is the cause of death in severe Pichinde virus infection in GP13s with an initial body weight <400 g?

2. What is the cause of death in severe Pichinde virus infection in GP13s with an initial body weight >700 g?

3. How does Pichinde virus infection affect the following endothelial cell functions: DNA and protein synthesis, cell morphology, monolayer permeability and leukocyte adhesion to GPAEC monolayers?

4. Does Pichinde virus inoculation of GP13 leukocytes produce increased adherence to uninfected GP13 aortic endothelial cells?

Although we found no major changes in a variety of cardiovascular functions, significant amounts of radioiodinated human serum albumin were detected in the lungs and heart of small (IBW <400 g) GP13s near death (>18 days). This accumulation was associated with a decline of arterial oxygen tension, hyperlactatemia, a normal blood pH and massive adherence of leukocytes to the pulmonary endothelium. These data suggest that respiratory failure in association with cardiac dysfunction may lead to death following P. virus infections in GP13s.

The pulmonary congestion in these small GP13 appeared similar to those seen in patients with severe Lassa fever (Edington and White, 1972; White, 1972).

Our preliminary data (n=5) in P. virus infected large (IBW >700 g) GP13 document a different disease process. No increased amounts of radiolabeled albumin were detected in any organs of animals near death (< 14 days). These animals showed normoxia with no elevation in arterial blood lactate but with a severe acidosis. These GP13 had low plasma bicarbonate, sodium and chloride ion concentrations with elevated blood glucose, creatinine, and blood urea nitrogen (BUN) values. These data are consistent with marked metabolic acidosis, a decreased renal perfusion and minimal cardiorespiratory failure. How can P. virus infection in small and large GP13 produce such divergent causes of death?

B. Methods

1. Comparison of the effects of P. virus in small (IBW <400 g) and large (IBW >700 g) strain 13 guinea pigs (GP13) on weight loss, blood gases, blood chemistries and lung anatomy.

Large and small GP13 (n=45) were inoculated i.p. with 10^4 plaque forming units (PFU) of Pichindé virus suspended in minimum essential media containing 10% fetal bovine serum. Each animal was returned to its cage with full access to food and water. Since the fatal progression of this disease is associated with substantial loss of body weight, each animal's body weight was measured at three day intervals.

Critically ill infected animals were anesthetized with an i.p. injection of pentobarbital sodium, 15 mg/ml. A carotid artery was cannulated with a polyethylene catheter containing physiological saline with 10U/ml of heparin. Approximately one hour after anesthesia, arterial pressure and heart rate were determined with a calibrated Statham pressure transducer, and 1 ml of blood was withdrawn for blood gas, hematocrit, hemoglobin and blood lactate measurements. These measurements were determined by standard techniques. An additional 6 ml of blood was withdrawn for a complete blood chemistry that included the following: 1) formed element counts with an automated hematology analyzer; 2) differential white blood cell counts by direct observation; 3) Blood chemical analyses as a clinical veterinary panel performed by Roche Laboratories. Finally, each animal received an overdose of anesthesia and all tissues except the lung were fixed for light and electron microscopic analysis by immersion fixation in physiologically balanced Karnofsky's fixative. Fixative was instilled into the trachea at 20 cm of H_2O for lung preservation.

2. Extravascular Lung Water Determination.

In a separate group of P. virus infected small GP13 near death, the extravascular lung water (EVLW), residual lung blood, and EVLW to bloodless dry lung weight (BDLW) ratio were determined as previously described (Schaeffer et al, 1984).

3. Blood Volume.

A separate group of P. virus infected small GP13 was prepared in a similar manner to that previously described (Schaeffer et al, 1985). After cannulation of the external jugular vein and internal carotid artery, blood volume was measured using radioiodinated (^{125}I) human serum albumin (RIHSA) 1 μCi/ml (Mallinckrodt, Inc., St. Louis, MO). After control arterial blood samples were taken for baseline radioactivity and hematocrit measurements, 200 μl of radioiodinated human serum albumin followed by 300 μl of physiological salt solution was injected into the venous catheter. The amount of free radioactive iodine was < 0.5% of the RIHSA injectate. Arterial blood (200 μl) was removed at 5 min intervals for 30 min after clearing the dead space of the catheter. Hematocrit was determined in duplicate and 100 ul of blood was added to 2 ml of deionized water for radioactivity counting. The hematocrit was multiplied by 0.96 to correct for trapped plasma (McGovern et al, 1955). Blood volume measurements using RIHSA were based upon linear extrapolation of the data to 0 time.

4. Organ RIHSA radioactivity index (ORI).

At the end of the RIHSA sampling period for blood volume determination, the intensity of radioactivity change in each tissue as compared to a control animal was determined. Animals were euthanised with an overdose of sodium pentabarbitol. The heart, lungs, liver, kidney, spleen, stomach, small and large intestine were removed and blotted dry to remove any residual blood. The organs were weighed and all samples were counted in a gamma counter. The ORI for RIHSA was calculated as follows:

$$\text{ORI} = \frac{\text{RIHSA emissions/min/g tissue wt}}{\text{RIHSA emissions/min/0.1 ml of blood}}$$

5. Brochioalveolar Lavage Studies.

In selected small GP13s, alveolar cells were obtained by bronchioalveolar lavage. The alveolar contents were centrifuged, and plated on a Lab-Tek (Nunc, Inc.; Naperville, Illinois) slide for morphologic and virus determination of fresh frozen cells by indirect immunofluoresence microscopy using a monoclonal antibody against Pichinde virus nucleocapsid glycoproteins.

6. Endothelial DNA synthesis.

GP13 aortic endothelial cells (GPAEC) were isolated with the following technique. GP13 aortas were cannulated and perfused with Ca++ and Mg++ free saline. The aorta was subsequently incubated with 2% collagenase for 30 min. After this period the cells were isolated, cultured and subcultured with trypsin-EDTA. GPAECs were grown into subconfluent monolayers (approx. 50% confluence), and then innoculated with various doses of Pichinde virus (106, 105, and 104 PFU/ml). GPAECs were incubated for 24 hours and then washed to remove debris and any non-adsorbed virus. Tritiated thymidine was added to each well and the cells were incubated another 24 hours. Incorporation of thymidine into endothelial cell DNA was measured using a scintillation counter.

7. GPAEC protein synthesis.

GPAEC (30 plates) were plated onto 96 well plates at a density of 37K cells/well and allowed to grow to approximately 90% confluence. Wells were inoculated with either 105, 104, or 0 PFU and incubated overnight at 37°C. Virus was removed and fresh 10% DMEM was added to each well. Wells were incubated 5-7 days at 37°C. Cells were starved for one hour by removal of old media, and addition of methionine free RPMI 1640. After one hour, media was replaced with methionine free RPMI 1640 containing 5% dialyzed serum. A 5 μCi volume of S-35 labeled methionine was added to each well and incubated at 37°C for four hours. Supernatant was removed and cells were lysed with lysis buffer and incubation at 4°C for one hour. Lysate was centrifuged at 5000 xg for one hour. An excess (50 μl) of polyclonal anti-Pichinde Ab (1:400) was added to the supernatant and incubated at 4°C overnight. A 10 μl aliquot of Pansorbin was added to each supernatant and shaken at 1100 rpm for one and one-half hours at room temperature. Supernatant was centrifuged at 5000 xg for five minutes to remove virus-Pansorbin pellet. Supernatant was placed into scintillation cocktail for radioactivity counting.

8. Electron microscopy GPAEC.

GPAEC were grown on transwells (n=25) for five days. Monolayers were infected with 105 PFU of P. virus for 18 hours. After this interval media was changed and monolayer fixed at one day intervals with half strengh Karnofsky's fixative and analyzed by scanning and transmission electron microscopy.

9. GPAEC intracellular calcium measurements.

GPAEC were grown on glass coverslips (n=25) for five days. Certain monolayers were infected with 105 PFU of P. virus for 18 hours. After this interval, media was changed and the monolayers cultured for an additional two days. After this interval control and P. virus infected GPAEC were loaded with the calcium binding dye Fura-2. The effects of the endothelial cell agonist, bradykinin (BK, 1 μM), were studied.

10. GPAEC monolayer permeability assay.

GP13 aortic endothelial cells (GPAEC) were plated onto a polycarbonate Transwell membrane insert at a density of 72K cells/well in 10% DMEM and incubated for three days at 37°C. After incubation, media was removed and cells were inoculated with either 105, 104, or 0 PFU of Pichindé virus and incubated overnight at 37°C. Virus was removed and cells were washed three times in PBS. The permeability of control and virus infected GPAEC monolayers were performed with fluorescein isothiocyanate hydroxyethyl starch (FITC-HES). This tracer was added to the top well of the transwell and allowed to diffuse across the monolayer. At selected times a sample was removed from the bottom well of this system for analysis on a calibrated size selective HPLC column.

11. Low density lipoprotein up-take by GPAEC.

In three experiments GPAEC monolayers were grown on a Lab-TEK slide and infected with 106, 105, 104 and 0 PFU of P.virus for 18 hours. After an additional day of culture, the uptake of the fluorescent tracer, 1,1'-dioctadecyl-3,3,3',3'-tetramethyl indocarbocyanine perchlorate labeled acetylated low density

lipoprotein (29; DIL-acetylated LDL, Biomedical Technologies, Inc., Stoughton, MA) was determined by observation with a fluorescence microscope.

12. GPAEC-lymphocyte adhesion assay.

In three preliminary experiments GPAEC monolayers were plated on 96 well plates and infected with 105 PFU of P. virus for 18 hours. Monolayers were grown for an additional day. At this time, GP13 mononuclear cells were isolated from three uninfected animals. These cells (105/well) were added to 7 control and infected monolayers. Adhesion was determined by observation with a light microscope.

In two preliminary experiments GP13 lymphocytes were isolated from uninfected controls on Histopaque (1084) gradients. These cells were washed with phosphate buffered saline and incubated with P. virus (105 PFU/ml) for 18 hours at 37°C. After this interval the washed cells were added to uninfected GPAEC in our standard adhesion assay.

13. Statistics.

All data are shown as the mean ± S.E. An analysis of variance was used to compare each variable of each group at the specified interval. The paired t test was used for comparision of each experimental time with the control group.

C. Results

1. Comparison of the effects of P. virus in small (<400 g) and large (>700 g) strain 13 guinea pigs on weight loss, blood gases, blood chemistries and lung anatomy.

F. (c)1 Figure (c)1 shows a comparison of the change in body weight in P. virus infected small (<400 g, n=18) and large (IBW > 700 g, n=8) GP13 vs time. Large GP13 demonstrated a different weight loss pattern than small GP13. Large GP13 lost approximately 15-20% of their IBW between days 10-12 as compared to the 5-7% for small GP13. All large GP13 expired by day 14 in comparison to >18 days for the small animals.

T. (c)1 Small and large GP13 showed different arterial blood gas results in comparison to the control group (Table (c)1). Blood gas and lactate values were within the normal range in the control group. Severely ill small GP13 at day >18, in contrast, showed marked hypoxemia with a slight elevation in PCO_2 and bicarbonate ion concentration, with normal pH. Arterial blood lactate was significantly above the control group. Hemoblogin was within normal limits. Severely ill large GP13 at day <14 showed a different blood gas profile. Normoxia in association with a low pH, PCO_2 and bicarbonate ion concentration was characteristic of the large animals with an increased respiratory rate. Arterial blood lactate was within normal limits. Hemoglobin was significantly elevated above the control levels.

T. (c)2 Small and large GP13 showed elevated blood enzymes levels in comparison to the control group (Table (c)2). Although the small animals showed a significant elevation in blood enzyme levels, large animals showed a nearly five-fold

higher level of most enzymes in comparison to the small animal group. Blood triglyceride levels were similar in the control and small GP13 groups in contrast to a 50% decline in the large animals.

A strikingly different pattern of electrolytes, creatinine, BUN and glucose values was seen between the small and large GP13 in comparison with the control group (Table 3). No major differences were seen between the control and
T. (c)3 small GP13 in all of these parameters. In contrast, the large GP13 (n=3) showed a marked reduction in electrolytes and bicarbonate ion. These data were associated with high values for blood creatinine, BUN and glucose.

An increase in the ORI of the lung and heart was observed after P. virus
. . (c)2 infection in the small but not large GP13 (Figure (c)2 and 3, respectively). No
F (c)3 differences in the gross features of the heart and lungs were noted bewteen the control and large GP13 at day 12-14. In addition, microscopic analysis of these two groups were unremarkable. In contrast, areas of the lungs of the small GP13 at day >18 showed a liver-like appearance. The lung from these animals showed marked binding of leukocytes to the pulmonary endothelium with some interstitial pneumonitis.

A detailed description of the pathophysiology effects of P. virus infection in small (IBW <400 g) GP13 at day 13 and day>18 on extravascular lung water, blood volume, organ RIHSA radioactivity index, brochioalveolar lavage and other data is described below.

2. Cardiovascular metabolic and respiratory effects.

There was little evidence of any major circulatory problems. Arterial pressure, heart rate, hematocrit, hemoglobin as well as blood volume index were
T. (c)4 not significantly different between the control and virus-infected groups at either day 13 or >day 18 (Table (c)4).

There was, however, a significant elevation in the cardiac enzyme, serum glutamic oxaloacetic transferase (SGOT), as well as lactate dehydrogenase (LDH)
F. (c)4 by day >18 (Figure (c)4). This effect was associated with a significant decline in heart weight as compared to the control group (1.14±.08 vs 1.51±0.13g, $p<.05$;
F. (c)5 respectively). Despite the fall in heart weight, this organ showed a significant elevation in RIHSA activity index (Figure (c)5).

A significant increase in lung wet weight was observed by day >18 in comparison to the control group (3.67±.26 vs 2.47±.09, $p<.005$; respectively). This effect was associated with a significant elevation in lung RIHSA activity index. Extravascular lung water (EVLW) to bloodless dry lung weight (BDLW) ratio
F. (c)6A was elevated at day 13 and day >18 in the infected animals (Figure (c)6A). Residual lung blood and EVLW were significantly increased above the control group
F. (c)6B by day >18 (Figure (c)6B).

Arterial blood gas measurements showed significant alterations by day >18
T. (c)5 after virus-infection (Table (c)5). By this period a marked decline in PO_2 (41 ± 5 mm Hg) was associated with a significant elevation in arterial blood lactate (3.35 ± 0.5 mM/L). Although pH and PCO_2 were not significantly altered, HCO^-_3 and respiratory rate were significantly above the control group.

3. Immunofluoresence Microscopy.

Pichindé virus antigen was observed in the visceral pleural epithelium (Figure (c)7A), mononuclear (MN) leukocytes bound to small pulmonary Blo(d)7 vessels (Figure (c)7B), alveolar macrophages (Figure (c)7D) as well as focal areas of the bronchiolar epithelium at day 13 (Figure (c)7C). Immunostaining increased at day 17 with marked deposits throughout the alveolar-capillary wall as well as within alveolar and capillary mononuclear cells (Figure (c)7D). This staining pattern was significantly decreased at day 20. In addition, alveolar cells obtained by bronchoalveolar lavage at day 13 and day >18 showed marked punctate fluorescent deposits throughout the cell cytoplasm (data not shown). These deposits were not seen in the control lungs (Figure (c)7E).

4. Light and Electon Microscopy.

Light microscopic evaluation of the lungs in the control group were unremarkable (Figure (c)7E). Modest perivascular edema was noted around small blood vessels and terminal bronchioles with clear alveoli in the infected animals at day 13. MN cells were bound to the intimal surface of many small pulmonary blood vessels and some capillaries (Figure (c)7B). This pattern progressively worsened until MN cells with some granulocytes were seen to occluded most pulmonary capillaries at day >18. A few unobstructed microvascular channels were seen around clear alveoli (Figure (c)7F). At this time, focal pneumonitis was characterized by alveoli filled with MN infiltrates without red cells. Many of the clear alveoli, however, contained activated macrophages with no hemorrhage or edema.

Transmission electron microscopic analysis of the uninfected GP13 lung
F. (c)8 showed clear lung fields with unobstructed blood vessels and capillaries (Figure
F. (c)9 (c)8). In contrast, lungs at day 19 after infection revealed vacuolated alveolar macrophages that appeared activated (pseudopod formation) without evidence of alveolar edema, hemorrhage or fibrin (Figure (c)9). Activated lymphocytes as well as monocytes were observed marginated to most microvascular walls. Granulocytes were less frequently seen in these cell aggregates. Most platelets and granulocytes did not show significant degranulation. A few plasma cells and megakaryocytes were also seen. Most pulmonary capillaries were occluded with lymphocyte-monocyte cell aggegates. This effect was seen in all lung lobes. The thick portion of the alveolar-capillary membrane contained macrophages. No significant alteration was noted in the thin portion of this membrane. Substantial ribosome deposits were seen in the cytoplasm of most leukocyte aggregates.

5. Blood Chemistry and Hematology.

Serum albumin (2.87±0.13 vs 2.14±.06, $p<.05$) and the albumin to globulin ratio (2.29±.21 vs 1.29±.07, $p<.001$) declined between the control and infected group at day >18. Serum globulin was increased from the control group to the infected group by this period (1.28±.1 vs 1.68±.07, $p<.05$, respectively). Serum proteins and all other serum determinations (electrolytes, BUN, creatinine, glucose) were not significantly different between any group.

Serum glutamic pyruvic transferase (SGPT) was significantly elevated above the control group at day 13 and day >18 (49.5±4.3 to 85±6.2, $p<.01$ and 63.5±3.4, $p<.05$). The decline in SGPT between day 13 and >18 is a different

pattern from the progressive rise in the activity previously described for SGOT and LDH. The other enzymes measured, gamma glutamyltransferase and alkaline phosphatase were not significantly different from the control group at any interval.

White blood cell count was elevated as compared to the control group by day >18 (3.1±.24 vs 4.56±.55, p<.01). An increase in granulocytes accounted for most of this gain (1.2±.1 vs 2.43±.13, p<.01). Blood platelets were strikingly below the control group by day >18 (614±44 x 103 vs 175±21 x 103/mm3, p<.001).

6. GPAEC DNA synthesis assay.

We were suprised to find that high levels of P. virus (10^6 PFU), caused a decreased H3-thymidine GPAEC up-take 39% below the untreated control cells (Figure (c)10). Our previous report of dead cells following treatment with 10^6
F. (c)10 PFU of P. virus was an error.

7. GPAEC protein synthesis assay.

F. (c)11 Figure (c)11 shows the amount of incorporation of S-35 methionine into GPAEC monolayers. The decrease in incorporation is apparently related to the inoculation dose, and higher doses seem to decrease incorporation of S-35 relative to control. This decreased incorporation suggests that protein synthesis may be inhibited in EC's infected with Pichinde virus.

8. Electron microscopy of GPAEC.

F. (c)12 Virus infected GPAEC showed marked amount of densely stained material within the cytoplasm and nucleus (, Figure (c)12). The prescence of an increased number of ribosomes are also seen. Vacuoles that appear to contain
F. (c)13 certain secretory material are also seen within theses cells (*, Figure (c)13). The effects of this distinct morphologic alteration in these cells remains unclear.

9. GPAEC intracellular Calcium measurements

F. (c)14 Figure (c)14 and Figure (c)15 show a comparison of representative experi-
F. (c)15 ments from each group. When Fura-2 binds to calcium, there is an increase in the emission energy at 340 nm and a decline in energy at 380 nm. This characteristic results in a marked increase in the 340/380 nm emission energy ratio. Figure (c)14 shows no difference on the BK stimulated increase in the 340/380 ratio on GPAEC monolayers that were exposed to 0 and 10^5 PFU of P. virus. Figure (c)15 shows that cells exposed to P. virus showed a slightly lower calcium elevation than that seen in the control cells. We are not certain if this difference results in a significantly different physiologic response of these cells. These data suggest that BK stimulates a calcium flux in both virus-infected and control GPAECs.

10. GPAEC monolayer permeability assay.

F. (c)16 Figure (c)16 shows the permeability vs molecular radius of FITC-HES that crossed each GPAEC monolayer in comparison with bovine pulmonary artery (c)17

endothelial cell (BPAEC) monolayers. Figure (c)17 shows these data plotted as
F. (c)17 the permeability coefficient/free diffusion coefficient (Do) of each sized probe. This is a measure of the relative restricted diffusion area per unit path length available for solute transport. Positive slopes are indicative of non-confluent layers (Katz and Schaeffer, 1991).

Figures (c)15 and 16 show that either control or virus-infected GPAEC monolayers were nearly an order of magnitude more permeable than the BPAEC monolayers. These data suggest that GPAEC monolayers do not form the substantial permeability barrier produced by BPAEC. These data show that the influence of P. virus on endothelial monolayer barrier function was not possible to determine.

11. GPAEC-lymphocyte adhesion assay.

GP13 lymphocytes bound infected GPAEC as distinct groups of 5-10 mononuclear cells per 1-2 endothelial cells. This adherence was 3-4X that seen on uninfected monolayers. These data suggest that virus infected GPAEC may express an adhesive molecule for mononuclear cells. This in vitro effect may model the massive adhesion of mononuclear cells in the lungs of small GP13 by day >18. The in vitro model may allow a characterization of the molecule(s) responsible for this increased adhesive effect in a defined manner.

When GP13 leukocytes were inoculated with P. virus (10^5 PFU/ml) in vitro (two preliminary experiments) these cells did not show the increased binding to uninfected GPAEC described above. Subsequent analysis of the mononuclear cells showed no significant virus within these cells. These data suggest that unlike GPAECs, overnight incubation of 10^5 PFU of P. virus does not lead to significant infection of GP13 mononuclear cells. Since significant virus has been detected in lymphocytes in vivo by day >18, the mechanism of virus infection of these cells remains unclear.

12. Low density lipoprotein up-take assay.

GPAEC did not show any significant differences in the scaverenger LDL receptor population density for the GPAEC P. virus infected or uninfected cells. These data suggest tha P. virus does not affect this receptor functon in these cells.

D. Discussion

Comparison of the effects of P. virus infection in small (young) (<400 g) and large (old) (>700 g) GP13 on weight loss, blood gases, blood chemistries and lung anatomy.

There appear to be two distinct causes of death in the small vs large P. virus infected GP13. Large GP13 appear to expire, in part, due to a severe metabolic acidosis without significant lactate production. This metabolic acidosis may be related to acute diabetes (no plasma ketones assay was performed) with a decrease in renal function. Anion gap is elevated at 18.7 with a control value of 10.5. The elevated glucose, hemoglobin, creatinine and BUN values in association with the decline in serum electrolytes and extremely low bicarbonate ion concentrations support this view. How can P. virus induce a non-lactate positive

anion gap, metabolic acidosis in large GP13 but a compensated lactacidosis in small GP13 near death? Anion gap in these animals is only 14.3. What are the mechanisms?

These data suggest that P. virus infection in large GP13 may not be a model of Lassa fever, since these animals do not display the lung pathology seen in severe Lassa fever in man. This disease process appears due to a fluid and electrolyte abnormality.

Severe hypoxemia is a hallmark of the fatal progression that leads to death in small P. virus infected GP13 by day >18. The elevation in lung RIHSA activity index, wet/dry weight ratio, residual lung blood and extravascular lung water that document modest pulmonary edema is consistent with this view. This finding, in association with severe congestion of the pulmonary circulation by mononuclear and polymorphonuclear cells, suggest that a substantial right to left shunt of unoxygenated blood may explain the severe hypoxemia and moderately elevated blood lactate levels. These data document a complex form of respiratory failure (modest pulmonary edema with increased intravascular mono/polynuclear cells). It is likely that lung failure is a major factor that leads to death in this disease process (Schaeffer and Bitrick, 1990).

Pulmonary hypertension is a likely consequence of the observed vascular congestion and dilation of the pulmonary capillaries. Although pulmonary pressures were not measured in the present study, the increase in residual lung blood in association with an elevation in lung RHISA activity index at day >18 are consistent with this view. Since an elevation in this parameter may be diagnostic of the initiation of the fatal progression of this disease process, documentation of pulmonary pressures at selected days after infection is an important priority.

The failure of arterial blood pH to decline in the setting of near normal partial pressure of carbon dioxide in association with elevaced respiratory rate and blood lactate is unclear. The significant increase in bicarbonate ion may explain this effect. Is it possible that a progressive increase in airway resistance in this disease process may lead to carbon dioxide retention in the lung and compensatory retention of bicarbonate ion by the kidney? The proof of this mechanism awaits further studies.

Although respiratory failure is a major factor that leads to death, a decrease in cardiac function is also likely to be involved. Although blood pressure and heart rate were not altered, we observed an increase in heart RIHSA activity index despite an absolute decline in heart weight. Monocyte invasion of the heart interstitium was also noted. These findings suggest that the heart capillaries were more permeable to albumin by day >18. Our observation of an elevation in SGOT and LDH is consistent with myocardial damage. A previous report (Peters et al, 1987) has shown that cardiac output is reduced by day 14 after Pichinde virus infection. These data suggest significant cardiac dysfunction in assocation with respiratory failure may be the cause of death following prolonged Pichinde virus infections.

We observed no evidence for significant peripheral vascular edema or alteration in blood volume in this disease process. We documented no significant increase in RIHSA index in the kidney, liver, small intestine, muscle or spleen.

Therefore, although it is not ruled out, hypovolemia does not appear to occur in prolonged virus infections.

Hepatic or severe renal failure do not appear to occur in this disease process, particularly in small or young GP13. We found no significant elevation in the liver enzymes GGT and SGPT. In addition, blood creatinine and blood urea nitrogen levels were not significantly elevated in these animals. Although there may be an alteration in liver blood flow and increased fatty deposition in this organ, these alterations appear to have minimal impacts on the cause of death.

It is unclear what influence the substantial thrombocytopenia has in this disease. We found no change in fibrinogen levels and no evidence of increase bleeding during surgical isolation of blood vessels. The presence of a consumption coagulopathy is not consistent with these data.

All small GP13 that expired showed a marked decline in body weight, and no adipose tissue was observed during blood vessel isolation by day >18. The mobilization of fat reserves leads to an elevation in blood triglyceride levels at day 13 in this study. This cachexic-like response may due to the increased release of tumor necrosis factor (TNF) by "activated" macrophages. It is likely, however, that weight loss, by itself, may not a major factor in the cause of death in small GP13.

The increased adhesion of mononuclear cells onto endothelial surfaces in the lung and heart that leads to vascular congestion may be the primary factor that leads to death. This process could explain the reports of pleural and pericardial effusions following Lassa fever in primates (Walker et al, 1982, Callis et al, 1982). Therefore, the sequence of events by which mononuclear leukocytes adhere to endothelial cells may be the penultimate mechanism that initiates the fatal sequence of events. Although this effect may be due, in part, to the increased release of a variety of products by "activated macrophages" onto vascular surfaces, the exact mechanisms of this process need further study.

GPAEC DNA and protein synthesis, transmission electron microscopy, intracellular Calcium measurements, monolayer permeability low density lipoprotein uptake and GPAEC-lymphocyte adhesion.

Although P. virus can decrease DNA and protein synthesis in GPAEC, these cells do not show major depression calcium metabolism or low density lipoprotein up-take. GPAEC appear to tolerate P. virus infection without massive cell death. Since these cells did not form any substantial barrier to macromolecules we could not determine if P. virus altered GPAEC interendothelial pores.

We observed an apparent increase in leukocyte adhesion to P. virus infected GPAEC in three preliminary experiments. Thus, P. virus infection of these cells may generate adhesive molecules that mediate the leukocyte binding seen in vivo.

Why P. virus did not directly infect GP13 leukocytes in our preliminary experiments is unclear. It suggests that lymphocytes may not directly take up this virus in vivo.

In conclusion, P. virus appears to produce two distinct disease processes in GP13 based upon initial body weight or age. Large or older animals appear to form a non-lactate based metabolic acidosis with a large anion gap. Small or young animals appear to die of leukocyte congestion of the pulmonary microcirculation similar to the histopathogy of Lassa fever in man. How the same virus can create such apparently distinct disease processes based upon initial body weight or age is not clear. The notion that P. virus infection of small GP13 that survive to >18 days is a more accurate model of the pulmonary changes seen in severe Lassa fever in man is supported by our findings. It may be possible to model the endothelial-mononuclear leukocyte interactions seen in these syndromes in vitro. Description of the molecules that create leukocyte sequestration in the pulmonary microcirculation would allow trial of precise therapy to prevent this insult, in vivo.

IV. Study (d) Assessment of free radical participation in pathogenesis of arenavirus infection by measurement of expired ethane by gas chromatography

A. First Study - Introduction

Guinea pigs strain 13 when infected with the eighth-passaged Pichindé Arenavirus develop syndrome with some similar features to hemorrhagic fever in man. The cause of death in hemorrhagic fever, as well as Pichindé virus in this strain of guinea pig, is believed to involve, at least in part, massive capillary leak syndrome. Studies a, b, and e of this project call into question this broad generalization, at least for the gut, mesentery, and liver. The characteristics of the illness both in animals and man has been poorly defined in terms of pathogenesis but the free radicals of oxygen are thought to play a role in the disease.

Ethane gas is a hydrocarbon byproduct of lipid peroxidation of the omega three fatty acids. It has been shown by Reily et al (1) to be a non-invasive marker of lipid peroxidation. We undertook to measure ethane in the exhaled breath from infected and non-infected guinea pigs to determine if increased lipid peroxidation occurs during Pichindé virus infection.

B. First Study - Methods

Ethane was measured in the expired breath of six guinea pigs both before and after infection with virus. Methods and validation procedures were developed under the aegis of the contract (2,3,4). Animals were studied prior to infection and every foure days after inoculation with Pichindé virus.

Air (zero grade air, Liquid Air, Tucson, AZ) was directed over a freshly prepared cold trap of activated charcoal (vacuum heated at 250° C for one hour) (Coconut Charcoal, Alltech, Deerfield, IL) at a flow rate of 200 ml/min (flowmeters, Cole Parmer), and this was directed into a sealed metabolic chamber housing a guinea pig. Effluent from the chamber was directed over a second cold trap of activated charcoal consisting of a 1/4 in diameter glass tube containing approximately 0.5 grams of charcoal. The contents of this tube were replaced at 30 minute intervals with fresh charcoal. Fresh charcoal was determined to contain no detectable ethane. The contents of the trap were poured into a 13.27 ml glass test tube and sealed with a screw cap housing a teflon septum. This tube

was placed into a heating block for 2 minutes at 230° C, and 5 ml of headspace gas was removed with an airtight gas sampling syringe. This was injected onto the column of a gas chromatograph (Hewlett Packard model 5890) kept at 220°C. The column was a 1/4 inch diameter, 2 meter long glass column (Alltech) packed with Carbosphere 60/80 (Alltech). Carrier gas was helium, the flame ionization detector (FID) used hydrogen and air. The retention time was 4.74 minutes. Pure ethane (Matheson) was diluted and used for calibration. The regression line for such calibration had a coefficient of linear regression of not less than 0.995 (2,3,4).

C. First Study - Results

Guinea pigs whose initial weight was 450-500 grams were used in this study. As shown in Figure (d)1, weight tended to increase after infection during
F. (d)1 the first four days as these were not full grown animals. At day 8, the animals had evidence of weight loss which was progressive, the animals losing an average of 32% of their initial weight by the 12th day.

Ethane elimination rose after inoculation with virus as shown in Figure
F. (d)2 (d)2. The variation in ethane elimination at various times after infection for
F. (d)3 each animal can be seen in Figure (d)3. Whether ethane produced was expressed based on final or initial weight, the ethane noted by day 12 was significantly higher than baseline.

D. First Study - Discussion

These data show that infected animals produce increased lipid peroxidative activity as the infection progresses. This increased ethane production may be related to the increased metabolic rate the animals are experiencing as they get more ill. The loss of weight they experience is a characteristic of this illness. By the 12th day, these animals had lost 32% of their initial weight. The severity of this degree of weight loss and hence the degree of illness can be brought into perspective when one realizes that these guinea pigs should have weighed about 550 grams based on the average weight gain over this time period seen in other uninfected animals whose initial weights were similar. Using the final predicted weight as an index, these infected animals weighed about 60% of their predicted weight at 12 days post infection. The animals died on the 12th or 13th day after infection.

Since ethane is considered to be a result of increased free radical production, anything which increases production of toxic oxygen metabolites or interferes with the scavenging of these toxic oxygen species may increase ethane. For example, increased metabolic rate, a result of the illness itself, may account for the increased ethane. This is a non-specific response to disease. It is unlikely to represent increased minute ventilation even though this event may have occurred, since we have previously shown that anesthetized, mechanically ventilated animals, ventilated at various rates, have ethane production rates that are independent of minute ventilation (3). This is not to say that increased work of respiratory muscles in conscious animals could not account for the increased ethane found in unanesthetized ill animals Thus, increased metabolic activity may have contributed to the increased ethane found in the ill animals.

The concern exists that weight loss alone may influence ethane production in that ethane is derived from the essential fatty acid linolenic acid. Recent data from this laboratory (5) in rats suggest that food restriction reduced ethane production. This is in contrast to the findings in the guinea pigs studied in this report where weight loss in the infected animals was associated with increased ethane elaboration. This finding in rats needs to be confirmed in guinea pigs.

In one of the animals whose demise was witnessed, the lungs were removed and wet/dry weight ratio performed. The normal value of 4.4 was found suggesting that the animal died without significant increase in lung water. This single observation does not obviate the more common experience that lungs are increased in weight (study a) and water (study c), in contradiction to modest capillary leak in the jejunum (study a) and no demonstrable capillary leak in liver, gut microvilli or mesentery (studies b-e).

Thus, ethane elaboration in infected guinea pigs increases by day 12 after infection at a time when the guinea pigs have lost 32% of their initial weight corresponding to about 60% of their final expected weight.

E. Second Study - Introduction

Ethane production from Pichinde virus infected guinea pigs was noted to be increased in spite of a 32% weight loss over the period of infection. Animals died at about 12 days after inoculation with, virus and the increased ethane resulting from the illness suggests that increased lipid peroxidative activity was seen with the infectious process. In order to determine if longevity can be increased after infection in these animals, we investigated the effects of pre-treatment of the animals with the antioxidants butylated hydroxytoluene (BHT) (6) as well as vitamin C which has been shown to possess some antioxidant activity and which is readily available for administration if efficacy can be shown. Antioxidants or scavengers of toxic oxygen metabolites should reduce the ethane produced during infection. To the extent that the syndrome leading to death from hemorrhagic fever these animals develop is related to increased toxic oxygen metabolites, these antioxidants may have the potential of being used as therapeutic agents.

F. Second Study - Methods

BHT (200 mg) was dissolved in corn oil (1 ml) and administered to guinea pig strain 13 by intraperitoneal injection (1 ml/kg) daily for three days prior to infection with Pichinde virus. This was performed in three animals.

F. (d)4 Animal weight was monitored and ethane was measured over time (see Figures (d)4 through (d)7 for exact times). The animals used in this group were larger than the animals used in the previous study (approx 700 grams initial weight).

Vitamin C

Other guinea pigs were administered vitamin C, 1 mg/ml in their drinking water for seven days prior to infection in one group and at the same concentration after infection with Pichindé virus. The absolute amount given to the animals could not be determined precisely since water was often found on the floor of the cages and it could not be determined precisely what had been consumed vs lost.

G. Second Study - Results

The time to death after infection was unaltered by the antioxidants administered in this set of experiments. Animals started to die around the 11th post inoculation day and were all dead by day 15. In the vitamin C group receiving vitamin C after infection, one animal died very early on possibly from intraperitoneal bleed from the i.p. injection of virus. Thus only two animals were followed in this group. All other groups contained three animals.

F. (d)5 Animals all lost weight as predicted by previous studies. Figure (d)5
F. (d)6 shows the weight change in the BHT treated animals, and Figure (d)6 shows the same for the vitamin C treated GP13s. The ethane production in the vitamin C
F. (d)7 pre-treated group rose along with that in the no treatment group (Figure (d)7). Although it appears that the group receiving vitamin C after inoculation with virus had less ethane elaborated, the N of 2 is small; and at 12 days there was no statistical difference between the no treatment, vitamin C pretreatment and the concurrent treatment group. Regardless of the results of the ethane studies, the time to death in all animals appeared not to be affected by the use of vitamin C either as pretreatment or during infection.

The BHT animals also did not survive any longer with the use of this antioxidant. Two of the three BHT treated animals died prior to our being able to study them on the 12th day. However, on day 8 post inoculation, there was a tendency for increased ethane elaboration to be found and in the one surviving animal; and a large rise in ethane was seen at day 12 (Figure (d)4). Again, weight after infection fell from the time of inoculation until death (Figure (d)5).

H. Second Study - Discussion

Antioxidants do not seem to be protective in infected animals. Perhaps they were not given in adequate doses at appropriate time points or were not accessing the site of increased free radical production. Which if any of these factors is at play cannot be elucidated with the data presented. This absence of protective effects does not preclude trials of other antioxidants. Further experiments with other antioxidants such as SOD and catalase, perhaps attached to polyethylene glycol or inside liposomes should be attempted. Further, the lack of effect of the antioxidants used in this study raises the need for other measures of lipid peroxidation in this model. These would include measure of lipid hydroperoxides, conjugated dienes and superoxide anion production of various cellular elements.

I. Third Study - Introduction

In preliminary work we have shown in rats that food restriction reduces ethane production during air breathing. The rationale was that if caloric restriction produces reduced ethane reduction, then this alone is not a factor in producing elevated ethane elaboration in Pichindé induced viral disease (3). We proposed to determine if the same holds for guinea pigs. Food restriction should lead to a decrease in the essential omega three fatty acid precursor of ethane, namely linolenic acid. Infusion of fatty acids in rabbits has been shown by Wispe et al (7) to increase ethane elaboration in that species. As noted, rats fed a restricted died for two weeks or fasted for 15 hours elaborate less ethane during air breathing than do rats not food restricted (5). Since ethane production in Pichindé infected GP13 results in increased ethane production at a time when weight loss is marked, we measured ethane production in fasted animals and compared results with ethane elaborated by infected but not food restricted animals.

J. Third Study - Methods

Application to the Institutional Animal Care and Use Committee resulted in approval for us to feed the guinea pigs 60% of the previously established daily food intake for two weeks. Thus their food allotment was reduced to 20 grams per 24 hours. Guinea pigs of different weight were used so that the final weight of the animals, both the infected and the fasted controls would be approximately equal.

Animals had ethane measured prior to diet restriction or inoculation and after 12 days in the infected group and 14 days in the diet restricted control group. Ethane was measured as described above. Weights were recorded weekly in the diet restricted group and every 4 days in the infected group. Time to death was also recorded and collection data were expressed per weight of animal at entry into study.

K. Third Study - Results

F. (d)8 Figure (d)8 shows the weight changes that the two experimental groups experienced as well as the expected weight gain. The infected group followed the established pattern whereby they lost approximately 21% of their initial weight. At day 12, they weighed 64% of their predicted weight (580 g) based on weight gain experienced by other guinea pigs housed in our facility. The diet restricted control animals were initially smaller than the infected ones. Hence, they were expected to gain weight rapidly during the two week period except for the fact that they were receiving only 60% of what was predicted they would have otherwise eaten. These animals gained less than 50 grams during a time when they should have gained over 250 grams. The final weights of these and the infected animals was about 350 grams.

F. (d)9 Ethane production rates were significantly higher in the smaller animals at the start of the study compared to the inoculated animals (Figure (d)9), a finding compatible with a higher metabolic rate in these less mature animals. By the end of the study, the infected animals were producing substantially more
F. (d)10 ethane than their diet restricted and similar sized counterparts. The absolute

difference in ethane production rates are shown in Figure (d)10. In the diet restricted animals, ethane was seen to decrease whereas it increased in the infected GP.

L. Third Study - Discussion

These data support the contention that weight loss is not a determinant of the increased ethane found in the infected guinea pigs. Indeed, weight loss (or less than appropriate weight gain) results in reduced ethane production. Since final weights in the two groups were similar, the ethane produced on the final days were from guinea pigs of approximately the same size. Thus, one cannot invoke discrepant animal size as a potential cause of the results. In study (a) weight reduction was shown to be unrelated to jejunal capillary leak in infected GP13.

M. Fourth Study - Introduction

Since some studies from our group have demonstrated that animals that survive around 19 days develop wet lungs, the cellular composition of the bronchoalveolar lavage (BAL) fluid during the course of infection was felt to be worthy of investigation. BAL fluid is usually predominated by macrophages (~95%). These cells produce monokines which can influence neutrophil chemotaxis and endothelial cell permeability among other phenomena. We studied superoxide anion production in the alveolar macrophage at various time points after infection with Pichindé virus and correlated this late finding with the increased ethane production that was expected. In addition, studies were made by other members of the team in identifying whether or not virus was present in these cells and at what time point after infection they appeared in the BAL. These studies were done with antibody to the virus.

N. Fourth Study - Methods

Guinea pigs were infected with Pichinde virus and studied at day 7 and either day 12 or 13 post inoculation. In addition, BAL fluid from five control animals was studied. Prior to BAL, animals were placed in metabolic chambers for ethane determination which was carried out over two hours. The animals were then anesthetized with 40 mg/kg sodium pentobarbital ip and a tracheotomy performed. BAL was performed in the standard way. Eight ml of a calcium free physiologic salt solution were injected into the trachea and once instilled, the chest was gently massaged. Fluid was removed and collected. This was performed 8 times, and the total fluid recovery approximated 50 ml. A BAL cell pellet was centrifuged and resuspended in 10 ml of Hanks balanced salt solution (HBSS) with glucose and placed on ice. Aliquots were used for determination of alveolar macrophage superoxide anion production, cell count, and differential cell count (by cytospin). Superoxide anion production was carried out on the alveolar macrophages by Dr. Clark Lantz at the University of Arizona. A modification of a previously reported procedure was employed (8). Cells from the BAL were poured into plastic dishes and are allowed to adhere. After washing, the individual macrophages were examined by videomicroscopy for their ability to reduce nitroblue tetrazolium (NBT). The reduction of NBT was determined by spectrophotometry during videomicroscopy. Ten cells were counted per BAL, and the mean was determined at each time point. In another experiment, the cells were maximally stimu-

lated with phorbol myristate acetate prior to the measurement of superoxide anion production as described (8). Statistical analyses included the use of analysis of variance for three or more data sets, and the Student t test for two data sets.

O. Fourth Study - Results

F. (d)11 Figure (d)11 shows that the total cells per mm^3 are increased at 7 days after infection. There were 5 animals at day 0, 4 at day 7 and 9 at day 12/13. By the 12/13th day, the total cells/mm^3 recovered is back to baseline.

The differential cell count on day 7 and day 12/13 (Figure (d)12) revealed that there were fewer macrophages than expected from controls which have 95% macrophages. The macrophages seen on cytospin preparation stained with Wright's stain were full of immense vacuoles indicating that they were activated. The reduction in macrophages at day 7 was replaced predominantly by the neutrophils whose differential count was 37%, much higher than the predicted 1-2% of most control BALs. At day 7, the lymphocyte concentration was normal. By day 12, the macrophage population remained similar to that at day 7 but the increased neutrophil infiltration was reduced (below its peak) and was being replaced by the lymphocytes.

F. (d)13 Figure (d)13 shows the superoxide anion production (SOAP) from the alveolar macrophages at day 0,7 and 12/13. The SOAP at day 7 was similar to that on day 0. The SOAP on day 12/13 showed a marked increase in NBT reduction under basal conditions. The maximum stimulation afforded by PMA showed that day 0 and day 7 macrophages had plenty of SOAP production potential in reserve but the day 12 macrophages produced significantly less than the day 0 or 7 animals, indicative of exhausted reserve capacity.

F. (d)14 Ethane production was increased at day 12 as compared to the day 0 and day 7 animals. This can be seen in Figure (d)14 and Figure (d)15. This is in
F. (d)15 keeping with our other data as shown in Figures (d)2 and Figure (d)3.

P. Fourth Study - Discussion

These data confirm that ethane rises after 12 days of infection with Pichinde virus in this Guinea Pig Strain 13. The source of this ethane production is unclear but it probably originates in the lipid peroxidation of the omega-3 fatty acids. This peroxidation occurs when the superoxide anion defenses are overwhelmed, and it appears that a potential source for this anion is the alveolar macrophage which from these studies is producing significantly more amounts of SOAP at day 12 post inoculation, a time that corresponds with the increased ethane elaboration by the animals.

It remains unclear from these data that increased ethane corresponds to the increased SOAP from the macrophage. One can derive the total number of alveolar macrophages per animal by multiplying the total number of cell/mm^3 of BAL fluid (Figure (d)11) (times the 10 ml in the resuspended pellet from which the cell counts were derived) by percent of macrophages in the BAL (Figure (d)12). The total number of macrophages multiplied by the average SOAP per macrophage during the unstimulated measurement (Figure (d)13) yields the total

SOAP by macrophages at that point in time after inoculation. The peak value of so derived total SOAP from alveolar macrophages occurs at 7 days after inoculation (due primarily to the large number of cells/mm^3 in the BAL fluid at that time, whereas the peak in ethane production occurs at day 12. This suggests that either some other source of superoxide anion is responsible for the peaks in ethane at day 12, or that there is a lag between the appearance of superoxide anion and ethane. This study was not designed to study this latter possibility. However, other potential sources of superoxide anion need consideration such as those derived from the neutrophils and those derived from the products of general cellular metabolism which is most likely increased in the host guinea pigs when they are ill with Pichindé virus.

References

Study (a)

1. Peters CJ (1984). Arenaviruses, Ch 19, in Textbook of Human Virology (ed RB Belshe), pp 513-545, PSG, Littleton.
2. Giles RB, Sheedy JA, Ekman CN (1954). The sequellae of epidemic hemorrhagic fever. Am J Med 16:629-638.
3. Lukes RJ (1954). The pathology of thirty-nine fatal cases of epidemic hemorrhagic fever. Am J Med 16:639-653.
4. McKee KT, Peters CJ, Craven RB, Francy DB (1984). Other viral hemorrhagic fevers and Colorado tick fever (ed RB Belshe), pp 649-677, PSG, Littleton.
5. Pinter GG, Liu CT, Peters CJ (1988). Capillary permeability to labelled albumin and cervical hemodynamics in Pichindé virus infected Strain 13 guinea pigs. FASEB J 2 A1524 (Abstr).
6. Liu CT, Pinter GG (1989). Transport of ^{125}I-albumin from interstitium of soft palate and peritoneum to cervical lymphatics and plasma in Pichindé virus infected strain 13 guinea pigs. Report on Contract DAA103-86-D-001, Feb 15.
7. Katz MA (1989). Report on Contract 87PP7853, Mar 25.
8. Katz MA (1982). System analysis of vascular membrane water and protein transport: general method and application to canine hindquarters. Microvasc Res 23:31-55.
9. Katz MA, Starr JF (1984). Effects of acetylcholine on peripheral vascular protein permeability. Lymphology 17:28-33.
10. Katz MA (1985). Comparison of crosspoint and least-squares regression methods in computation of membrane protein flux parameters from lymph flux analysis. Microvasc Res 30:207-221.
11. Katz MA (1985). New formulation of water macromolecular flux which corrects for nonideality: theory and derivation, predictions, and experimental results. J Theor Biol 112:369-401.
12. Jahrling PB, Hesse RA, Rhoderick JB, Elwell MA, Moe JB (1981). Pathogenesis of a Pichindé virus strain adapted to produce lethal infections in guinea pigs. Infect Immun 32:872-880.
13. Peters CJ, Jahrling PB, Liu CT, Kenyon RH, McKee KT Jr, Barrera Oro JG (1987). Experimental studies of arenaviral hemorrhagic fevers. Current Topics in Microbiol Immunol 134:5-68.
14. Brace RA, Granger DW, Taylor AE (1977). Analysis of lymphatic protein flux data. Effects of capillary heteroporosity on estimates of reflection coefficients and PS products. Microvasc Res 14:215-226.
15. Brigham KL, Harris TH, Bowers RE, Roselli RJ (1979). Inferences from measurements of plasma to lung lymph protein transport. Lymphology 12:177-190.
16. Katz MA (1981). Changes in transcapillary protein flux by permeative and convective mechanisms as functions of increasing transcapillary water flux. Microvasc Res 22:271-195.
17. Rutili G, Granger DN, Taylor AE, Parker JC, Mortillaro NA (1982). Analysis of lymphatic protein data: IV. Comparison of the different methods used to estimate reflection coefficients and permeability surface area products, Microvasc Res 23:347-360.

18. Taylor AE, Granger DN (1984). Exchange of macromolecules across the circulation. In Handbook of Physiology, Section 2, the Cardiovascular System, Vol IV, The Microcirculation, pt. 1, Ch 11 (eds EM Renkin, CC Michel), pp 467-520, Am Phsyiol Soc, Bethesda.
19. Witte CL, Myers JF, Witte MH, Katz MA (1983). Transcapillary water and protein flux in the canine intestine with acute and chronic extrahepatic portal hypertension. Circ Res 53:622-629.
20. Katz MA (1985). The effect of hydrostatic gradient on solvent drag reflection coefficient in heteroporous membranes: differences between model-dependent and model-independent computations. Microcirculation, Endothelium, Lymphatics 2:417-441.
21. Katz MA, Starr JE (1990). Pichindé virus infection in strain 13 guinea pigs reduces intestinal protein reflection coefficient with compensation. J Infec Dis, In Press.
22. Dowdy S, Wearden S (1983). Statistics for Research, pp 194-195, 263-275, 295-297, John Wiley & Sons, New York.
23. Siegel S (1956). Nonparametric Statistics for the Behavior Sciences, pp 116-127, McGraw-Hill, New York.
24. Granger HJ, Laine GA, Barnes GE, Lewis RE (1984). Dynamics and control of transmicrovascular fluid e changes, Ch 8. In Edema (eds NC Staub, AE Taylor), pp 189-228, Raven Press, New York.
25. Granger DN, Barrowman JA (1984). Gastrointestinal and liver edema, Ch 26. In Edema (eds NC Staub, AE Taylor), pp 615-626, Raven Press, New York.
26. Katz MA, Johson PC (1985). Capillary Exchange, Ch 2. In The Kidney: Physiology and Pathophysiology (eds DW Seldin, G Giebisch), pp 15-29, Raven Press, New York.

Study (b-e)

1. Peters CJ (1984). Arenaviruses, in Textbook of Human Virology (ed RB Belshe), pp 513-545, Littleton.
2. Tandon BN, Acharya SK (1987). Viral diseases involving the liver. Baillieres Clin Gustrovent 1:211-230.
3. McCuskey RS (1986). Hepatic microvascular dysfunction during sepsis and endotoxemia, in Cytoprotection and Cytobiology, Vol III (ed M Tsuchiya), Excerpta Medica, Amsterdam, pp 3-17.
4. McCuskey RS, McCuskey PA, Urbaschek R, and Urbaschek, B (1987). Kupffer cell function in host defense. Rev Infect Dis 9:5616-5619.
5. Jahrling PB, Hesse RA, Rhoderick JB, Elwell MA, and Moe JB (1981). Pathogenesis of a Pichinde virus strain adapted to produce lethal infections in guinea pigs. Infect Immunity 32:872-880.
6. Murphy FA, Buchmeirer MJ, Rawls WE (1977). Reticuloendothelium as the target in a virus infection. Lab Invest 37:502-515.
7. Peters CJ, Jahrling PB, Liu CT, Kenyon RH, McKee KT, Barrea Ore JG (1987). Experimental studies of arenaviral hemorrhagic fevers. Current topics in Microbiol Immunol 134:5-68.
8. McCuskey RS (1991). Microscopic Methods for Studying the Microvasculature of Internal Organs, in Physical Techniques in Biology and Medicine. Microvascular Technology, (eds CH Baker, WF Nastuck), Academic Press, New York, In Press.
9. McCuskey RS, Urbaschek R, McCuskey PA, Urbaschek B (1983). In vivo microscopic observations of the responses of Kupffer cells and the hepatic

microcirculation to Mycobacterium bovis BCG alone and in combination with endotoxin. Infect Immunity 42:362-367.
10. McCuskey RS, McCuskey PA, Urbaschek R, Urbaschek B (1984). Species differences in Kupffer cells and endotoxin sensitivity. Infect Immunity 45:278-280.
11. McCuskey RS, Urbaschek R, McCuskey PA, Sacco N, Stauber WT, Pinkstaff CA Urbaschek B (1984). Deficient hepatic phagocytosis and lysosomal enzymes in the low endotoxin-responder, C3H/HeJ mouse. J Leukocyte Biol 36:591-600.
12. Wisse E, DeZanger RB, Jacobs R, and McCuskey RS (1983). Scanning electron microscopic observations on the structure of portal veins, sinusoids and central veins. SEM/1983/III:1441-1452.
13. Wisse E, DeZanger RB, Jacobs R, Charels K, Van der Smissen P, McCuskey RS (1985). The liver sieve: consideration concerning the structure and function of endothelial fenestrae, the sinusoid wall and the space of Disse. Hepatology, 5:683-692.
14. Steffan A-M, Gendrault J-L, McCuskey RS, McCuskey PA, Kirn A. Phagocytosis, an unrecognized property of murine endothelial liver cells. Hepatology, In press.
15. McCuskey RS, McCuskey PA, Gendrault J-L, Ditter B, Becker K-P, Steffan A-M, Kirn A (1986). In vivo and electron microscopic study of dynamic events occuring in hepatic sinusoids induced by Frog Virus 3, in Cells of the Hepatic Sinusoids, Vol I, (eds A Kirn, DL Knook, E Wisse), Kupffer Cell Foundation, Leiden, pp 351-356.
16. Urbaschek B, Becker KP, Ditter B, Urbaschek R (1985). Quantification of endotoxin and sample-related interferences by using a kinetic limulus Amebocyte lepate microtiter test, in Microbiology - 1985, (ed L Leive), Amer Soc Microbiol, Washington, DC.
17. Murphy FA, Whitfield SG (1965). Morphology and morphogenesis of arena-viruses. Bull World Health Organiz 52:409-419.
18. McCuskey RS, Urbaschek R, McCuskey PA, and Urbaschek B (1989). Hepatic microvascular responses to tumor necrosis factor, in Cells of the Hepatic Sinusoid, Vol 2, (eds E Wisse, DK Knook, K Decker), Kupffer Cell Found, Leiden, pp 272-276.
19. Decker K (1989). Hepatic mediators of inflamation in cells of the hepatic sinusoids, in Cells of the Hepatic Sinusoid, Vol 2, (eds E Wisse, DL Knook and K Decker), Kupffer Cell Found, Leiden, pp 171-175.

Study (c)

1. Callis PT, Jahrling PB, DePaoli A (1982). Pathology of Lassa virus infection in the Rhesus monkey. Am J Trop Med Hyg 31:1038-1045.
2. Edington GM, White HA (1972). The pathology of Lassa fever. Trans R Soc Trop Med Hyg 66:381-389.
3. Jahrling PB, Hesse, RA, Rhoderick JB, Elwell MA, Moe JB (1981). Pathogenesis of a Pichinde virus strain adapted to produce lethal infections in guinea pigs. Infec Immun 32:872-880.
4. Katz MA, Schaeffer RC Jr (1991). Convection of macromolecules is the is the dominant mode of transport across horizontal 0.4 and 3 μm filters in diffusion chambers: Significance for biologic monolayer permeability assessment. Microvasc Res, In Press.

5. Peters CJ, Jahrling PB, Liu CT, Kenyon RH, McKee KT Jr, Barrera Oro JG (1987). Experimental studies of arenaviral hemorrhagic fevers. Curr Trop Microbiol Immunol 134:5-68.
6. Schaeffer RC Jr, Chilton S-M, Hadden TJ, Carlson RW (1984). Pulmonary fibrin microembolism with Echis carinatus venom in dogs: Effects of a synthetic thrombin inhibitor. J Appl Physicl 57:1824-1828.
7. Schaeffer RC Jr, Chilton S-M, Carlson RW (1985). Puff adder venom shock: a model of increased vascular permeability. J Pharmacol Exp Thera 2133:312-317.
8. Schaeffer RC Jr, Bitrick, MS Jr (1990). Effects of lethal Pichindé virus infection in strain 13 guinea pigs on organ permeability index. FASEB J 4:A287.
9. Walker DH, Johnson KM, Lange JV, Gardner JJ, Kiley MP, McCormick JB (1982). Experimental infection of Rhesus monkeys with Lassa virus and a closely related arenavirus, Mozambique virus. J Infec Dis 146:300-368.
10. White HA (1972). Lassa fever: a study of 23 hospital cases. Trans R Soc Trop Med Hyg 66:390-399.

Study (d)

1. Reily CA, Cohen G, Lieberman M (1974). Ethane evolution: A new index of lipid peroxidation. Science 183:208-210.
2. Habib MP, Eskelson CD, Katz MA (1988). Ethane production rates in rats exposed to high oxygen concentrations. Am Rev Resp Dis 137:341-44.
3. Habib MP, Katz MA (1989). Ethane production rates and minute ventilation. J Appl Physiol 66(3):1264-1267.
4. Habib MP, Katz MA (1989). Source of ethane in expirate of rats ventilated with 100% oxygen. J Appl Physiol 66(3):1268-1272.
5. Habib MP, Dickerson F, Mooradian AD (1990). Ethane production rate is reduced with dietary restriction. J Appl Physiol 68:2588-2590.
6. Babich H (1982). Butylated hydroxytoluene (BHT): A review. Environmental Research 29:1-29.
7. Wispe JR, Bell EJ, Roberts RJ (1985). Assessment of lipid peroxidation in newborn infants and rabbits by measurements of expired ethane and pentant: influence of parenteral lipid infusion. Pediatr Res 19:374-379.
8. Sedgwick J et al (1990). Superoxide generation by hypodense eosinophils from patients with asthma. Am Rev Respir Dis 142:120-123.

Figures Legends

Study (a)

Figure a-1. Baseline comparisons in weight, mean arterial pressure (MAP), hematocrit (Hct), and serum protein concentrations between groups, Groups IV (infected, hydropenic) and Group V (control, hydropenic). The infected GP group weighed significantly less than normals (476 ± 47 g as opposed to 643 ± 21 g, $2P < .001$). The weight loss of 20 ± 2.4 % over 12 days in the infected group with marked decrease in subcutaneous and organ fat in this group. No evidence of hemorrhage nor effusions were seen. MAP was 38 ± 5.7 mmHg; Hct was 52 ± 2.4, and serum protein was 4.6 ± .22 g/dl. These values were not different from the normal group.

Figure a-2. Differences between values for lymph variables in Groups IV and V. Although mean lymph flux, J_v, was decreased in the infected group (4.9 ± 1.5 µl/min/(100 g) vs 5.5 ± .4), the large variance of the infected group resulted in no significant difference between groups. The infected group had a larger lymph/plasma protein concentration ration, R, than the normal group (.70 ± .05 vs .55 ± .02, $2P < .01$). Thus, although mean protein clearance across jejunal capillaries, J_vR, was increased slightly in the infected group (3.1 ± .6 vs 2.9 ± .2), this increase was not statistically significant.

Figure a-3. Differences between Groups IV and V for the values of σ and PS by the crosspoint method. Note that the method is not always successful in locating such crosspoints. Only 23 of the 38 normal animals had solutions for values. σ was significantly lower in infected GP than in normals with mean values of .52 ± .03 and .73 ± .02 respectively ($2P < .001$). The mean values for PS were not greater for the infected group, but actually less than normal (2.5 ± .30 vs 3.2 ± .29). This small difference was not significant.

Figure a-4. Differences between Peclet number, which is the ratio of convective to diffusive coefficients for protein transport, and the percent of total transport which is attributable to permeative or diffusive processes between Groups IV and V. The Peclet numbers were not different between groups and were .97 ± .10 for the normals and 1.20 ± .19 for the infected GPs. However, there was a shift in fractional diffusive transport from 51 ± 2.7% in normals to 32 ± 3.5% in the infected group ($2P < .001$). This relative decline in diffusive transport, or relative increase in convective transport was due to the decrease in reflection coefficient in the infected group.

Study (b-e)

Figure (b-e)1. In vivo photomicrograph of hepatic sinusoid (S) with blood flow obstructed by leukocyte (L) adherent to the endothelium. Other leukocytes (L) are adherent to endothelium of central venule (CV) 14 days post injection (400x).

Figure (b-e)2. In vivo photomicrograph of central venule (CV) having leukocytes (L) adherent to the endothelium 14 days post injection (400x).

Figure (b-e)3. SEM of leukocytes (L) adhering to endothelium of central venule 16 days post injection (500x).

Figure (b-e)4. In vivo fluorescence photomicrograph of 170 kD FITC-dextran in a mesenteric 35 μm arteriole (A) and 40 μm venule (V) 16 days post injection. Note there is no leakage of the fluorescent material.

Figure (b-e)5. In vivo photomicrograph of: A. Capillaries (C) in intestinal villi contained good flow 14 days post injection. B. The capillaries did not leak 170 kD FITC-dextran.

Figure (b-e)6. TEM of Kupffer cell (KC) containing tissue debris and material suggestive of viral ribonucleocapsid (arrows). Note the reduced number of filopodia suggestive of reduced phagocytic capability (13,300x).

Figure (b-e)7. TEM of macrophages (M) containing material suggestive of viral ribonucleocapsid (↖) that have infiltrated between hepatic parenchymal cells (H) which contain large lipid droplets (L) (13,300x).

Figure (b-e)8. SEMs of endothelial fenestrae in: A. non-infected guinea pig and B. 14 days post injection. Note reduction in number and increase in size of the fenestrae in the injected animal (20,000x).

Figure (b-e)9. TEM of thickened sinusoidal endothelium (E) having few fenestra (↖) 14 days post injection. Note lack of microvilli projecting from hepatocytes (H) into the space of Disse. L; lipid (13,300x).

Figure (b-e)10. TEM of enlarged bile canaliculus (BC) 14 days post injection. Note reduction in the size and number of microvilli projecting from hepatocytes (H) into the bile canaliculus and the space of Disse (SD). Also note lack of fenestrae through the thickened sinusoidal endothelium (E) (13,300x).

Figure (b-e)11. Macrophages in the top of an intestinal villus containing phagolysomes (P) and material suggestive of viral ribonucleocapsids (↖) 14 days post injection (9,880x).

Figure (b-e)12. TEM of capillary in intestinal villus 16 days post injection. The endothelium (E) is intact and contains closed fenestrae (↖) (16,380x).

Figure (b-e)13. Intestinal epithelium 14 days post injection. Note the intercellular junction (↖) is intact (13,300x).

Study (c)

Figure c-1. The per cent change in body weight of small (initial body weight (IBW, <400 g, n=18) with large (IBW, >700 g, n=8) Strain 13 guinea pigs over time following injection of 104 PFU, i.p., is shown (n=26). Error bars are ± in SEM.

Figure c-2. The organ radioactivity index of the lungs from P. virus small and large GP13 as well as uninfected control GP13 is shown. The increase in lung and

heart ORI of the small GP13 are significantly ($p<.05$) above those of the control or large animals.

Figure c-3. The organ radioactivity index of the heart from small, large and control animals is shown. The increase in lung and heart ori of the small GP13 are significantly ($p<.05$) above those of the control or large animals.

Figure c-4. Blood serum glutamic oxaloacetic transferase (SGOT), and lactate dehydrogenase units (LDH) from the control, day 13 and day >18 groups. The elevation in blood SGOT and LDH activities was assessed in 6 animals from each group. * statistically significant from the control group.

Figure c-5. Organ radioiodinated 125 human serum albumin activity index (RIHSA index) in the heart and lung of control ($n=6$) and virus infected animals at day 13 ($n=3$) and day >18 ($n=7$) groups. Although no elevation in RIHSA index was noted at day 13, a significant increase in RIHSA index was noted for the heart and the lung in the day >18 group. * statistically significant from the control group.

Figure c-6. Time course of the increase in extravascular lung water to bloodless dry lung weight ratio (EVLW/BDLW) in the control ($n=4$) and virus infected animals at day 13 ($n=6$) and day > 18 ($n=3$). A: A significant elevation in EVLW/BDLW is present by day 13 and day 18. B: Although there was a significant increase in EVLW by day 13, the increase in residual lung blood (RLB) was only seen in the day >18 group. * statistically significant from the control group.

Figure c-7. Light micrographs of paraffin (5 μ) lung sections from Pichindé virus-infected GP13 series at day 13 GP (A, B and C), day 17 (D) and uninfected control (E) series treated with the indirect immunoperoxidase technique for the presence of virus antigen. A, B and C panels that show marked immunostaining in the visceral pleural epithelium, bronchiolar epithelium and mononuclear cells, respectively (↖). In panel B, most of the mononuclear cells show punctate deposits of virus antigen. An aggregate of immunostained cells appears to block a 20 μ branch of a large pulmonary blood vessel (↖). In panel C, the focal appearance of virus-infected bronchiolar epithelial cells (↖) of an airway (A) is contrasted with non-stained adjacent cells (☆). Panel D shows marked staining of a large alveolar cell (↖) as well as punctate deposits throughout the pulmonary microcirculation. Panel E shows an unobstructed 20 μm blood vessel (b), alveolus (a) and the pulmonary microcirculation without immunostaining in a control lung. Panel F is a thin (1 μm) plastic section of a day 19 infected GP13 lung alveolus (a) stained with toluidine blue. This panel shows a dilated pulmonary throughfare channel (c) with red blood cells. All other capillaries that surround this alveolus appear filled with aggregates of mononuclear cells (↖). At least three macrophages (↖) are seen in the alveolar space (a).

Figure c-8. Transmission electron micrographs of uninfected GP13 lung. The clear alveoli (a) showed type II pneumocytes (*) in the alveolar corners. The alveolar capillaries (c) show many red blood cells (r) with no leukocytes.

Figure c-9. Transmission electron micrographs of a lung at 19 days after Pichindé virus-infection in GP13. Alveolar macrophages (M) are seen with different degrees of vacuolation. The alveolus (A) is free of edema fluid, red

cells or fibrin. A small blood vessel (☆) shows a monocyte (m) and large lymphocytes (l) and plasma cell (P) bound to the endothelium that appear to impede the movement of red blood cells. Pseudopods that extend from the endothelial cell, as well as the monocytes and lymphocytes appear to interdigitate. Most of the pulmonary capillaries (c) appear blocked with monocyte-lymphocyte cell plugs. One capillary (↖) is occluded by a granulocyte (g)-lymphocytes aggregate. No degranulation of the polymorphonuclear leukocyte is seen. The cytoplasm of these cells contain massive numbers of ribosomes. A type II pneumocytes is seen in an alveolar corner (*).

Figure c-10. The effects of P. virus (10^6, 10^5, 10^4 PFU and no virus, control) on tritiated thymidine uptake in GPAEC is shown.

Figure c-11. The effects of P. virus (10^5, 10^4 PFU and no virus, control) on S-35 methionine uptake in GPAEC is shown.

Figure c-12. Transmission electron micrograph of P. virus (10^5 PFU for 18 hours) infected GPAEC. The arrow (↖) indicates dense particles throughout the nucleus and cytoplasm. Many polyribosomes are also seen.

Figure c-13. Transmission electron micrograph of P. virus (10^5 PFU for 18 hours) infected GPAEC. The asterisk (*) indicates vaculoes with secretory material and small ribosome-like particles.

Figure c-14. The effects of bradykinin (10^{-6}M) on the alteration in the 340/380 ratio of Fura-2 over time in GPAEC with and without P. virus infection for three days.

Figure c-15. The effects of bradykinin (10^{-6}M) on the alteration in the calculated intracellular calcium over time in GPAEC with and without P. virus infection for three days.

Figure c-16. The effects of P. virus (10^6, 10^5 PFU and no virus) on GPAEC permeability vs solute molecular radius in comparison with a bovine pulmonary artery endothelial cell monolayer given no virus. The means ± S.E. are shown.

Figure c-17. The effects of P. virus (10^6, 10^5 PFU and no virus) on GPAEC permeability/free diffusion coefficient (Do) in comparison with a bovine pulmonary artery endothelial cell monolayer given no virus. The mean ± S.E. are shown.

Study (d)

Figure d-1. Weight change in 6 GP strain 13 before (day 0) and at various time points after inoculation with Pichinde virus.

Figure d-2. Average (± SEM) ethane production rates in 6 GP strain 13 before (day 0) and at various time points after inoculation with Pichinde virus.

Figure d-3. Individual ethane production rates in six strain 13 guinea pigs before (day 0) and at various time points after inoculation with Pichinde virus.

Figure d-4. Ethane production rates in three GP strain 13 before (days -2 and 0) and at various time points after inoculation with Pichindé virus. These animals were pretreated with butylated hydroxytoluene daily for three days prior to inoculation with virus.

Figure d-5. Weight of the three BHT treated animals (whose ethane production rates are shown in Figure d-4) before and after inoculation with virus. One animal died prior to being studied on day 12.

Figure d-6. Mean (± SEM) weight change before and after inoculation in three strain GP before and after inoculation with virus. The open triangles represent those three animals receiving vitamin C in their water for seven days prior to inoculation and the open circles those three animals receiving vitamin C only after inoculation. Note that different six animals were used for the studies.

Figure d-7. Ethane production rates for the guinea pigs receiving vitamin C whose weight changes are shown in Figure d-6. The three animals represented by the open triangles (Vitamin C at infection) were slightly lower than the other two groups but overall, there was no difference.

Figure d-8. Mean (± SEM) weight changes in infected (open circles) and diet restricted (open triangles) strain 13 guinea pigs. The diet restricted animals were not inoculated. The filled circles and triangles represent the expected weight gain otherwise normal animals would have shown for the infected and diet restricted groups respectively. Note that final actual weights are quite similar in the two groups.

Figure d-9. Mean (± SEM) ethane production rates for the infected and diet restricted animals before (day 0) and two weeks after either inoculation or the start of the diet restriction period respectively.

Figure d-10. The absolute differences (± SEM) in ethane production rates in the infected and diet restricted animals. Diet restriction resulted in the reduction in ethane elaboration whereas the infection increased ethane production.

Figure d-11. Total cell counts per mm^3 (± sd) in bronchoalveolar lavage fluid from guinea pigs before and at 7 and 12 days after inoculation with Pichinde virus. Cell counts were markedly elevated at day 7.

Figure d-12. Differential cell counts (± sd) in BAL fluid from guinea pigs at day 7 and 12 after inoculation. Macrophages are reduced at both time points from expected levels (95%) and whereas neutrophils predominate early (day 7) lymphocytes predominate by day 12.

Figure d-13. Effect of Pichindé virus infection on unstimulated (baseline) and PMA stimulated superoxide anion production from alveolar macrophages. Values are in relative optical density units ± sd.

Figure d-14. Ethane production rates (± SEM) in animals inoculated at baseline and followed at 7 and 12 days. The ordinate represents the total cumulated ethane production from the animals studied. The slopes of these lines is the

ethane production rate in pm/min/100 gm. Note the increased ethane elaborated at day 12 after infection with virus.

Figure d-15. The bars represent the mean slopes (± SEM) of the lines in Figure d-14. Baseline means all animals are included (total 18 animals). Baseline day 7 represents the 4 animals sacrificed at day 7 so that a direct comparison can be made in this group. Day 12 baseline represents the nine animals sacrificed at day 12 so that a direct before and after comparison can be made in this group. (* signifies statistical significance at the $P<.05$ level for the day 12 animals compared to 12 day baseline group.)

Figure (a) - 1

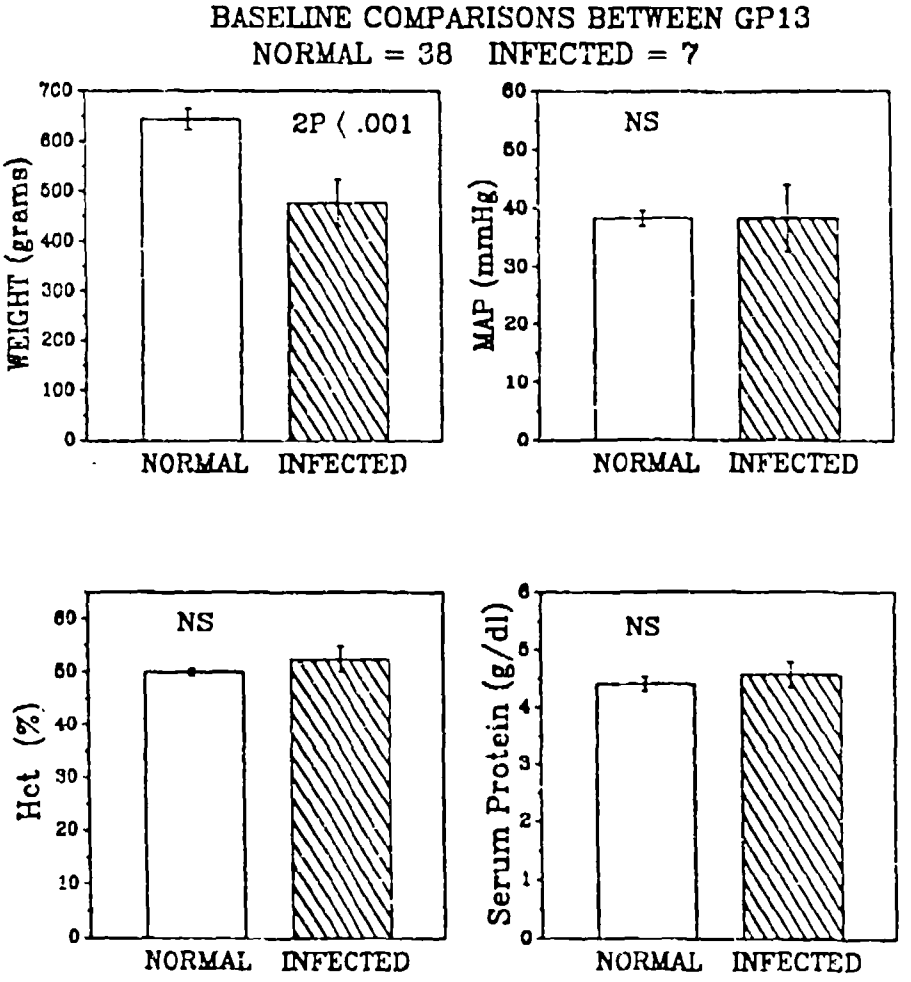
BASELINE COMPARISONS BETWEEN GP13
NORMAL = 38 INFECTED = 7
WEIGHT (grams)
2P < .001
NORMAL
INFECTED
MAP (mmHg)
NS
NORMAL
INFECTED
Hct (%)
NS
NORMAL
INFECTED
Serum Protein (g/dl)
NS
NORMAL
INFECTED

Figure (a) - 2

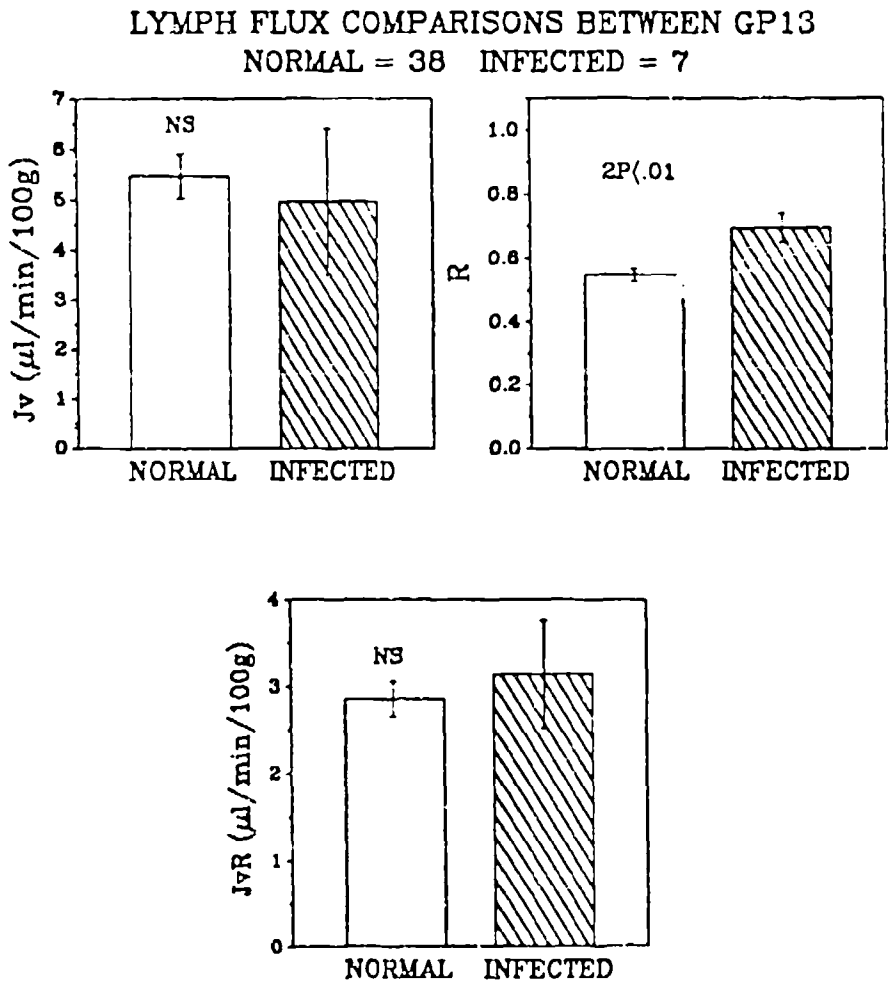
LYMPH FLUX COMPARISONS BETWEEN GP13
NORMAL = 38 INFECTED = 7
Jv (µl/min/100g)
NS
NORMAL
INFECTED
R
2P(.01
NORMAL
INFECTED
JvR (µl/min/100g)
NS
NORMAL
INFECTED

Figure (a) - 3

TRANSPORT DESCRIPTOR COMPARISONS BETWEEN GP13

NORMAL = 23 INFECTED = 7

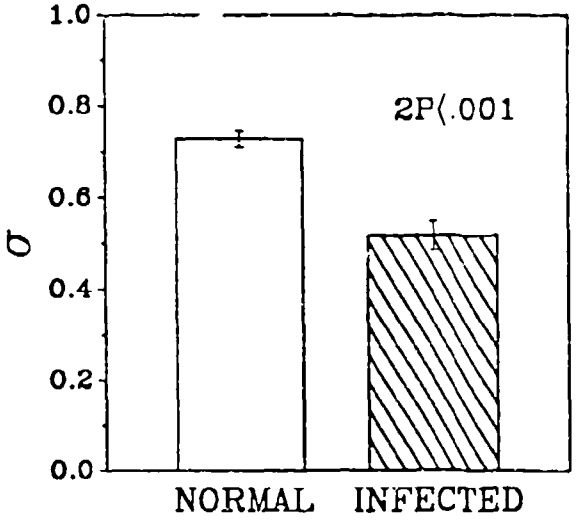

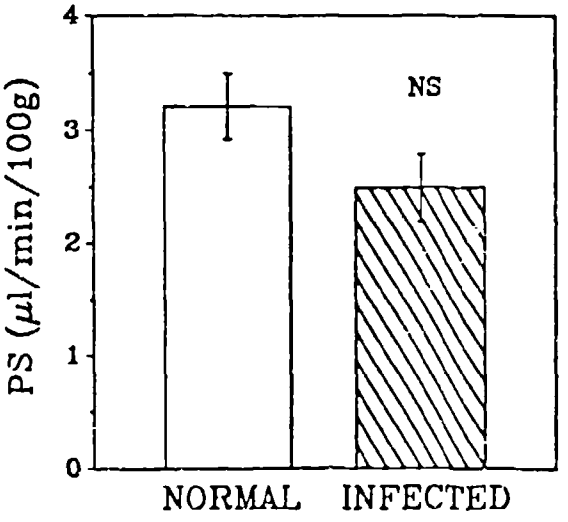

Figure (a) - 4

TRANSPORT DERIVED VALUES COMPARISONS BETWEEN GP13

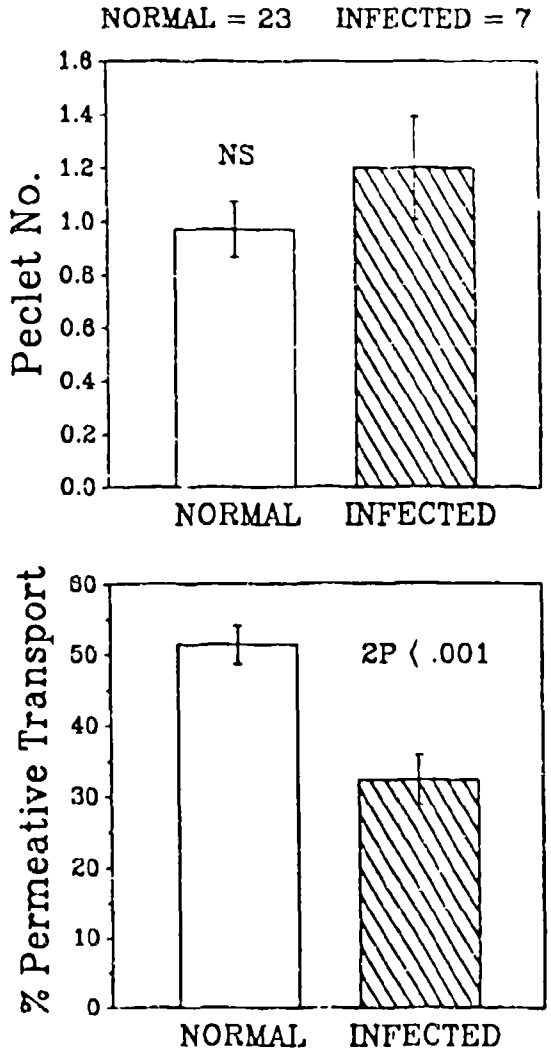

Figure (b - e) - 1

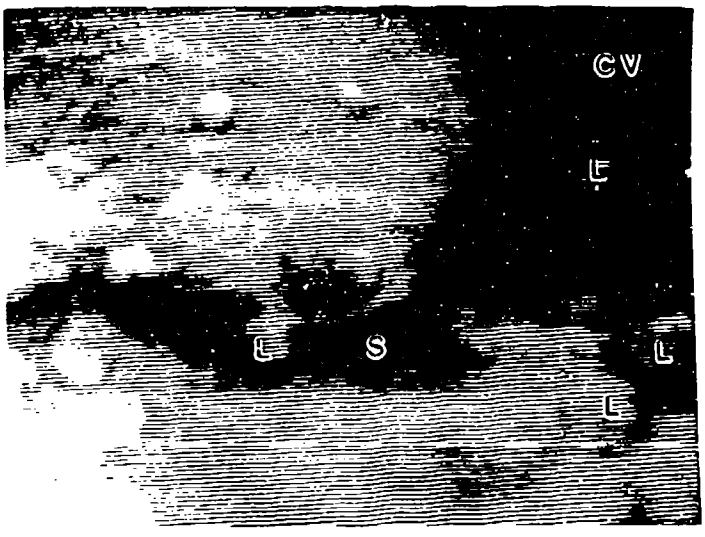

Figure (b - e) - 2

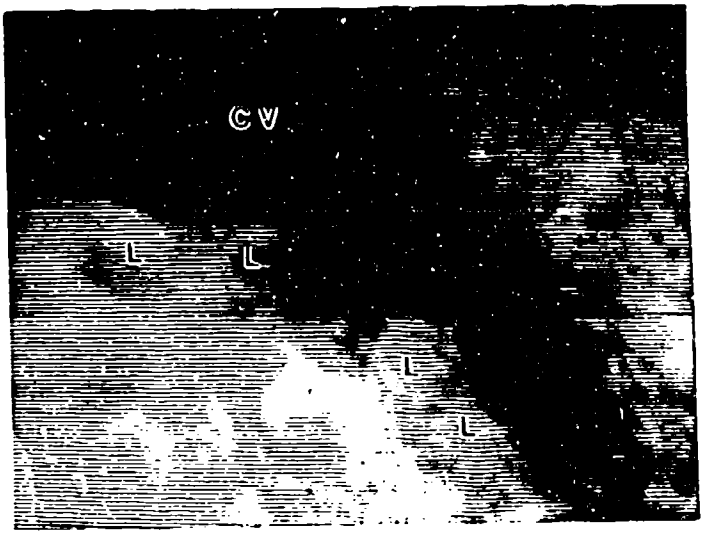

Figure (b - e) - 3

Figure (b - e) - 4

Figure (b - e) 5A and 5B

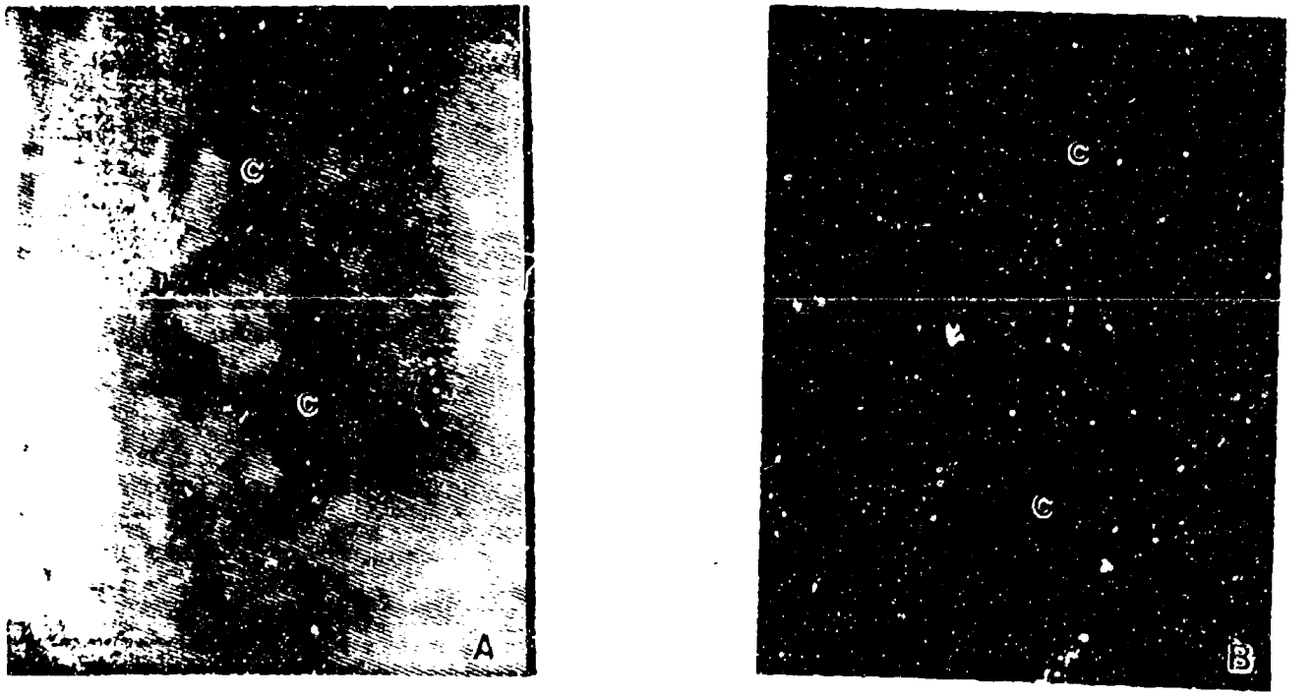

Figure (b - e) - 6

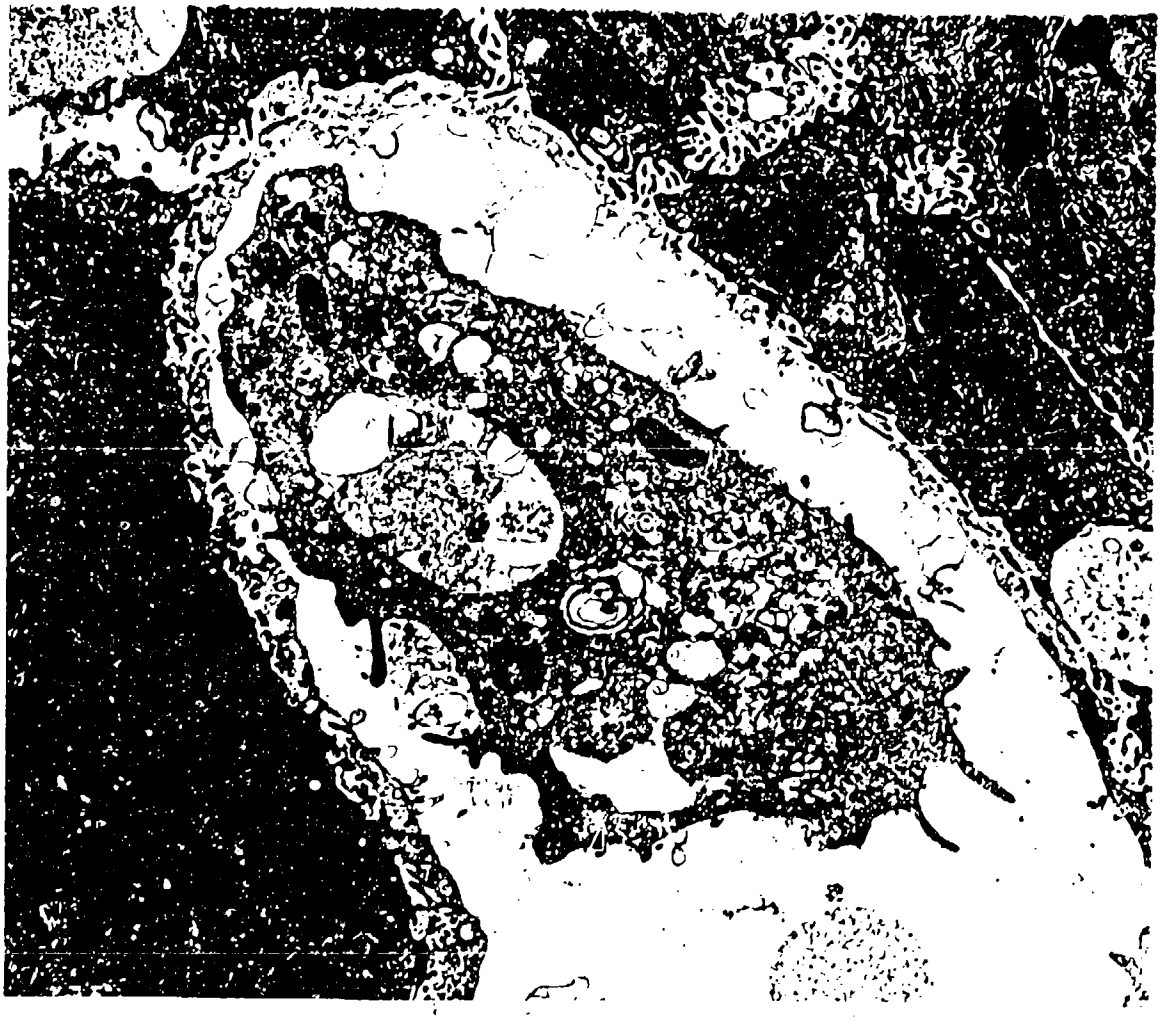

Figure (b - e) - 7

Figure (b - e) - 8A

Figure (b - e) - 8B

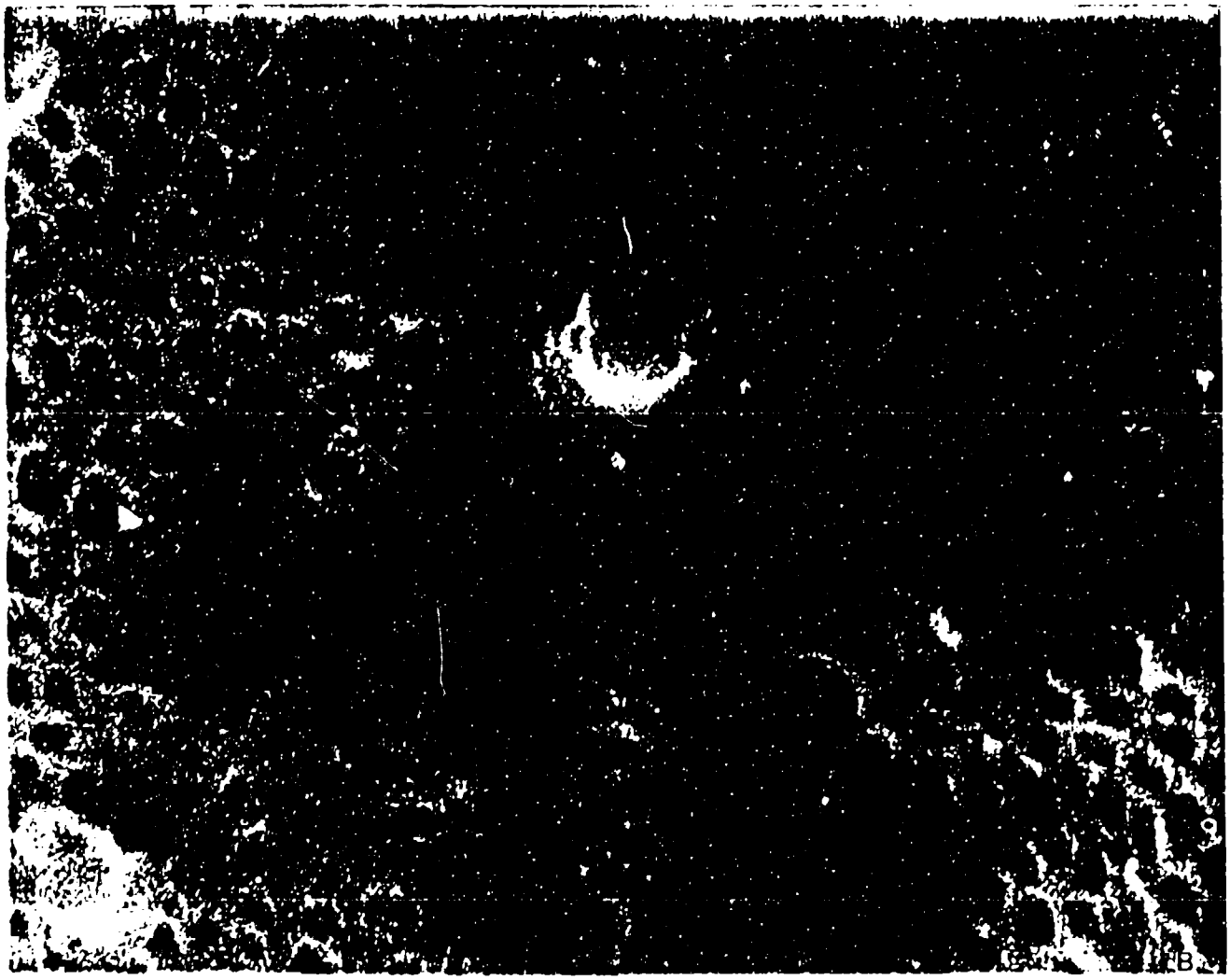

Figure (b - e) - 9

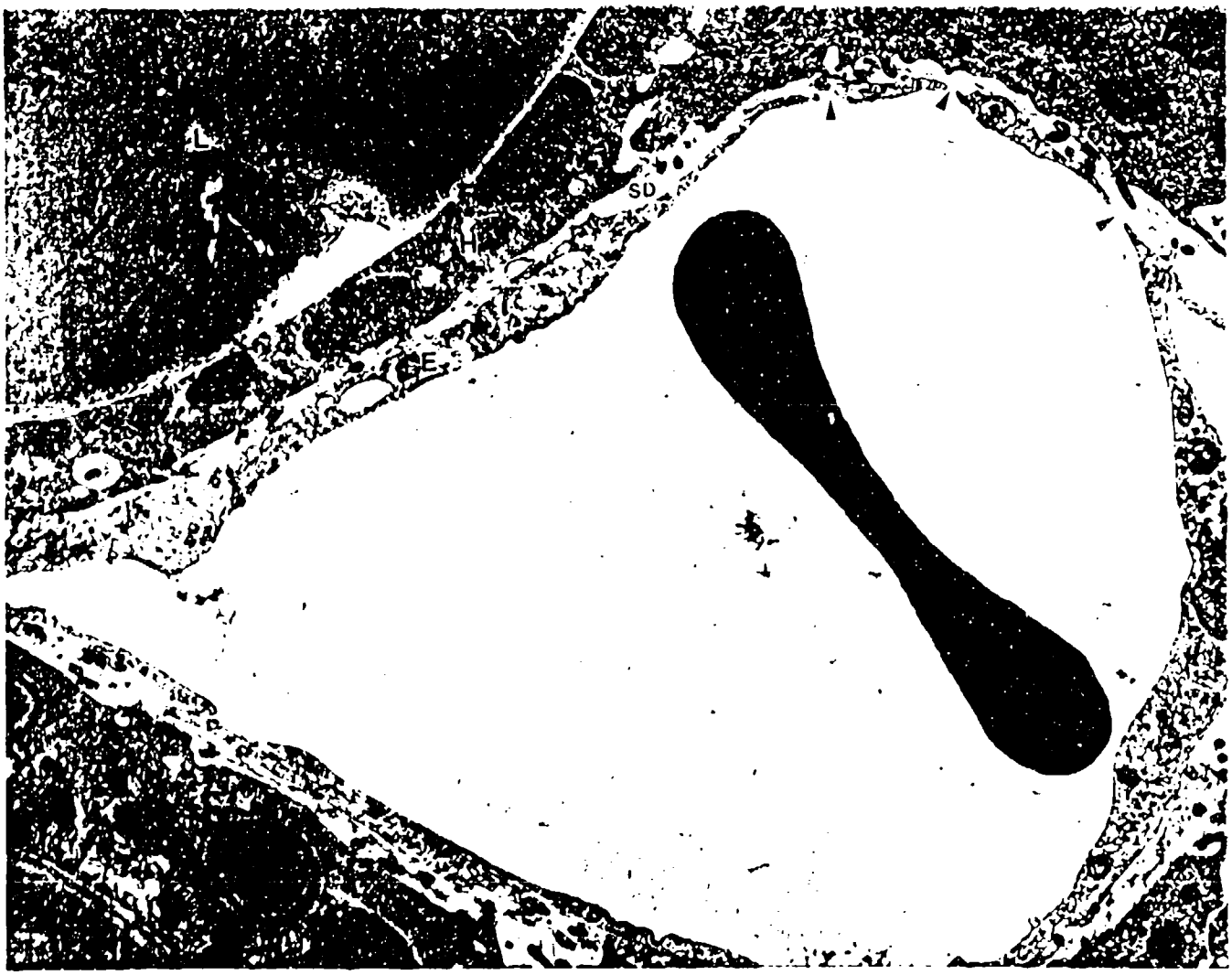

Figure (b - e) - 10

Figure (b - e) - 11

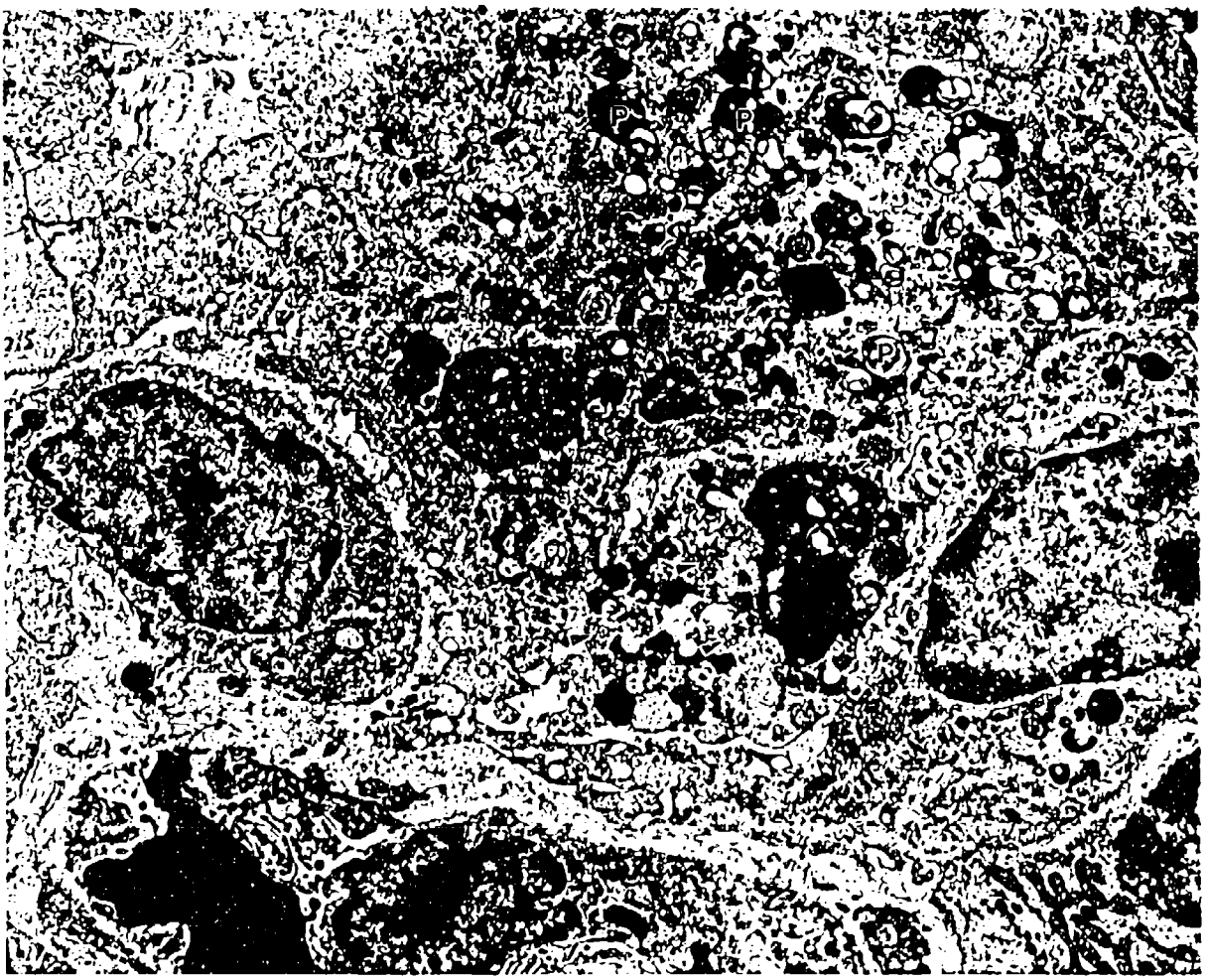

Figure (b - e) - 12

Figure (b - e) - 13

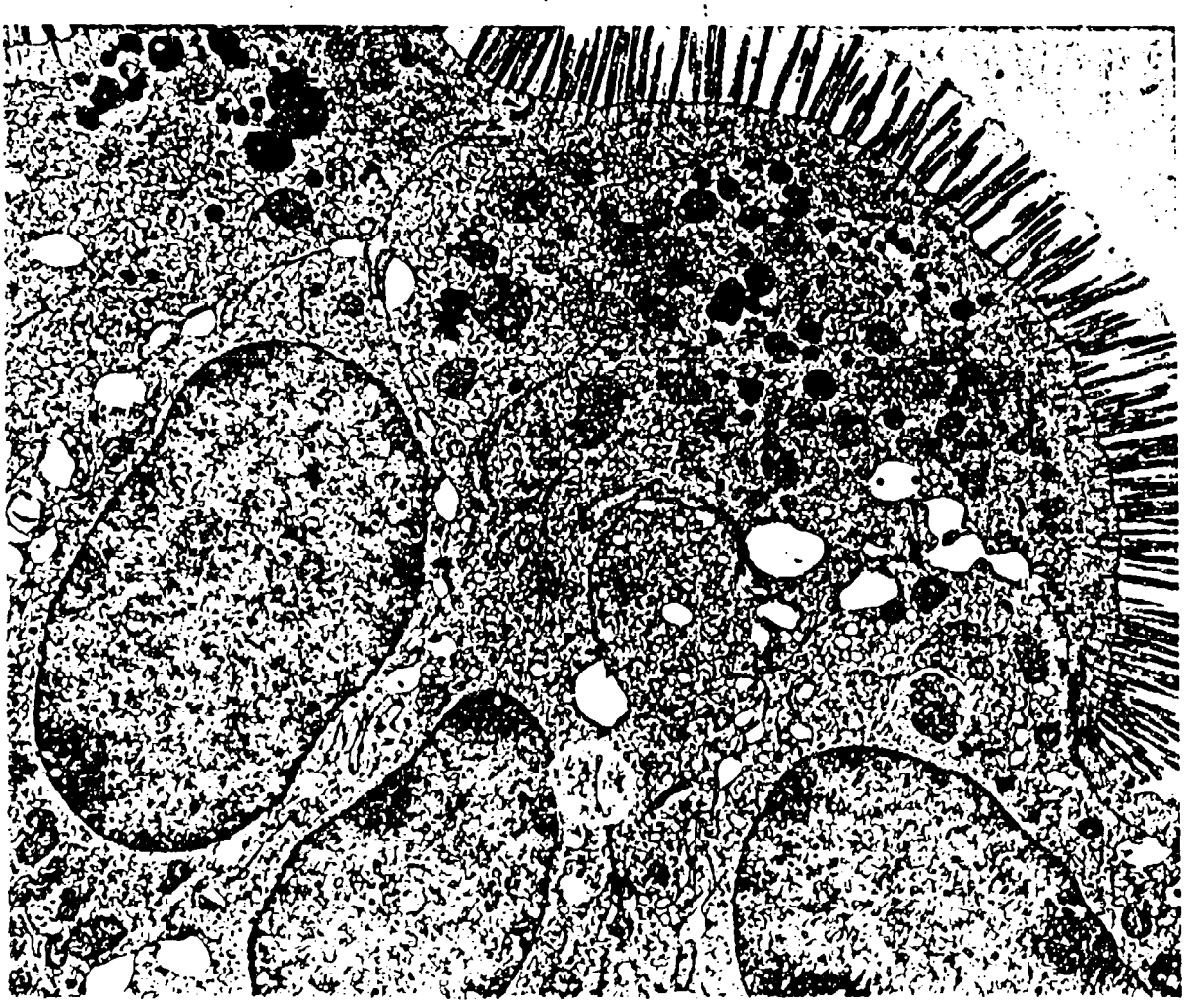

Figure (c) - 1

Change in Initial Body Weight after P. virus infection in Large and Small GP13

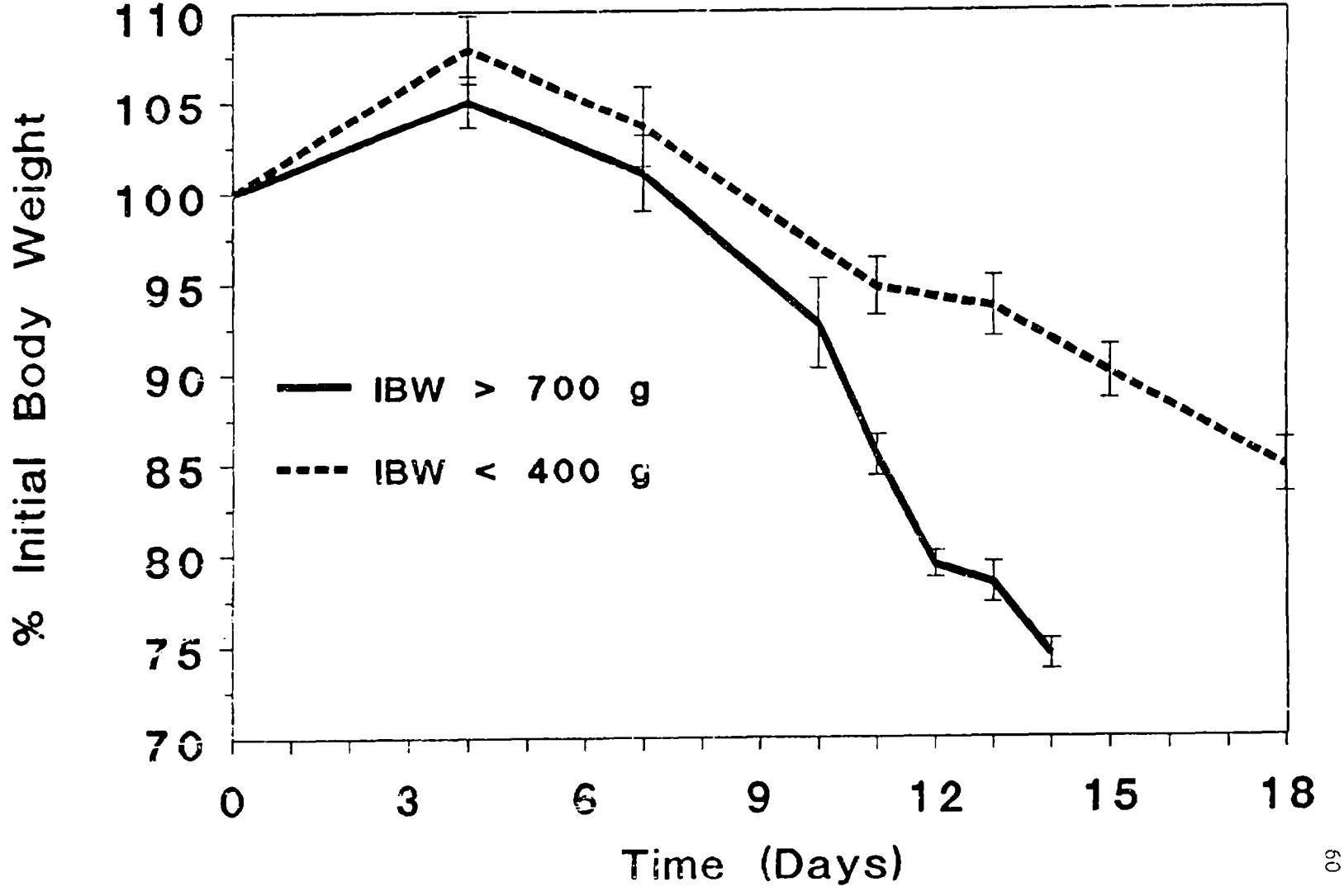

Figure (c) - 2

Organ Radioactivity Index of Large vs. Small Animals as compared to Control

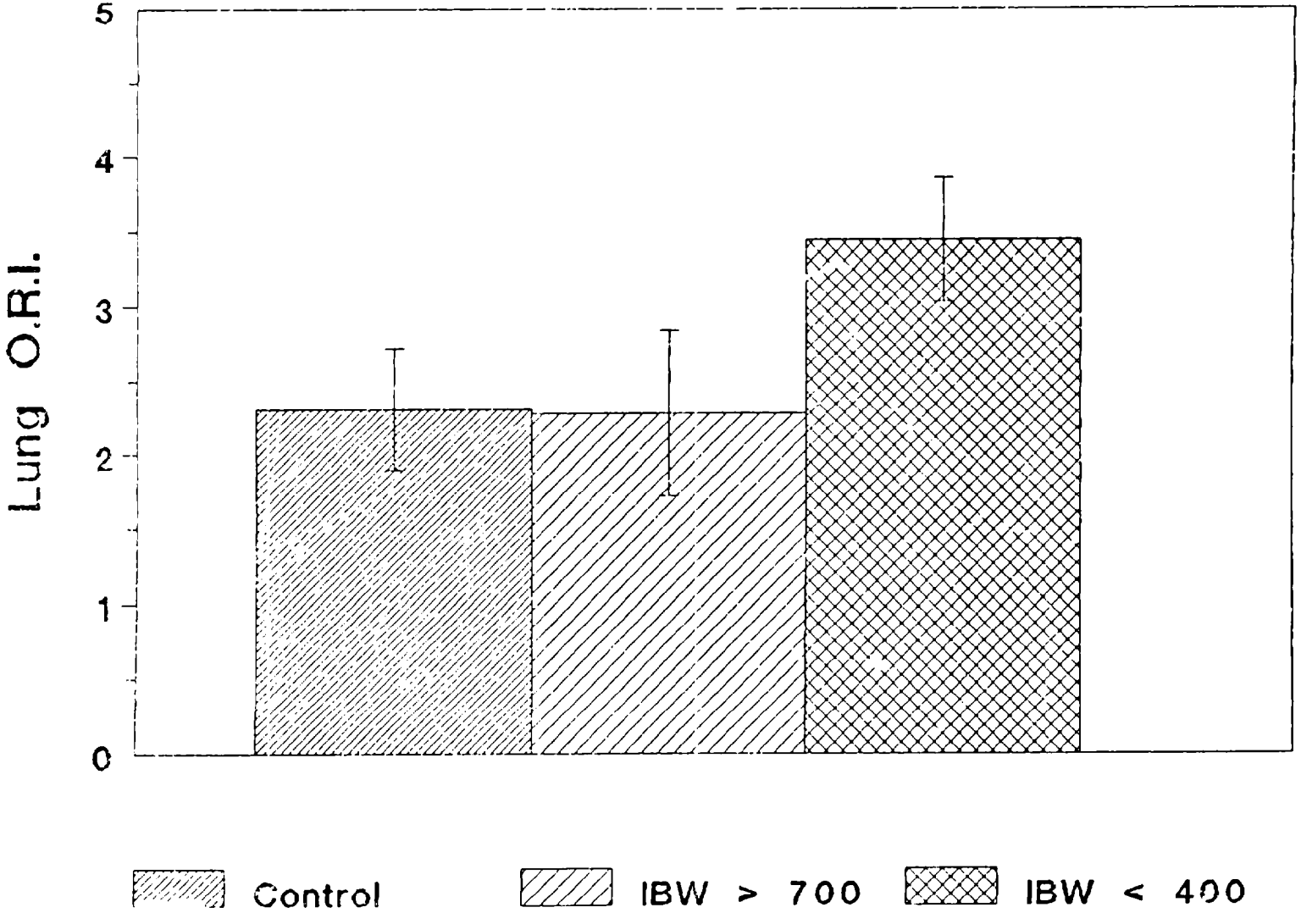

Organ Radioactivity Index of Large vs. Small Animals as compared to Control

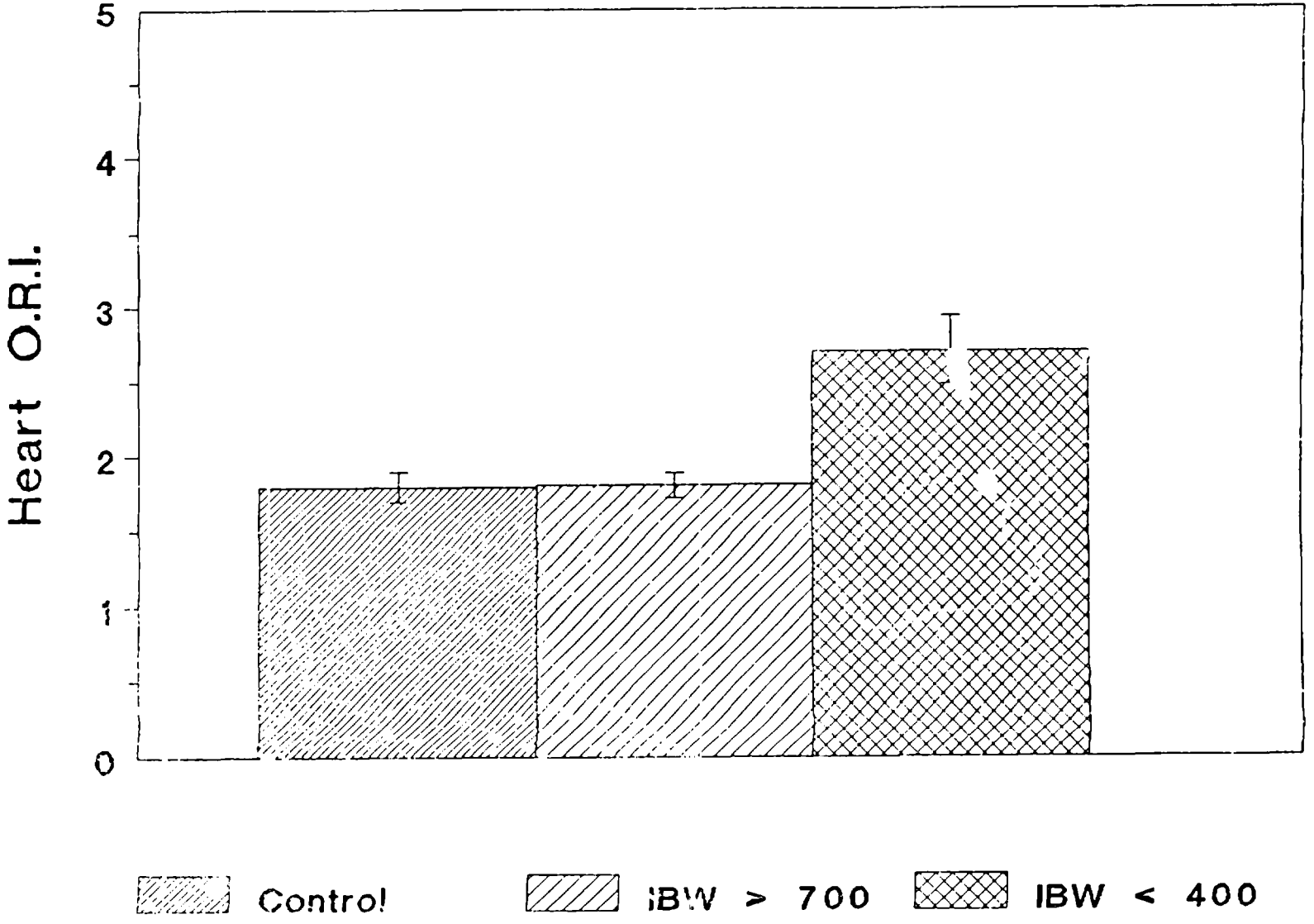

Figure (c) - 4

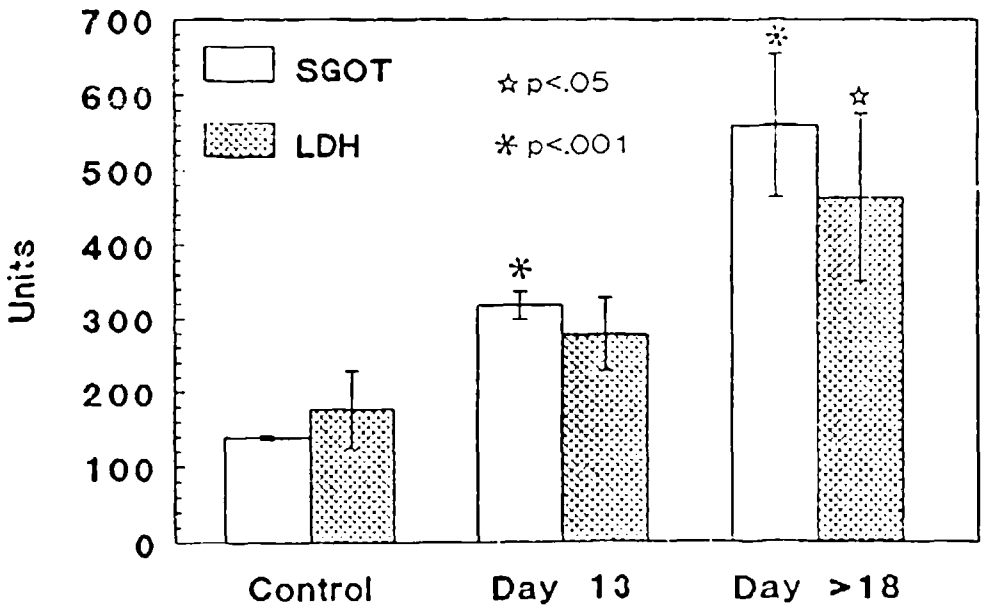
700
600
500
400
300
200
100
0
Units
SGOT
LDH
☆ p<.05
* p<.001
Control
Day 13
Day >18

Figure (c) - 5

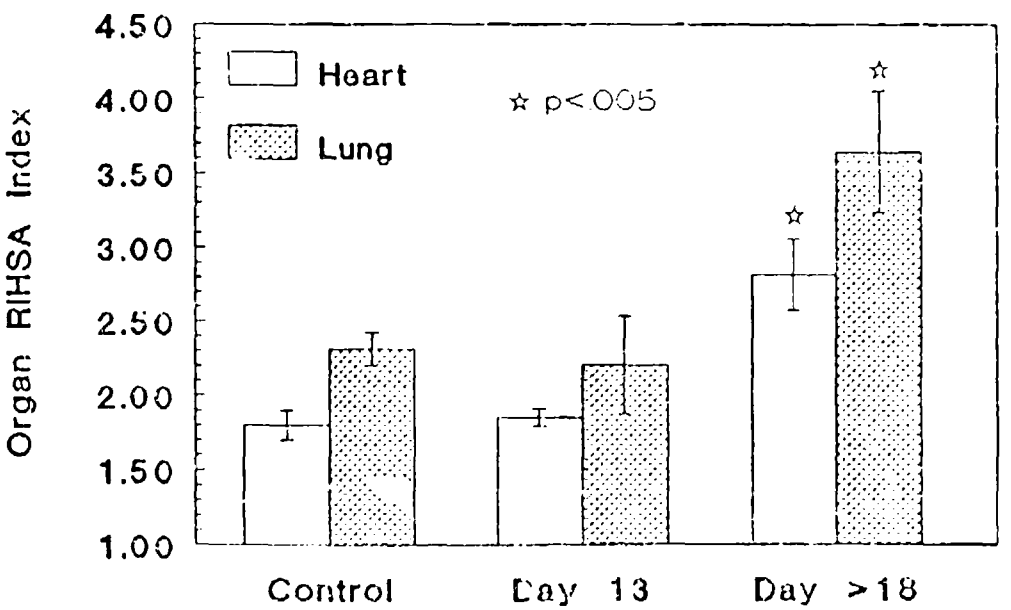
Organ RIHSA Index
4.50
4.00
3.50
3.00
2.50
2.00
1.50
1.00
Heart
Lung
☆ p<.005
☆
☆
Control
Day 13
Day >18

Figure (c) - 6

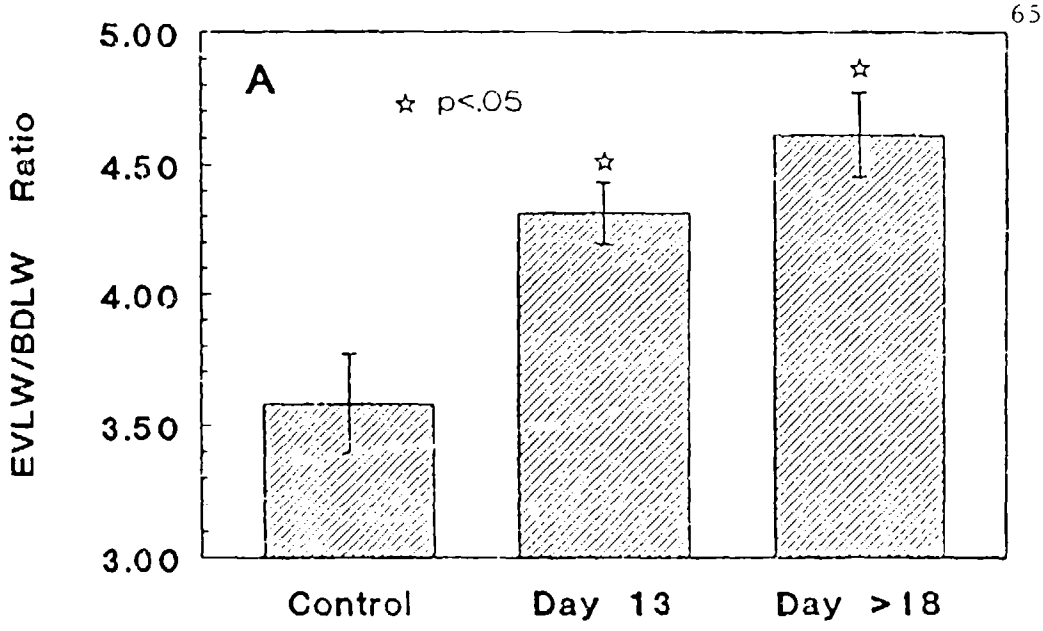
A
☆ p<.05
EVLW/BDLW Ratio
5.00
4.50
4.00
3.50
3.00
Control
Day 13
Day >18

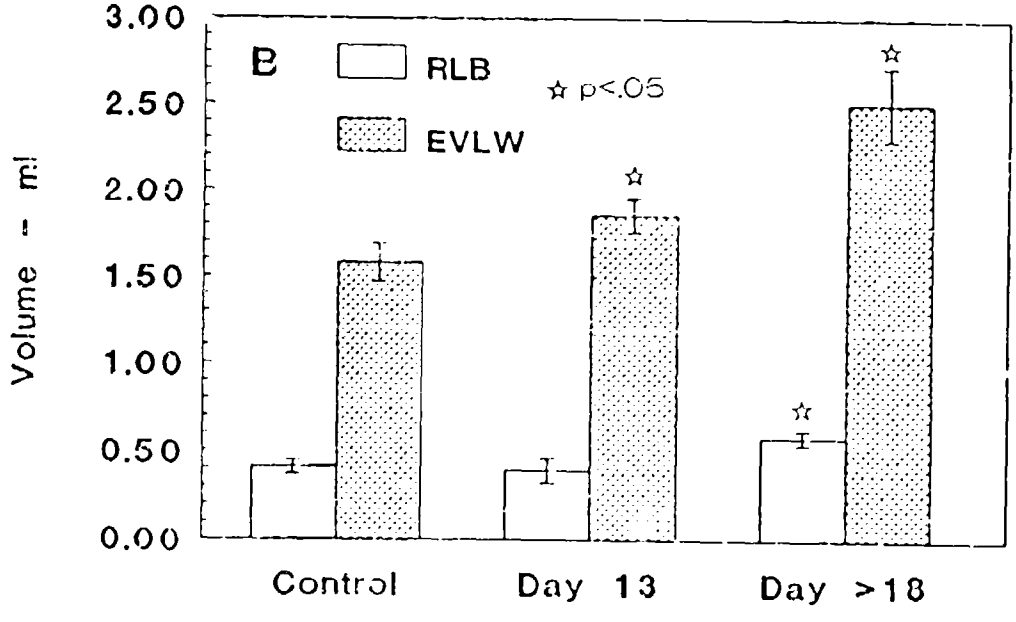
B
RLB
EVLW
☆ p<.05
Volume - ml
3.00
2.50
2.00
1.50
1.00
0.50
0.00
Control
Day 13
Day >18

Figure (c) - 7

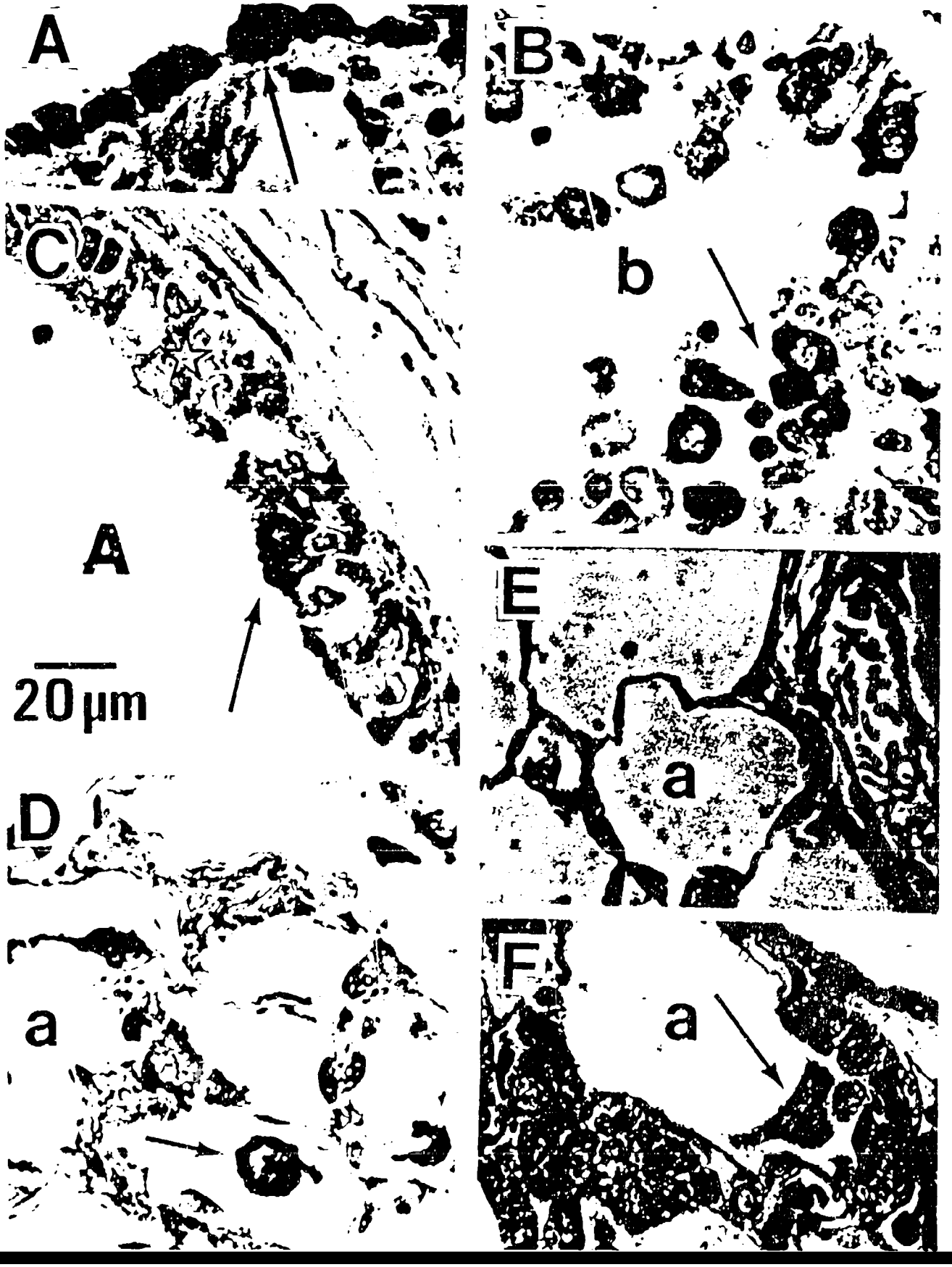

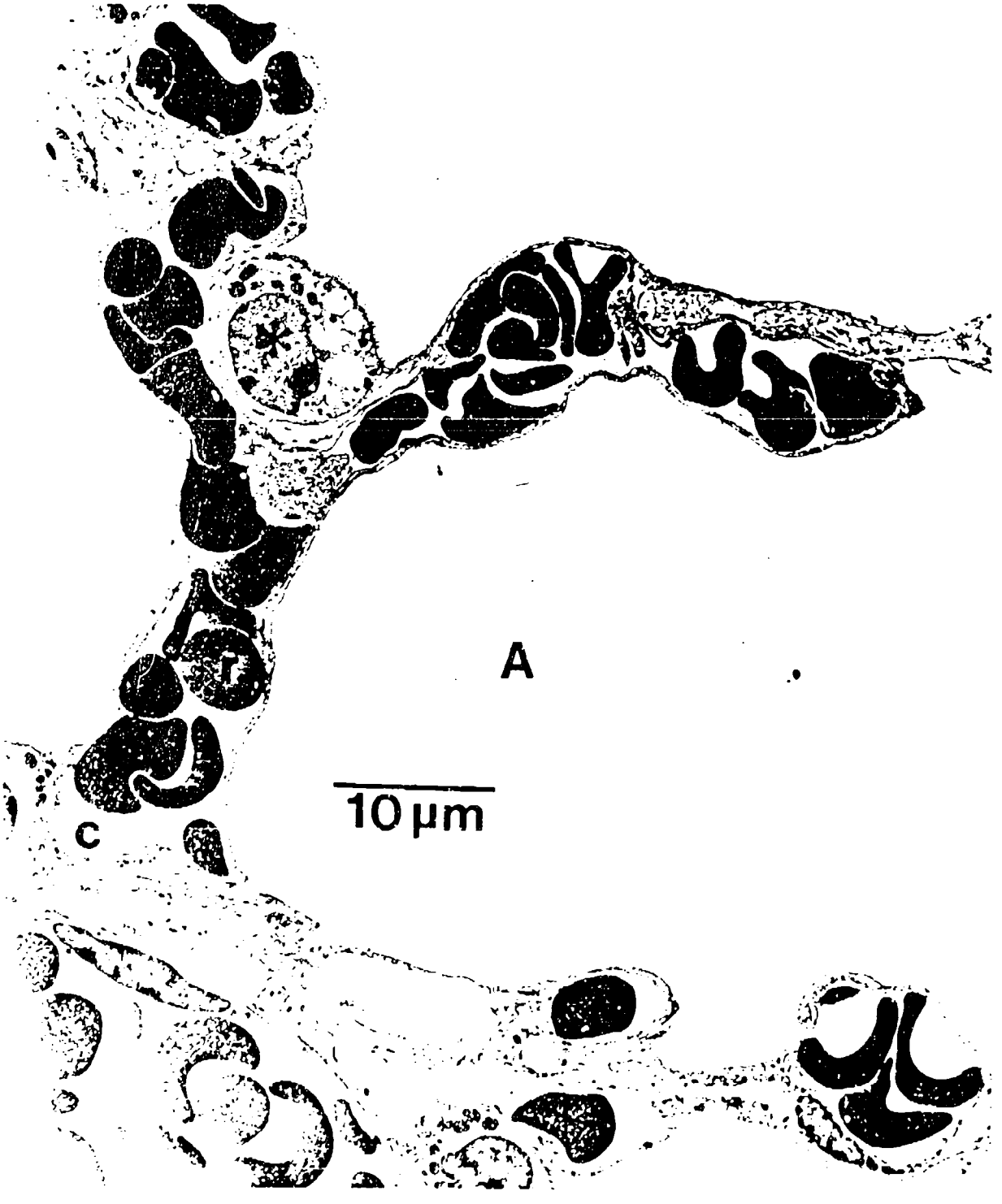
A
10 µm
C

Figure (c) - 9

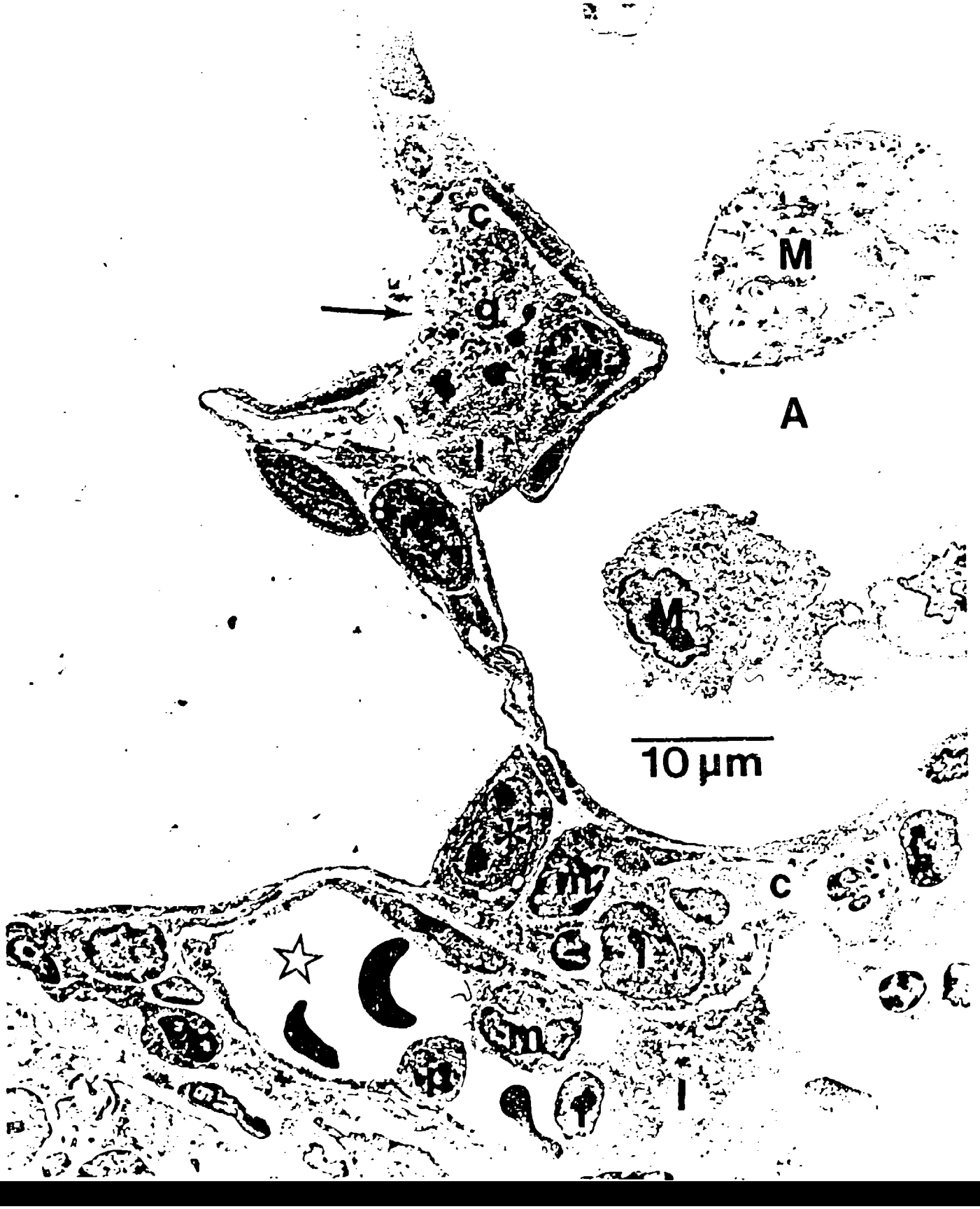

H^3Thymidine Uptake

GP Endothelial Cells

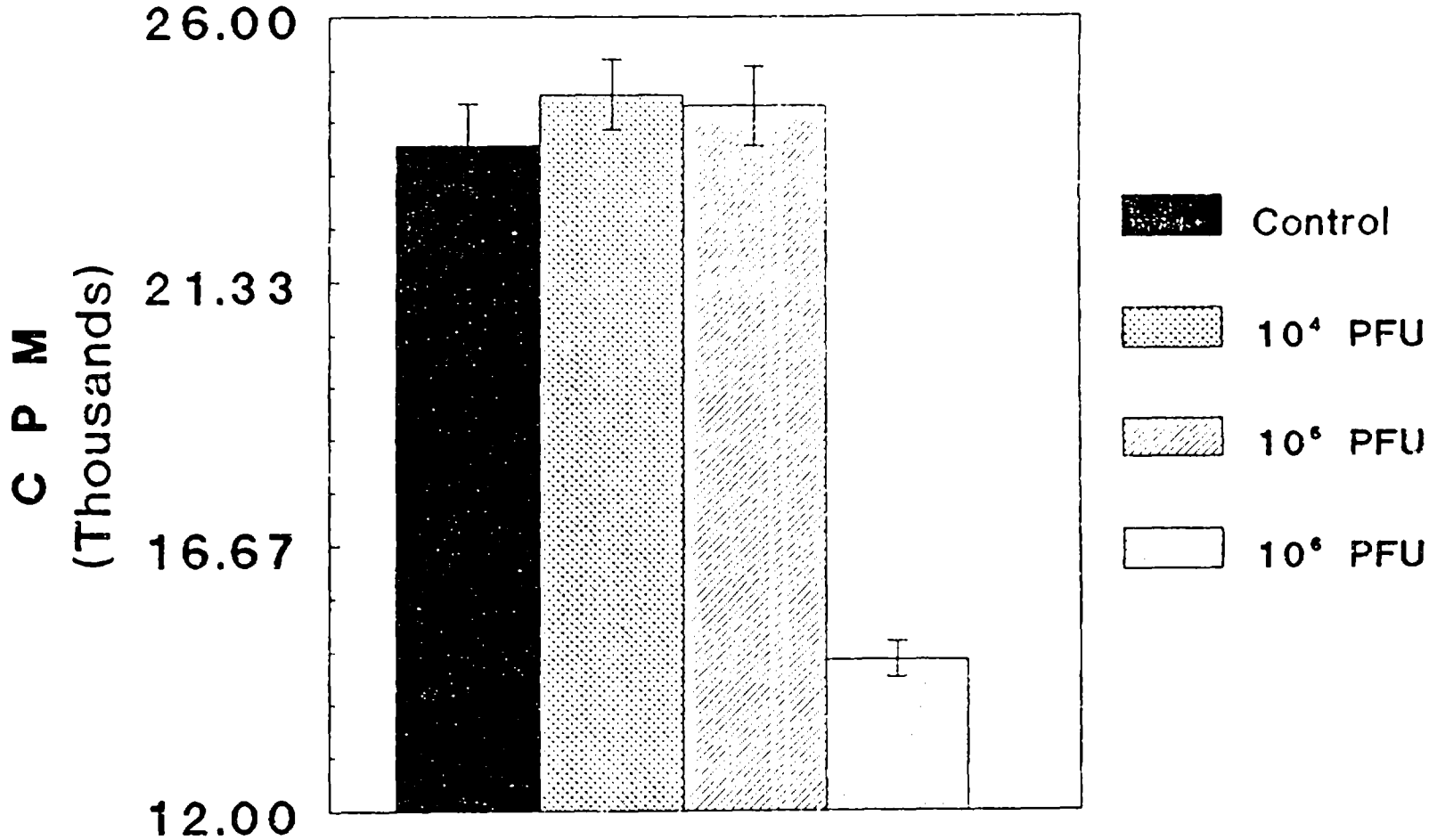

Figure (c) - 10

Figure (c) - 11

S-35 Methionine Incorporation in GP13 Aortic Endothelial Cells

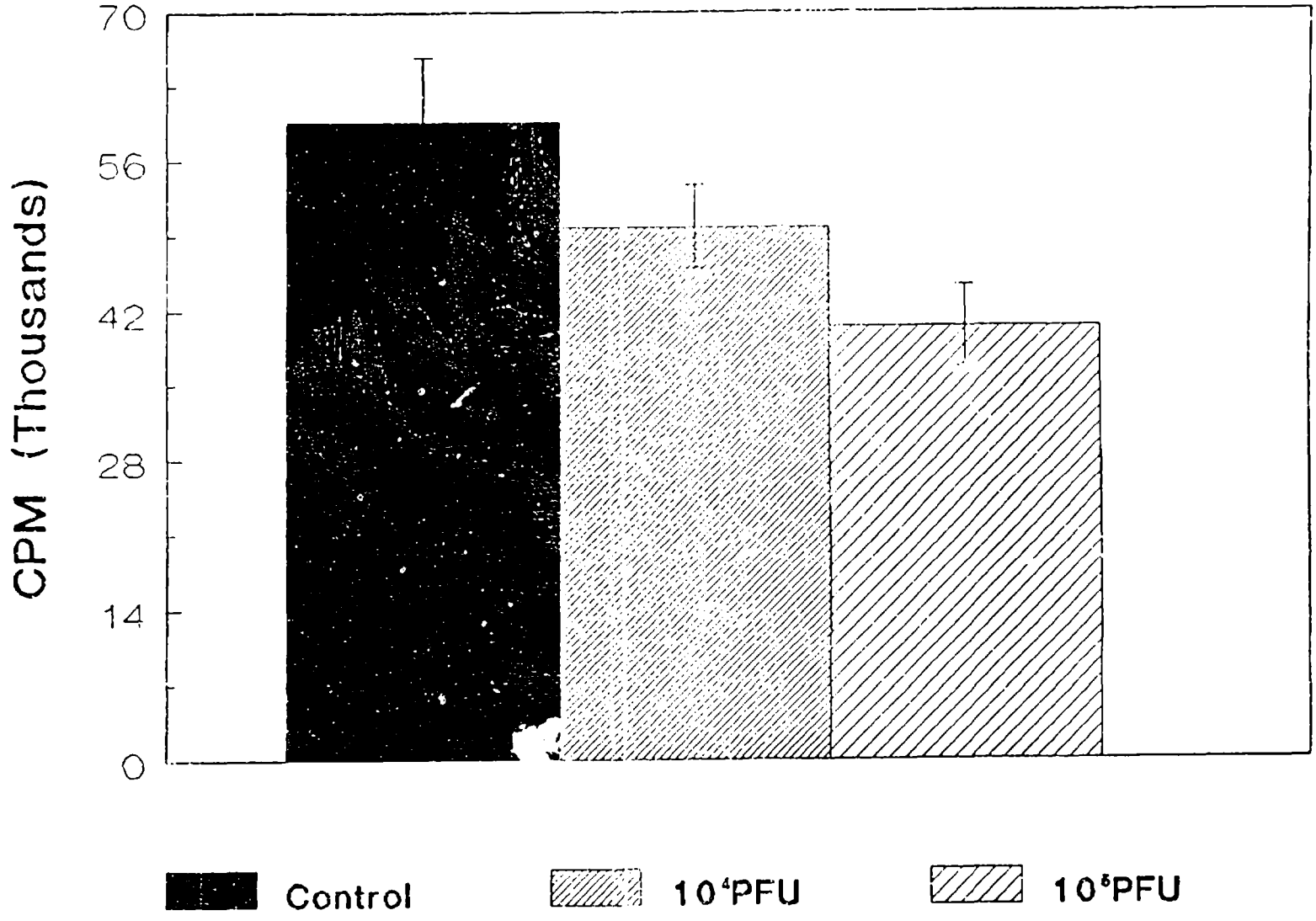

Figure (c) - 12

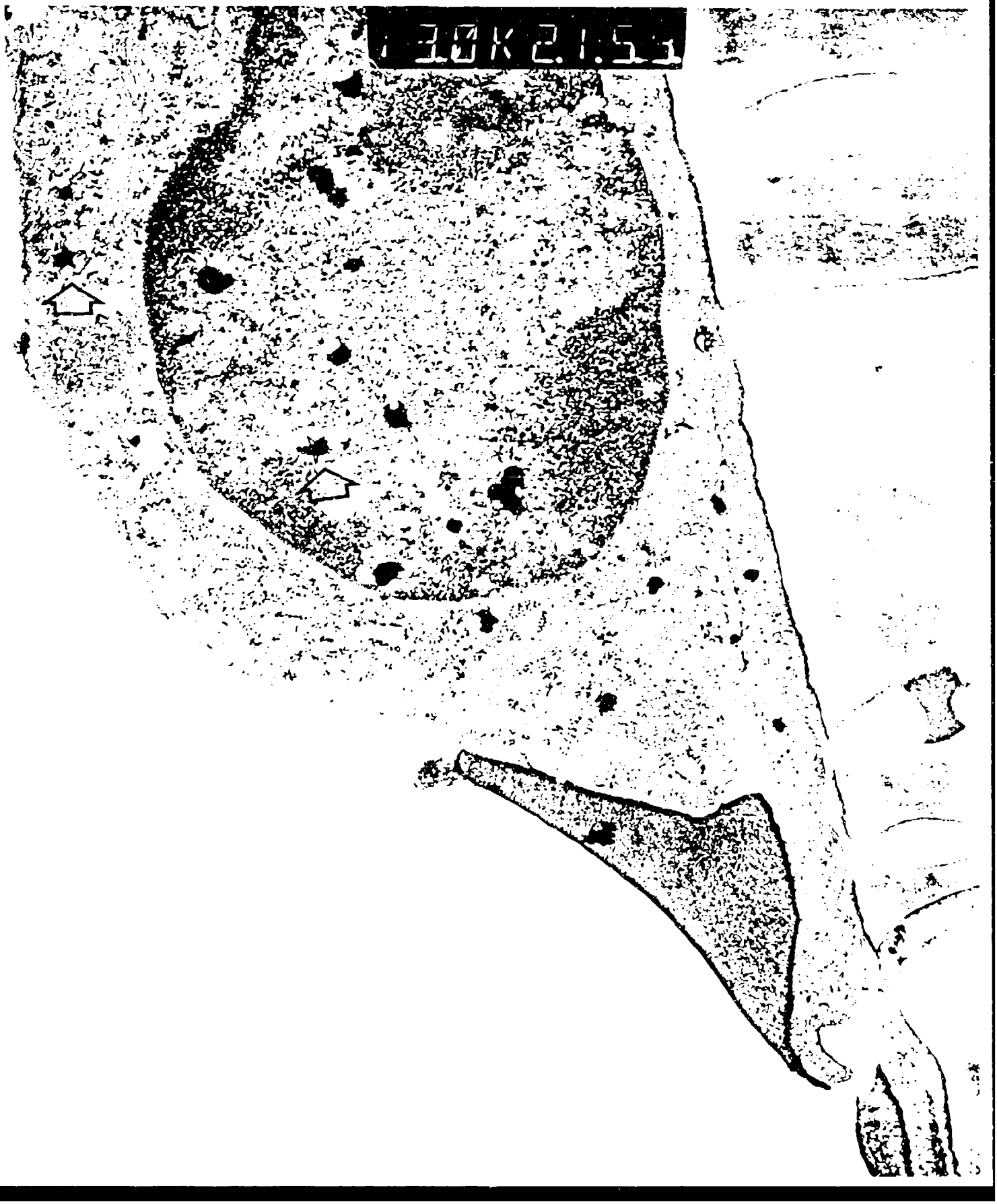

Figure (c) - 13

Figure (c) - 14

Effects of P. virus on GP 13 Endothelial Cell Calcium

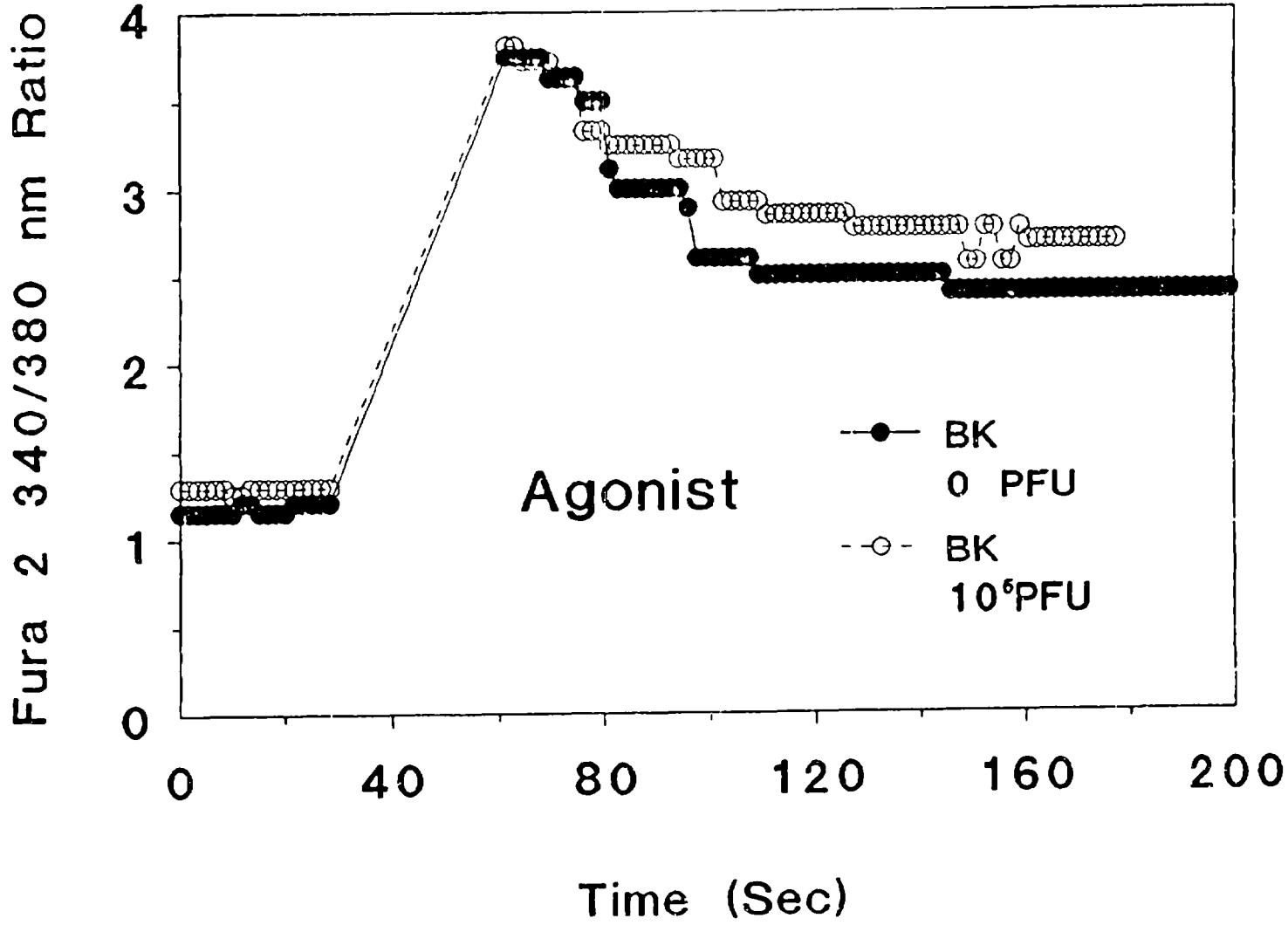

Figure (c) - 15

Effects of P. virus on GP13 Endothelial Cell Calcium

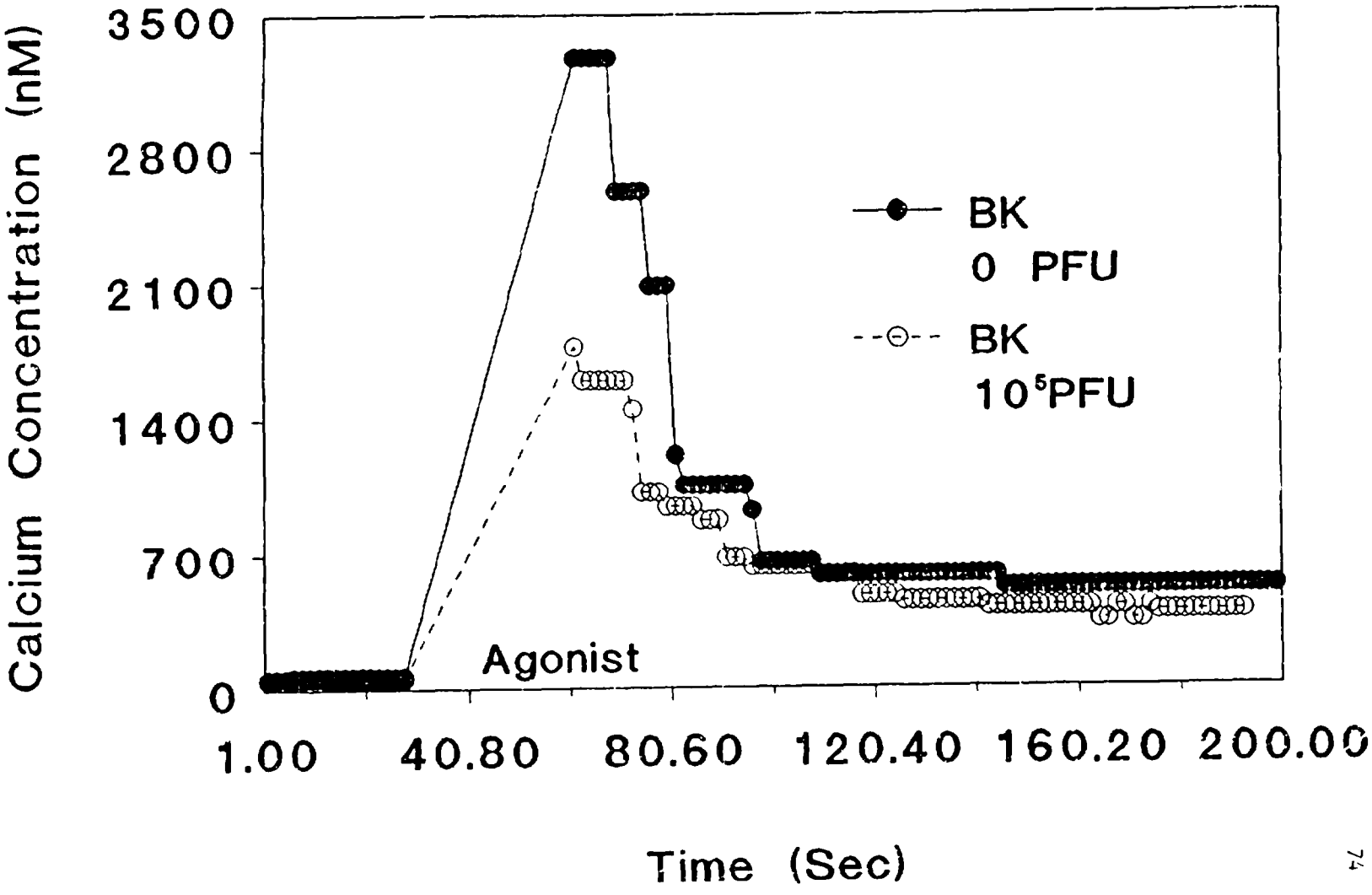

Comparison of GPAEC and Bovine Pulmonary Artery EC Monolayers

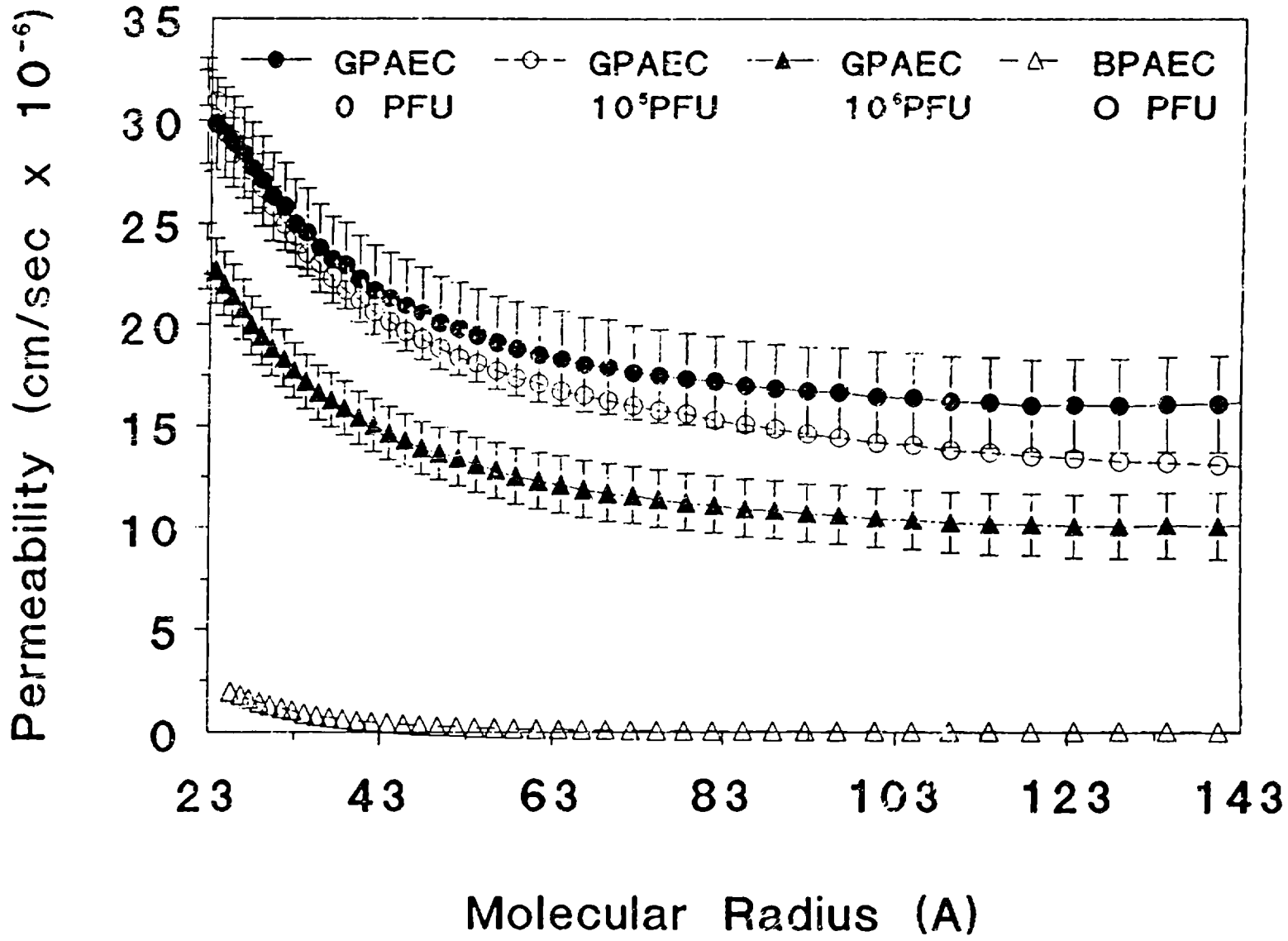

Permeability/Do of GPAEC and Pulmonary Artery EC Monolayers

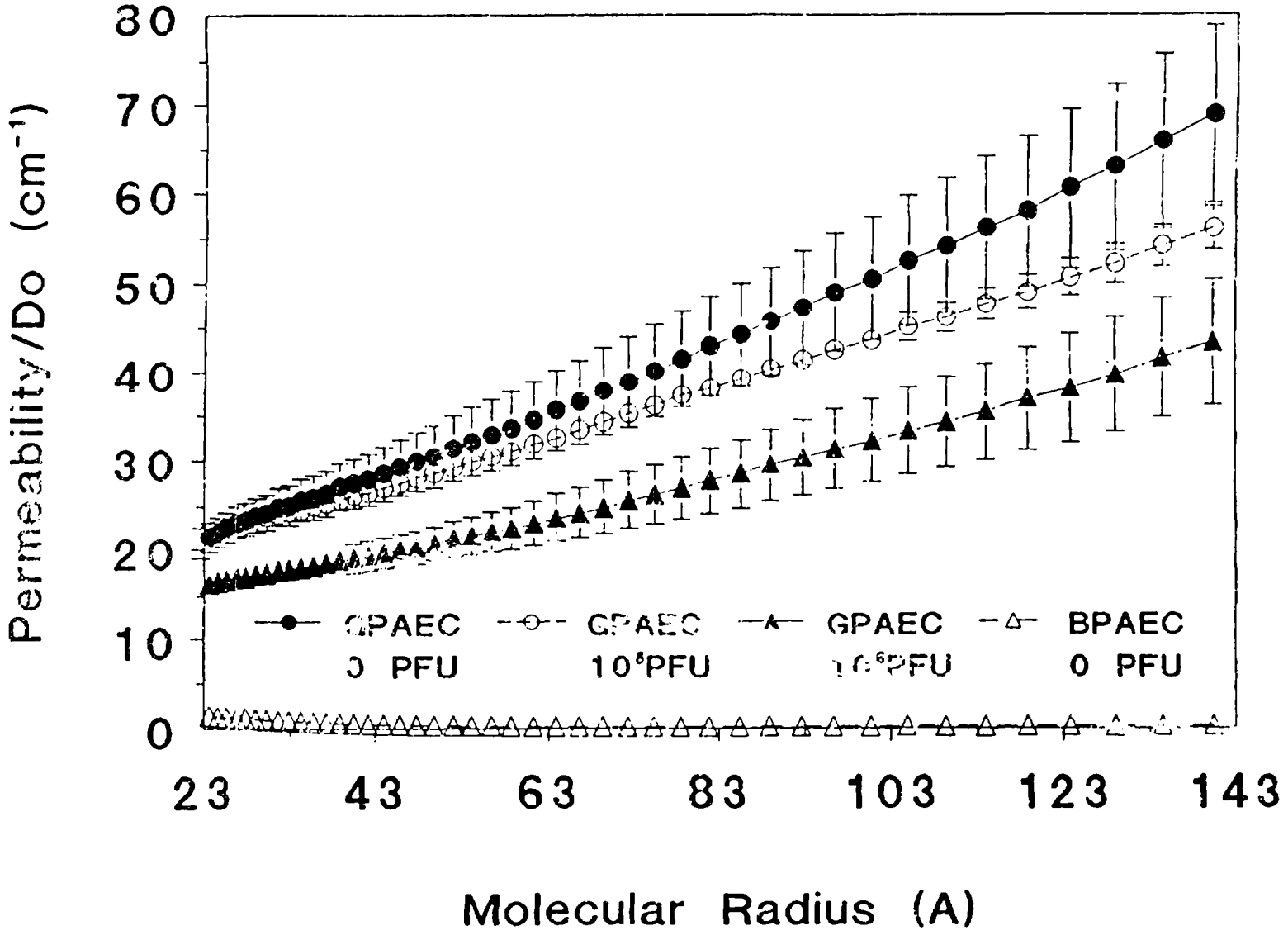

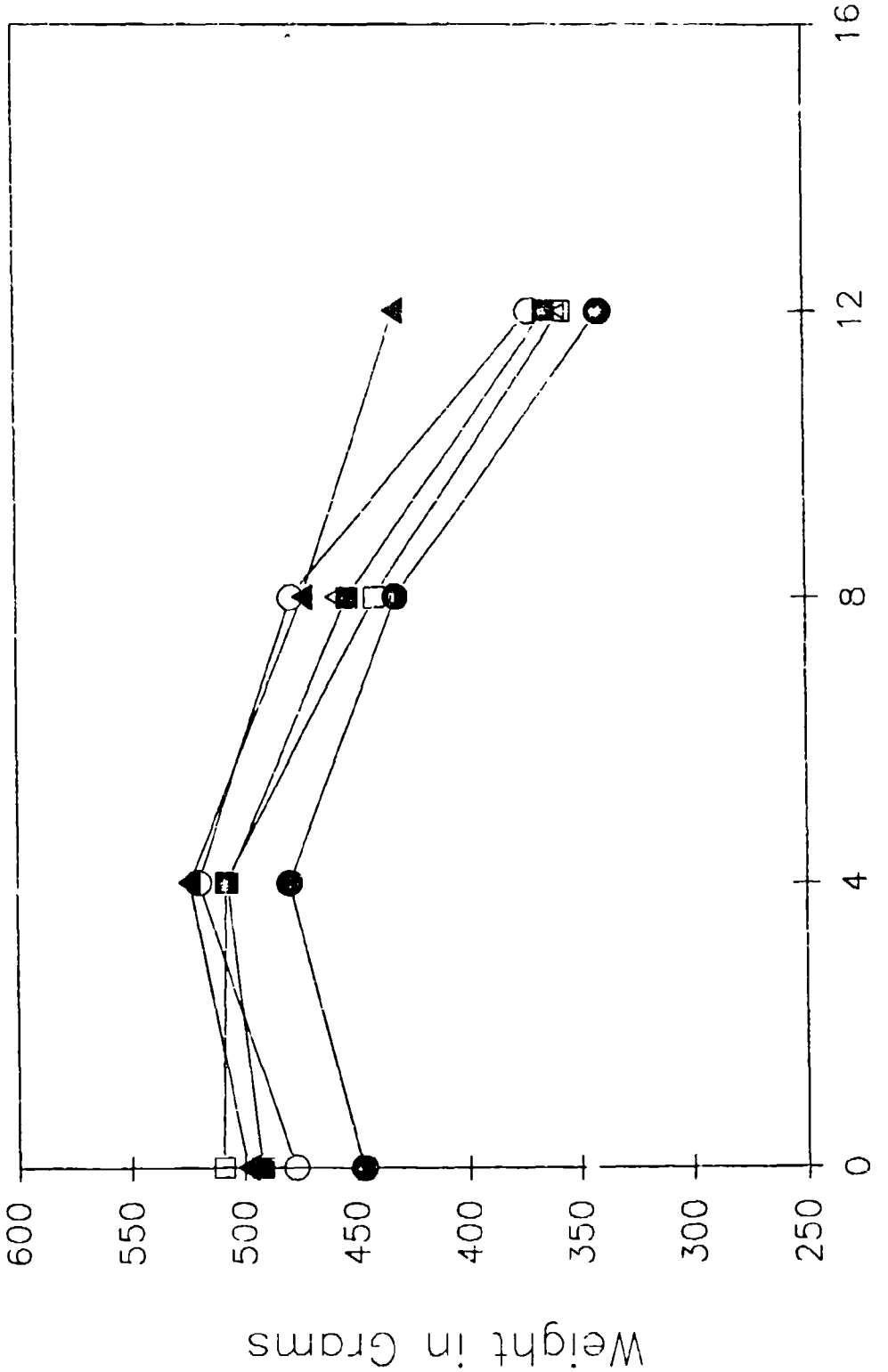
Weight in Grams
600
550
500
450
400
350
300
250
0
4
8
12
16
Days After Inoculation

Figure (d) - 1

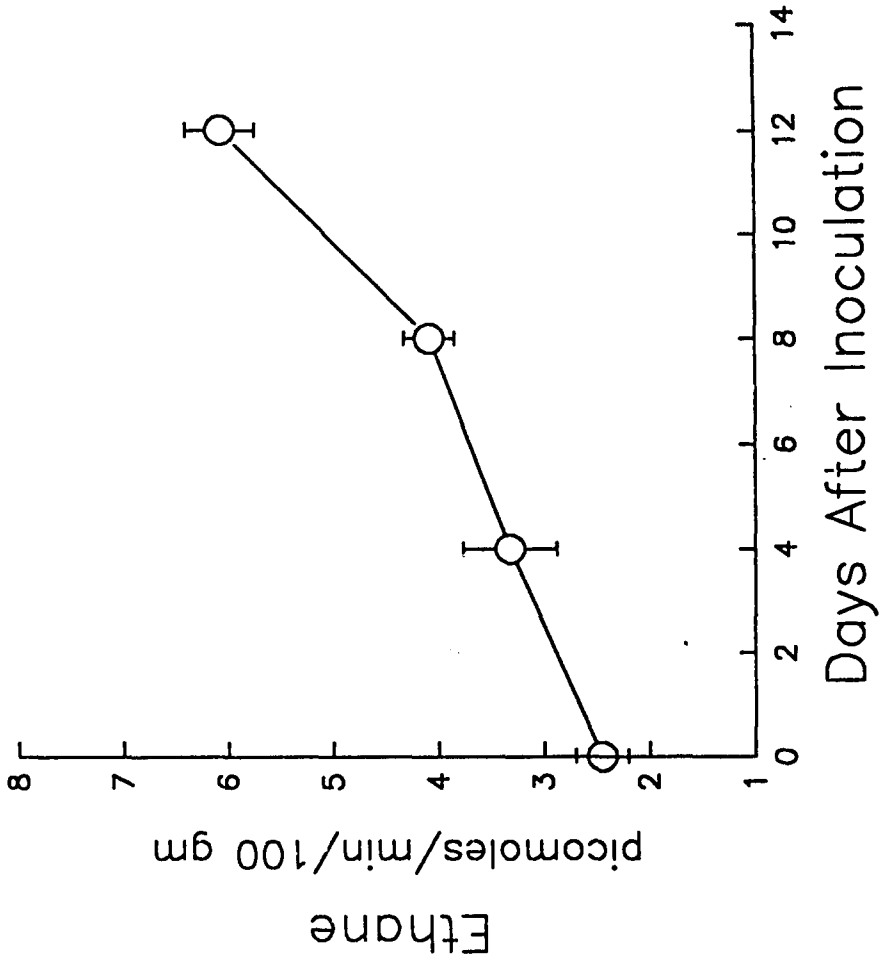
Ethane
picomoles/min/100 gm
8
7
6
5
4
3
2
1
0
2
4
6
8
10
12
14
Days After Inoculation

Figure (d) - 2

Figure (d) - 3

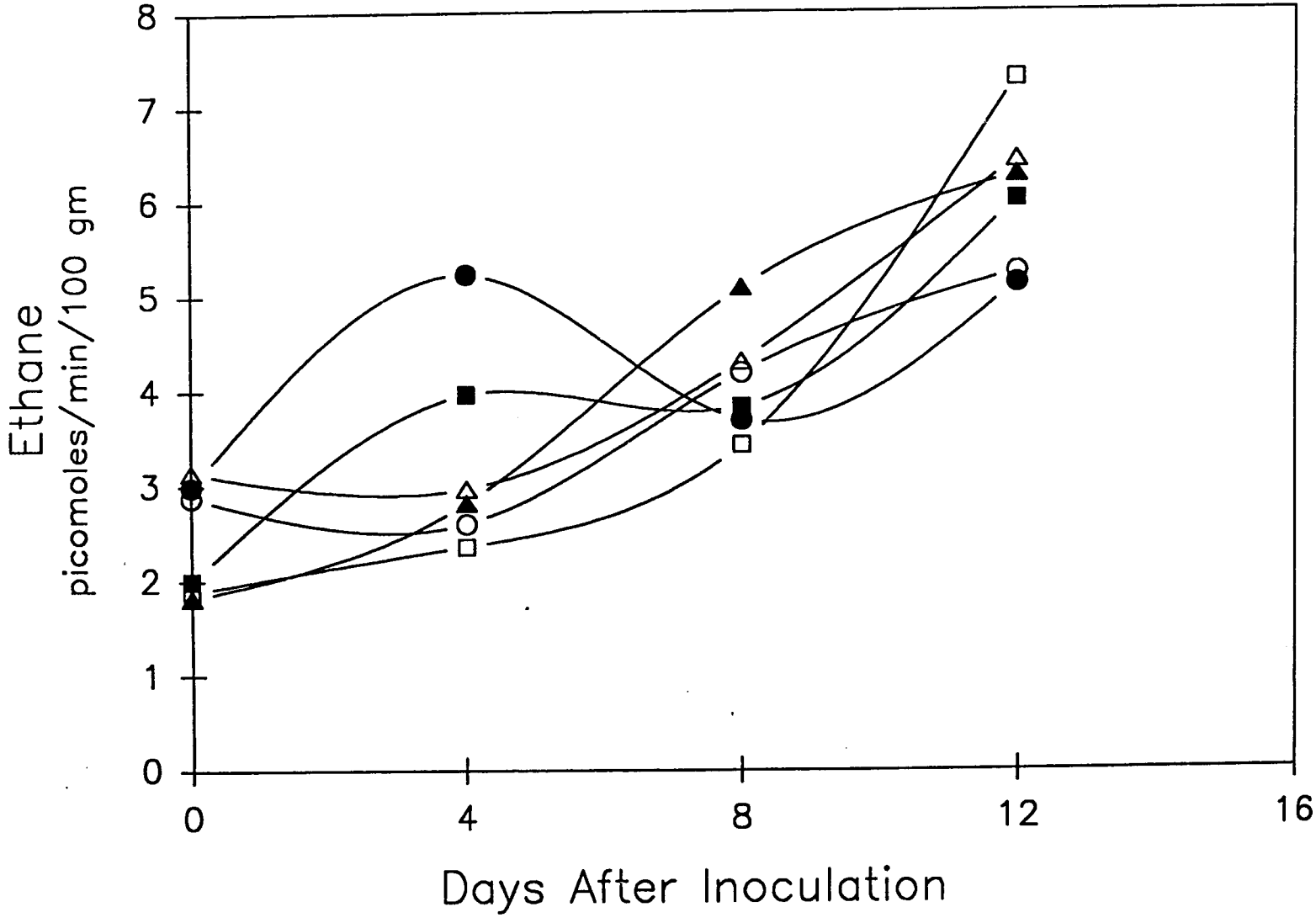
Ethane
picomoles/min/100 gm
0
1
2
3
4
5
6
7
8
0
4
8
12
16
Days After Inoculation

Figure (d) - 4

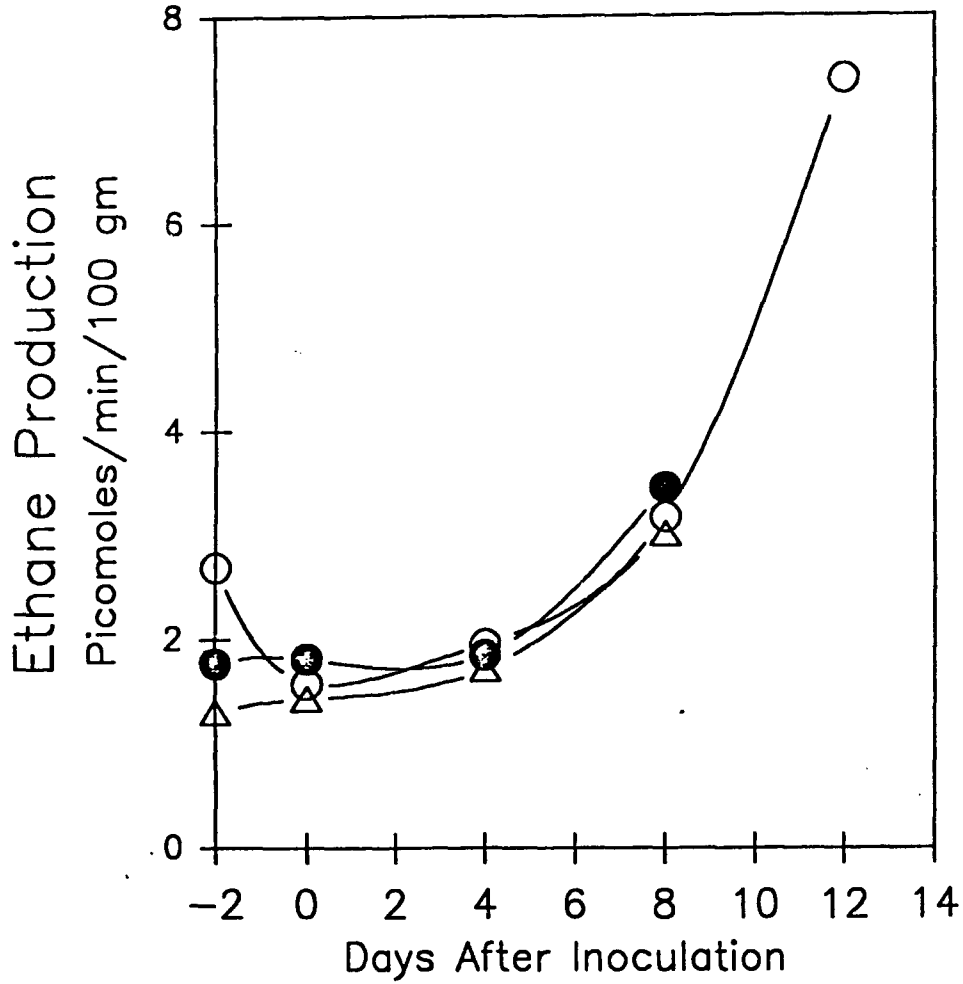

Figure (d) - 5

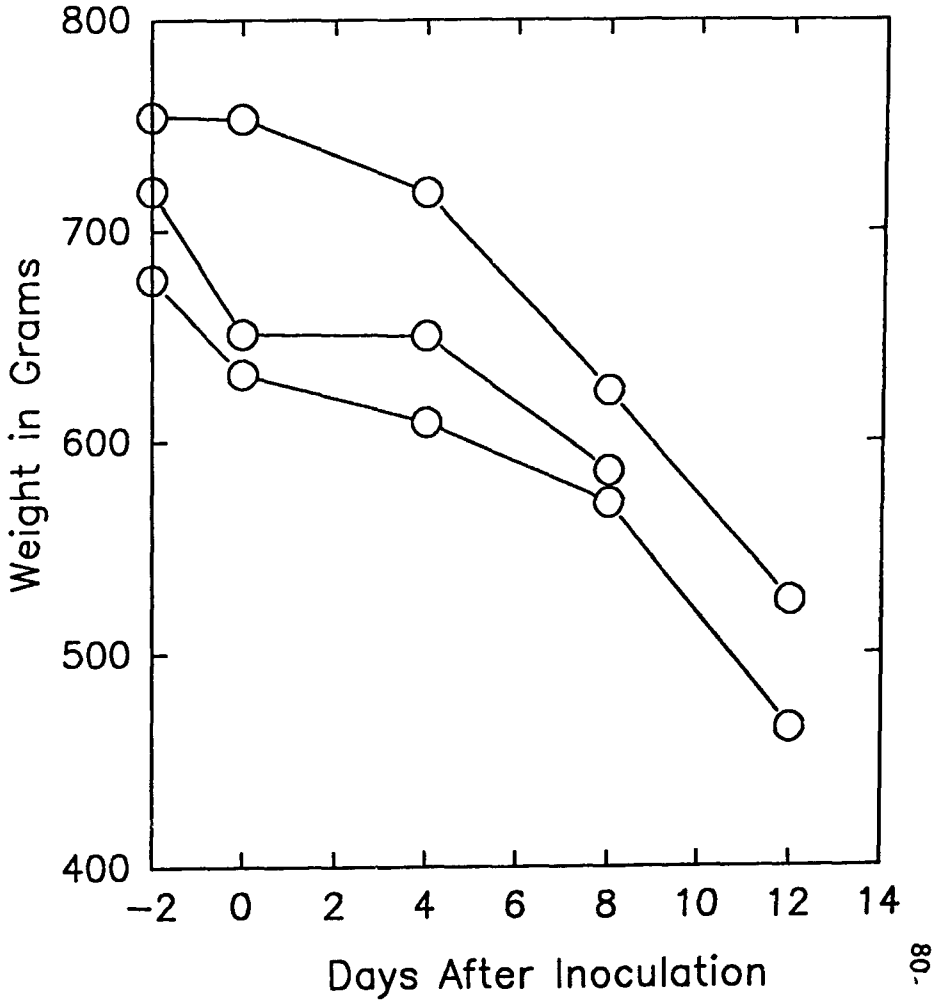

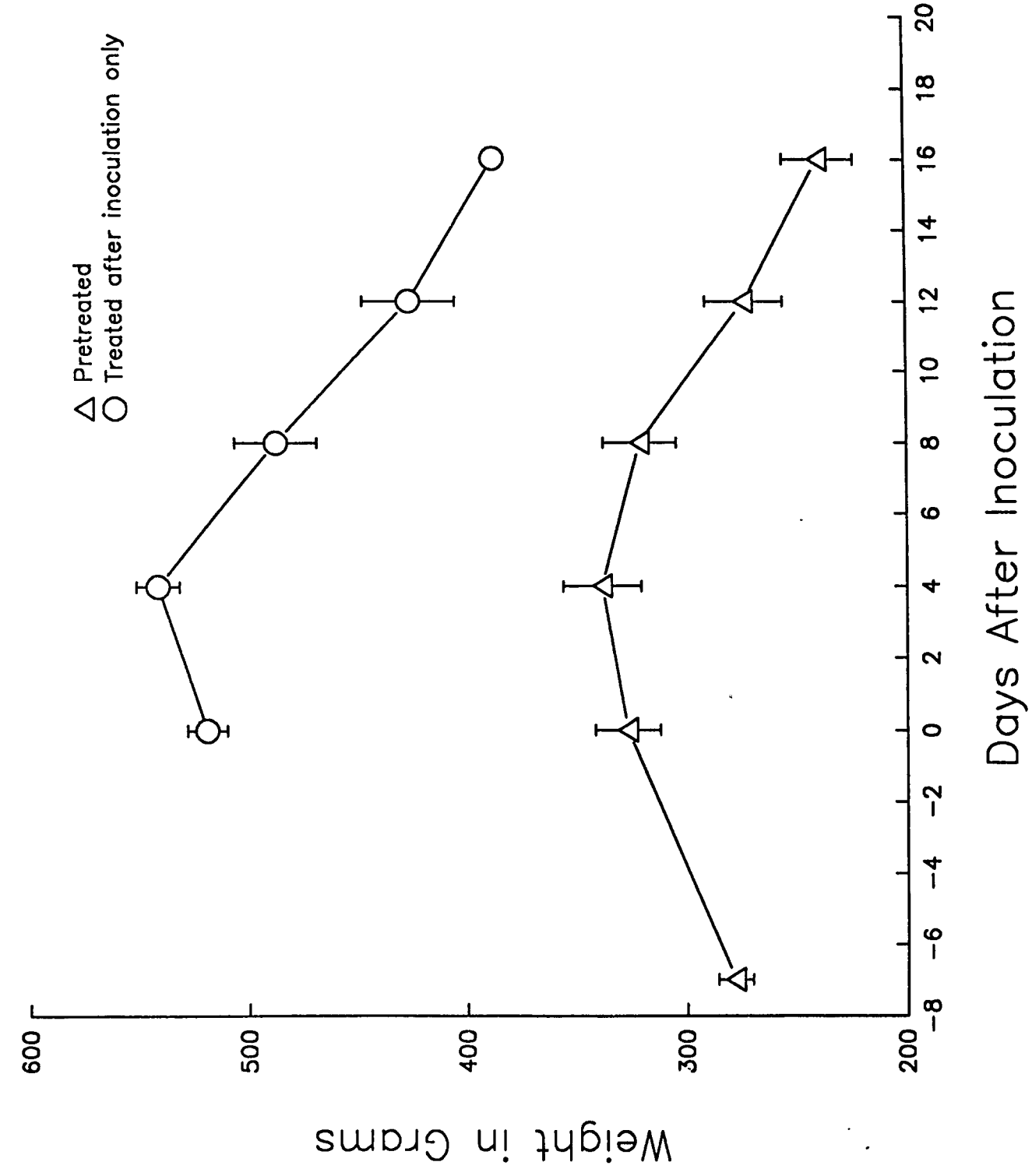
Pretreated
Treated after inoculation only
Weight in Grams
600
500
400
300
200
-8
-6
-4
-2
0
2
4
6
8
10
12
14
16
18
20
Days After Inoculation

Figure (d) - 6

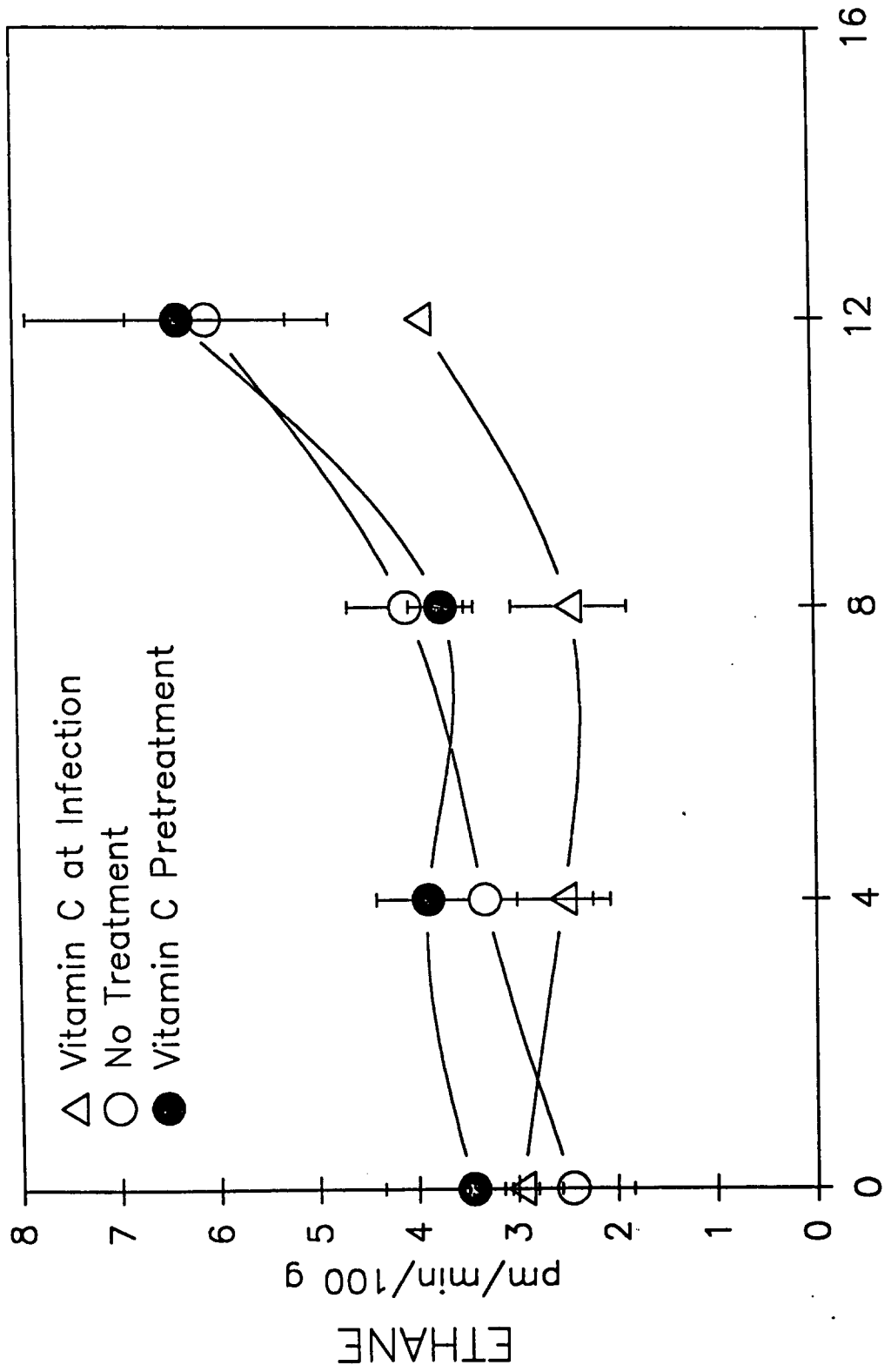
ETHANE
pm/min/100 g
0
1
2
3
4
5
6
7
8
0
4
8
12
16
Days After Infection
Vitamin C at Infection
No Treatment
Vitamin C Pretreatment

Figure (d) - 7

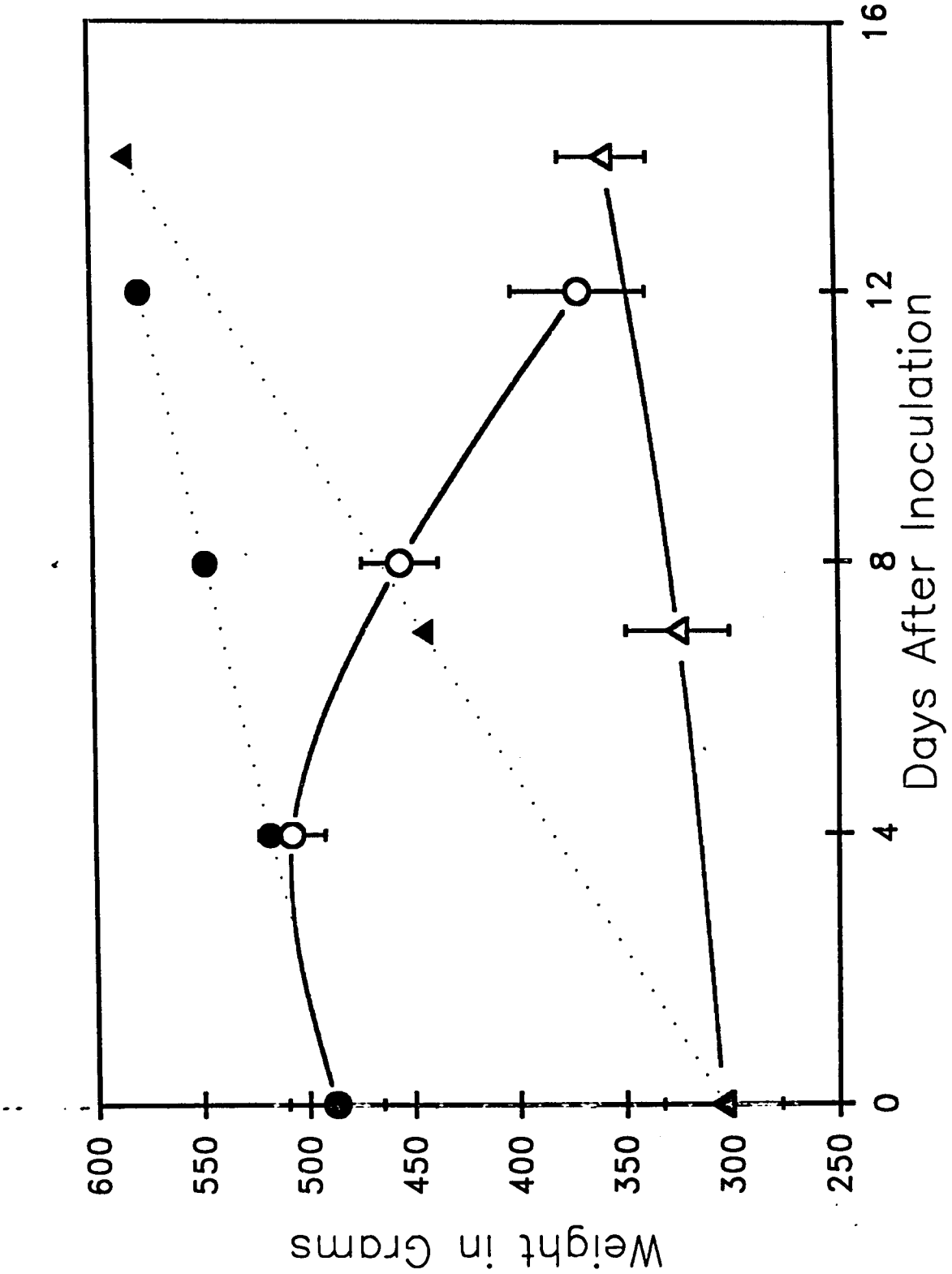
Weight in Grams
600
550
500
450
400
350
300
250
0
4
8
12
16
Days After Inoculation

Figure (d) - 8

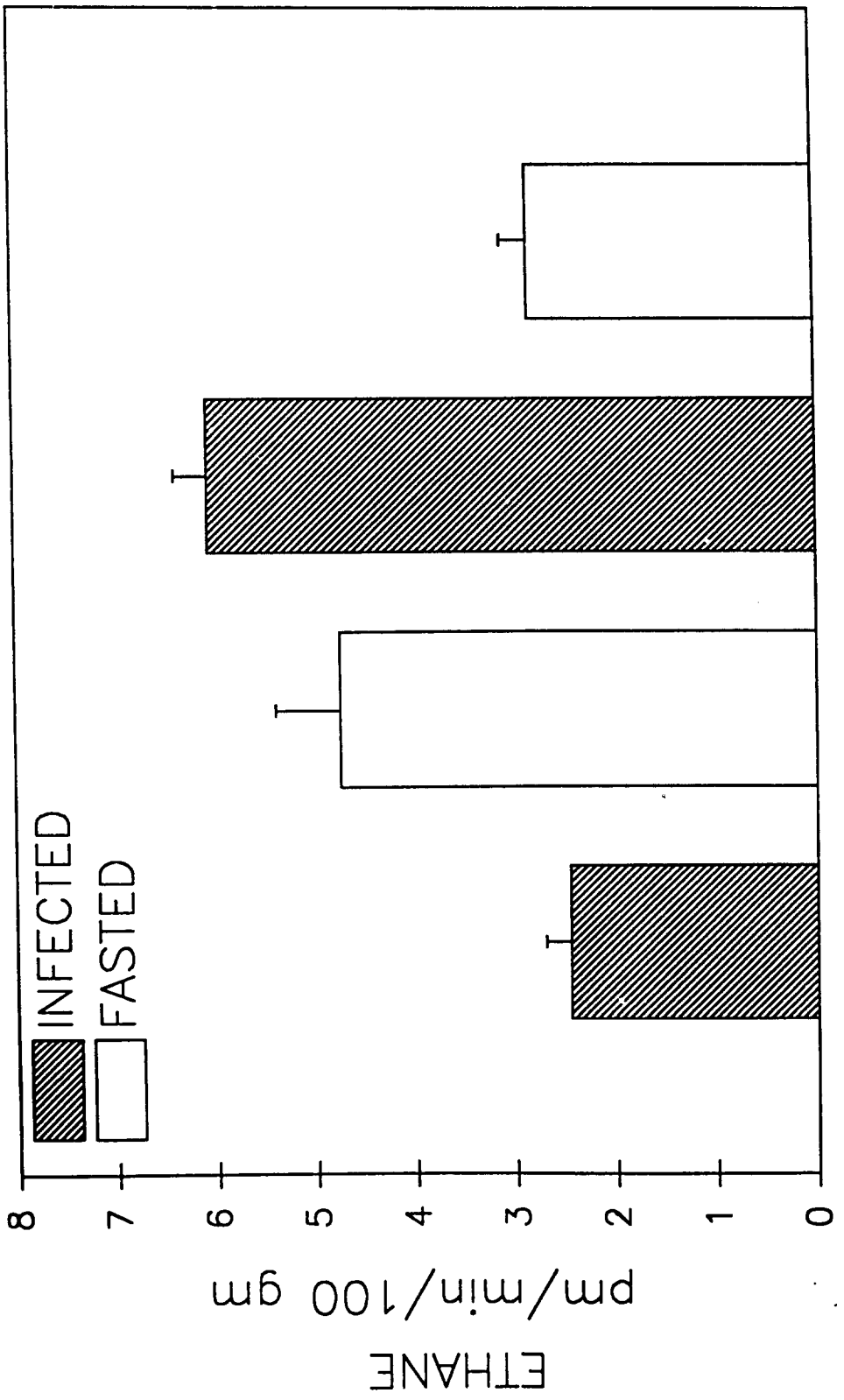

Figure (d) - 9

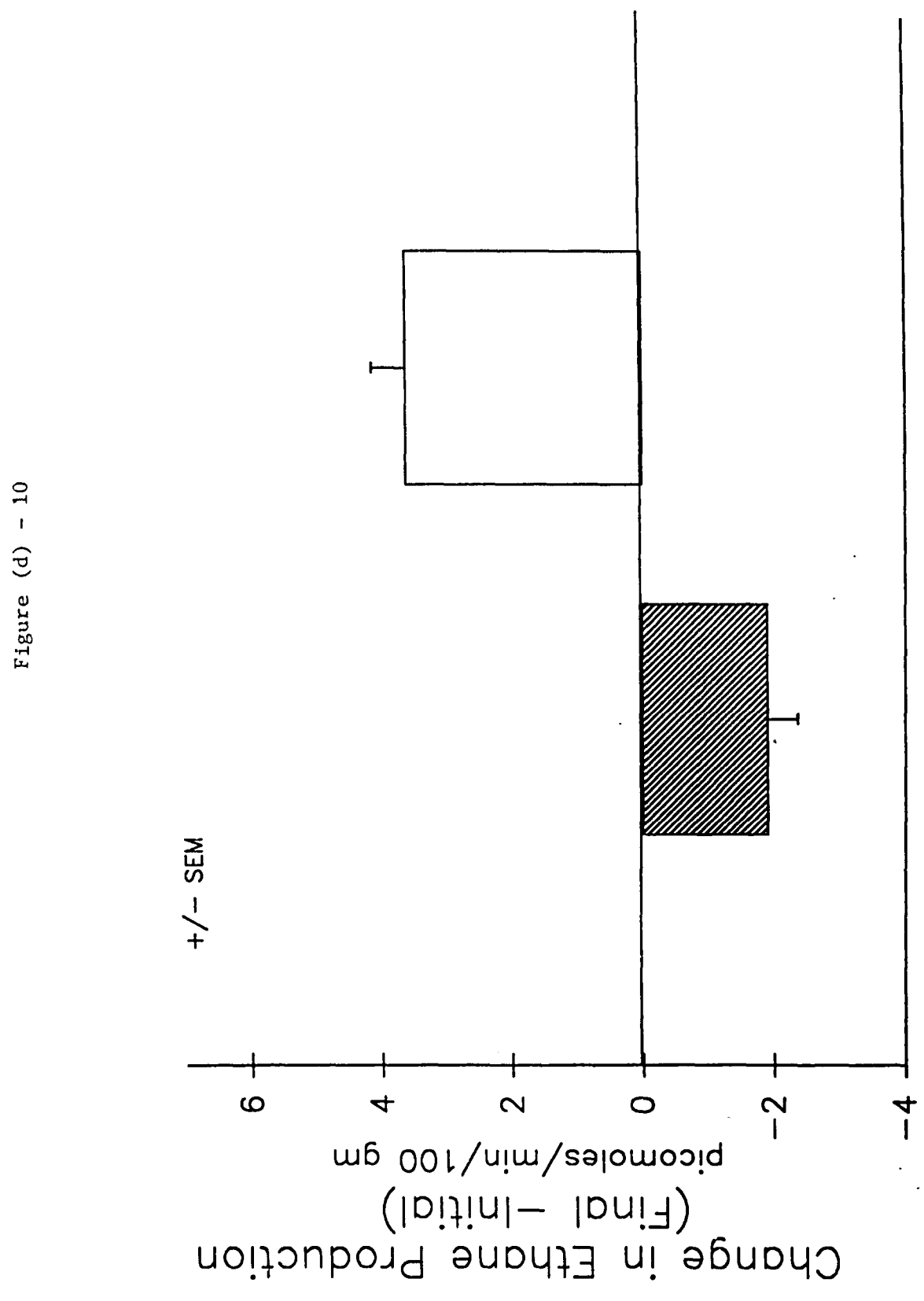
Change in Ethane Production
(Final –Initial)
picomoles/min/100 gm
6
4
2
0
−2
−4
+/− SEM
Food Restricted
Not Infected
Infected

Figure (d) - 10

Figure (d) - 11

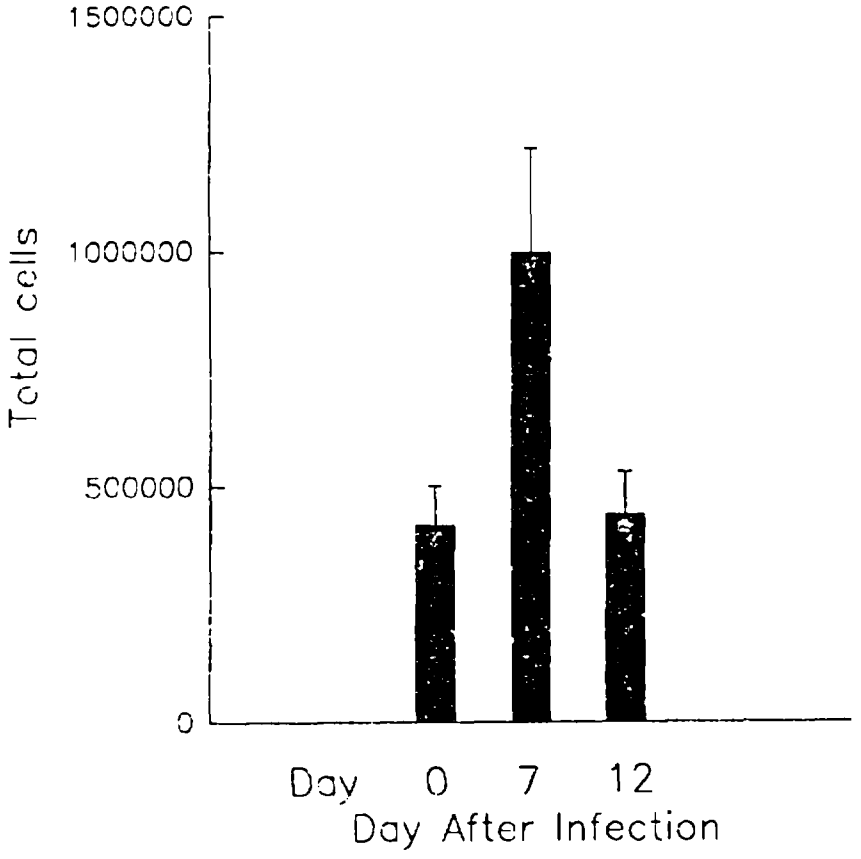

Figure (d) - 12

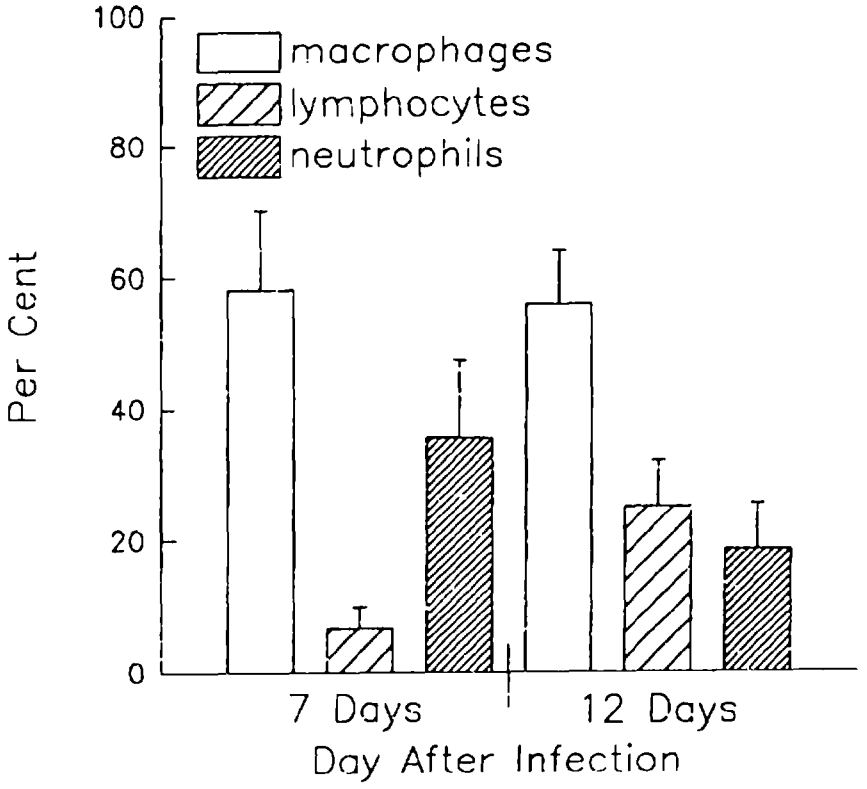

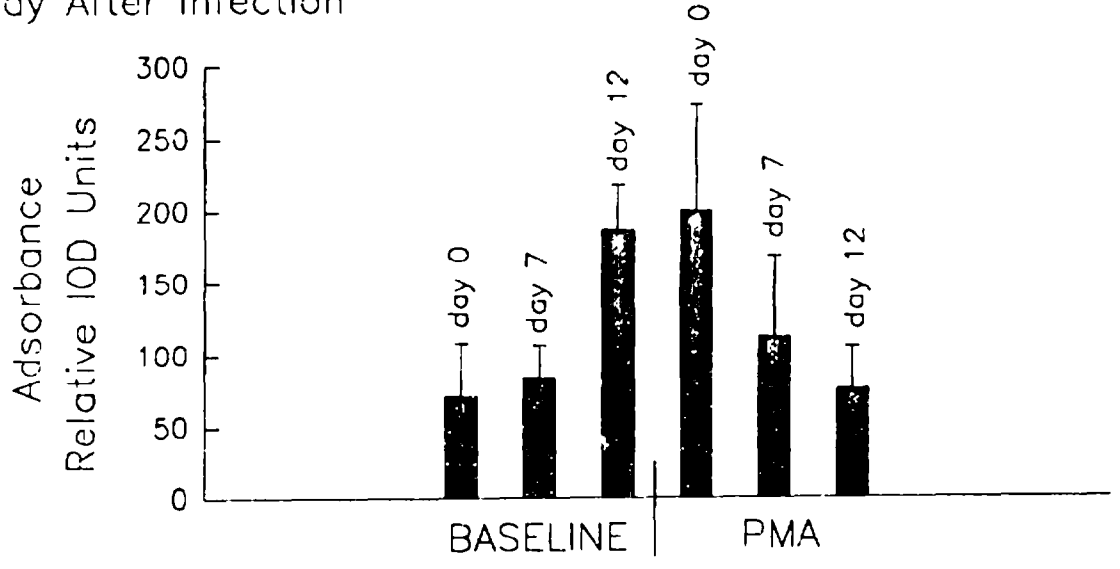

Figure (d) - 13

Figure (d) - 14

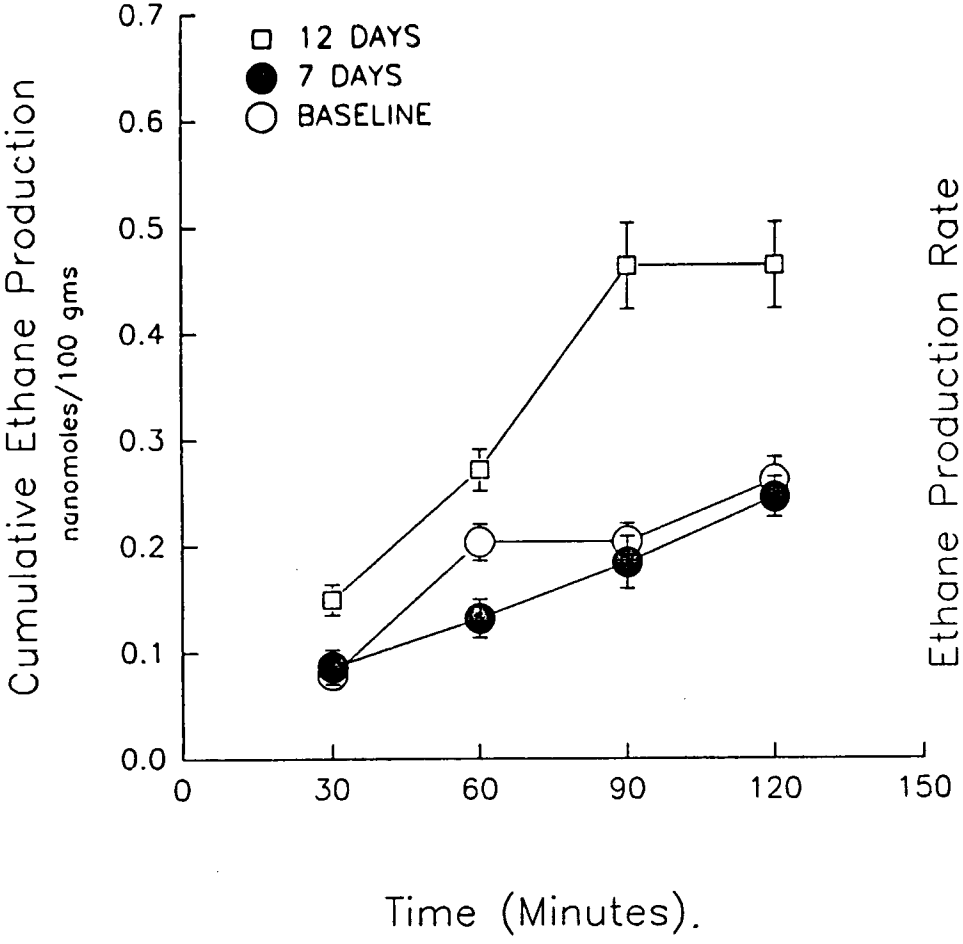

Figure (d) - 15

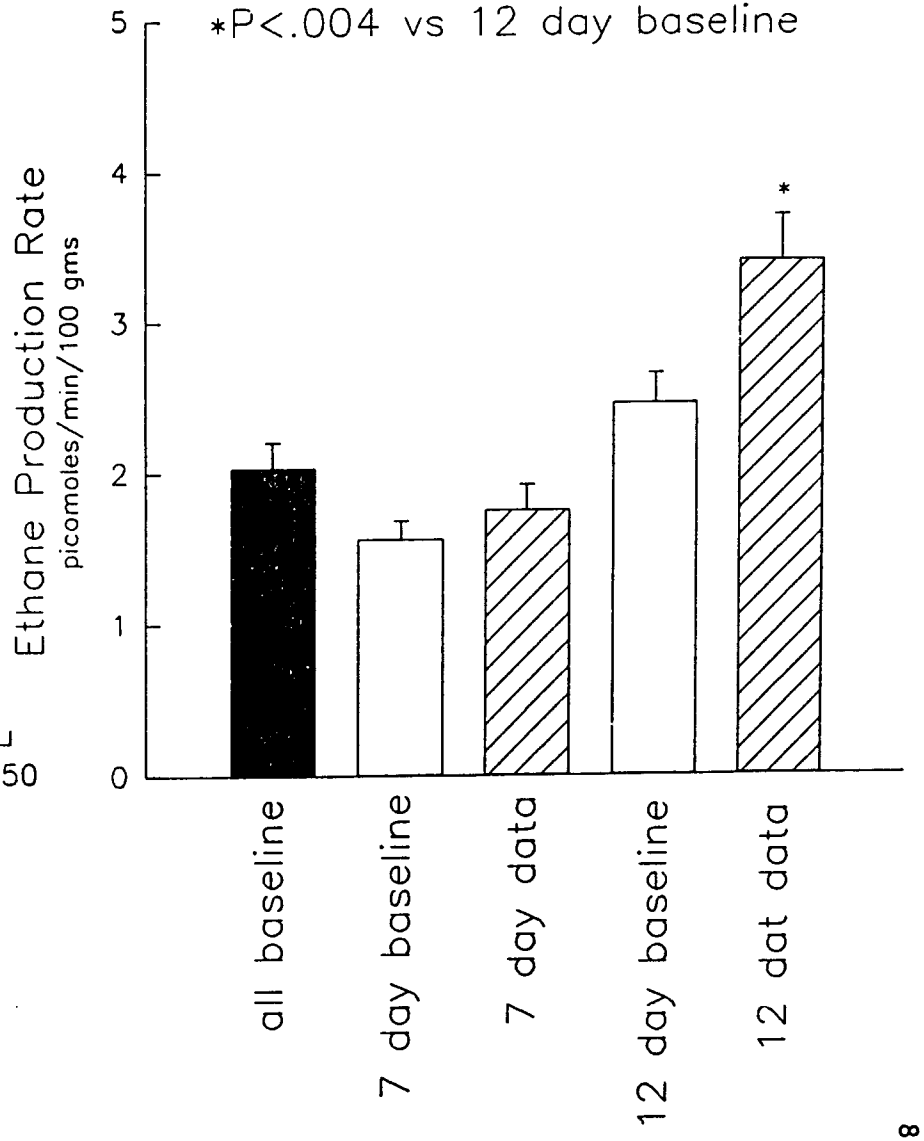

Table a-1

Differences among Initial Conditions (± SEM) of Experimental Groups

Variable	I	II	III	TYPE	2P Values I vs II	I vs III	II vs III	I, II vs III
Weight (g)	351 ± 73	427 ± 90	374 ± 41	(S)	NS	NS	NS	NS
MAP (mmHg)	41 ± .5	49 ± 8.7	47 ± 2	(MW)	NS	NS	NS	NS
Hct (%)	54 ± 1.5	54 ± 2.0	49 ± 1.4	(S)	NS	NS	NS	NS
Serum P (g/dl)	4.1 ± .3	4.5 ± .2	4.1 ± .3	(S)	NS	NS	NS	NS
J_V(µl/min/100g)	8.5 ± .8	9.6 ± 2.0	15.8 ± 3.4	(S)	NS	NS	NS	NS
R	.56 ± .04	.53 ± .10	.33 ± .03	(S)	NS	<.05	NS	<.05
J_VR(µl/min/100g)	4.6 ± .2	4.7 ± .4	5.1 ± .9	(S)	NS	NS	NS	NS

Abbreviations: MAP = Mean arterial pressure, Hct = hematocrit, P = protein, J_V = lymph flow rate, R = lymph/plasma protein concentration ratio, J_VR = lymph clearance rate.
2P = two tail probabilities that populations are the same, NS = not significant, i.e. 2P > .05, (S) = Scheffé's Method, (MW) = Mann-Whitney U Test. Note that (S) or (MW) applies to all entries of a given variable.

TABLE a-2

Differences among Lymph Measurements (± SEM) of Experimental Groups During the Course of the Study (Numbers of Measurements are Noted)

Variable	I (10)	II (8)	III (22)	TYPE	2P VALUES IvsII	IvsIII	IIvsIII	I,IIvsIII
J_v (µl/min/100g)	8.2 ± 1.7	12.7 ± 2.2	17.4 ± 2.2	(S)	NS	<.05	NS	NS
R	.56 ± .06	.23 ± .02	.29 ± .03	(MW)	.0014	.0026	NS	NS
J_vR(µl/min/100g)	3.8 ± .4	2.8 ± .4	4.1 ± .4	(S)	NS	NS	NS	NS
σ	.54 ± .05	.86 ± .02	.83 ± .02	(MW)	.0004	.00012	NS	.0033
PS(µl/min/100g)	2.65 ± .50	2.16 ± .34	3.44 ± .32	(S)	NS	NS	NS	NS
Peclet No.	1.86 ± .56	.89 ± .20	.75 ± .11	(MW)	.07	.018	NS	.05
%FrD	28 ± 4.6	60 ± 5.6	61 ± 3.6	(S)	<.01	<.01	NS	<.05

Abbreviations: σ = protein solvent drag reflection coefficient, PS = permeability - surface area product for protein, %FrD = percent of total protein transport carried by diffusion. Other abbreviations are the same as Table a-1.

TABLE a-3

Differences among Organ Weights as Percentages of Body Weight (± SEM) of Experimental Groups

				TYPE	2P VALUES			
Organ	I	II	III		I vs II	I vs III	II vs III	I, II vs III
Heart	.45 ± .02	.41 ± .02	.39 ± .02	(S)	NS	NS	NS	NS
Lung	.97 ± .12	1.03 ± .17	.66 ± .02	(MW)	NS	.016	.036	.002
Spleen	.24 ± .02	.19 ± .02	.16 ± .02	(S)	NS	NS	NS	NS
Stomach	.88 ± .09	.85 ± .13	.89 ± .04	(S)	NS	NS	NS	NS
Liver	5.60 ± .27	5.35 ± .32	3.74 ± .41	(S)	NS	<.05	<.05	<.05
Kidney	.72 ± .05	.72 ± .04	.50 ± .03	(S)	NS	<.01	<.05	<.05
Brain	.79 ± .12	.63 ± .11	.69 ± .06	(S)	NS	NS	NS	NS

Abbreviations: Same as Table a-1.

TABLE a-4

Differences between Initial Variables and Those During the Course of Studies of Present Study (Volume Expansion) compared to Previous Study (No Volume Expansion)

I = Current Study - Virus Injected, Unresponsive, III = Current study - Controls (Calorie Restricted), IV = Previous Study - Virus injected, V = Previous Study - Controls (Ad lib diet)

					2P Values	
Variable	I	IV	III	V	I vs IV	III vs V
n =	4	7	5	38		
Weight	351 ± 73	476 ± 47	374 ± 41	643 ± 21	NS	<.001
MAP_i	41 ± .5	38 ± 5.7	47 ± 2.1	38 ± 1.4	NS	<.05
Hct_i	54 ± 1.5	52 ± 2.4	49 ± 1.4	50 ± .7	NS	NS
Serum P_i	4.1 ± .3	4.6 ± .2	4.1 ± .3	4.4 ± .1	NS	NS
Jv_i	8.5 ± .8	4.9 ± 1.5	15.8 ± 3.4	5.5 ± .4	NS	<.05
R_i	.56 ± .04	.70 ± .04	.33 ± .03	.55 ± .02	NS	<.001
JvR_i	4.6 ± .2	3.1 ± .6	5.1 ± .9	2.9 ± .2	NS	≈.05
n =	10	15	22	56		
Jv_c	8.2 ± 1.7	5.4 ± .8	17.4 ± 2.3	8.1 ± .5	NS	<.001
R_c	.56 ± .06	.61 ± .03	.29 ± .03	.44 ± .02	NS	<.001
JvR_c	3.8 ± .4	3.1 ± .3	7.1 ± .4	3.3 ± .2	NS	NS
σ_c	.54 ± .05	.52 ± .03	.33 ± .02	.73 ± .02	NS	<.005
PS_c	2.65 ± .50	2.48 ± .30	3.44 ± .32	3.21 ± .29	NS	NS
Peclet No.$_c$	1.86 ± .56	1.20 ± .19	.75 ± .11	.97 ± .10	NS	NS
$\%PrD_c$	23 ± 4.6	32 ± 3.5	61 ± 3.6	51 ± 2.7	NS	≈.05

Abbreviations: Subscripts i, c refer to initial values and those taken during the course of study. Tests of probability are non paired t when variances of groups are not different, and the Behrens-Fisher t' test when the variances are different by F test. Units are the same as for Tables a-1 and a-2.

Table (c)1 Comparison of Arterial blood gases, blood lactate, hemoglobin, hematocrit and respiratory rate from P. virus infected GP13 with distinct initial body weight (IBW) in comparison with uninfected controls.

	Control (n=7)	IBW < 400 g (n=8)	IBW > 700 g (n=5)
pH (Units)	7.39 ± 0.02	7.38 ± 0.02	7.12 ± 0.04
pCO_2 (mm Hg)	41 ± 2	45.1 ± 4	24.4 ± 1.9
pO_2 (mm Hg)	78 ± 3	41.1 ± 4.6	125 ± 8.4
HCO_3 (meq/L)	25.2 ± 1	28.5 ± 2	8.0 ± 0.9
Lactate (mmol/L)	1.1 ± 0.2	2.35 ± 0.54	1.15 ± 0.05
Hematocrit (Vol %)	46.1 ± 1.7	42.1 ± 1.5	49.5 ± 1.2
Hemoglobin (g/dl)	13.6 ± 0.2	12.5 ± 0.3	17.9 ± 0.7
Resp. Rate (#/min)	61±5	128±3	113±3

Table (c)2 Comparison of plasma enzyme and triglyceride values from P. virus infected GP13 with distinct initial body weight (IBW) in comparison with uninfected controls.

	Control (n=7)	IBW < 400 g (n=8)	IBW > 700 g (n=5)
SGPT (IU/L)	49.5 ± 4.3	63.5 ± 6.5	283 ± 22.7
LDH (IU/L)	282 ± 22.1	461 ± 113	798 ± 128
SGOT (IU/L)	139 ± 3.4	558 ± 96	2626 ± 245
GGT (IU/L)	19.3 ± 2.1	9.0 ± 1.2	199 ± 2.1
Triglyc. (mg/dl)	85 ± 5.9	93.8 ± 26.4	47 ± 7.2

Table (c)5 Effects of Pichinde virus on arterial blood pH, PO_2, PCO_2, HCO^-_3, lactate and respiratory rate at day 13 and day >18 after infection as well as no infection (control).

	Control [7]	Day 13 [6]	Day >18 [8]
pH (units)	7.39±.02	7.51±.01	7.38±.02
PCO_2 (mm^2 Hg)	41±2	32±2	45±5
PO_2 (mm^2 Hg)	78±5	90±9	41±5*
HCO^-_3 (mEq/l)	25.2±1	25.7±1	28.5±2**
Lactate (mM)	1.1±0.2	1.3±0.2	3.35±.6*
Respiratory Rate (breaths/min)	60±5	60±3	128±3*

[ ] indicate the number of values for each determination.
*indicates $p<.001$ from the control group
** indicates $p<.05$ from the control group

Table (c)3 Comparision of plasma electrolytes, bicarbonate, creatinine, BUN, and glucose from P. virus infected GP13 with distinct initial body weight (IBW) in comparison with uninfected controls.

	Control (n=7)	IBW < 400 g (n=8)	IBW > 700 g (n=3)
Sodium (meq/L)	139.2 ± 6.1	139.6 ± 2.8	118.3 ± 7.9
Potassium (meq/L)	6.35 ± 1.5	6.74 ± 1.2	2.6 ± 0.4
Chloride (meq/L)	103.5 ± 5.7	96.8 ± 4.1	92.7 ± 6.4
HCO_3 (meq/L)	25.2 ± 1	28.5 ± 2	6.9 ± 0.4
Creatinine (mg/dl)	0.56 ± 0.02	0.54 ± 0.01	2.5 ± 0.6*
BUN (mg/dl)	21 ± 4.7	26.4 ± 3.5	73 ± 22
Glucose (mg/dl)	150 ± 5.1	81.5 ± 13	355.3 ± 33.0

Values marked with * indicate n=2

Table (c)4 Effects of Pichinde virus on arterial blood pressure heart rate, hematocrit, hemoglobin and blood volume index at day 13 and day >18 after infection as well as no infection (control). No significant difference was noted between any groups.

	Control	Day 13	Day >18
Arterial pressure (mm Hg)	52±5 (3)	56±6 (6)	60±14 (3)
Heart Rate (beats/min)	250±24 (3)	228±8 (5)	225±21 (3)
Hematocrit (Vol %)	46±2 (5)	50±2 (3)	42±2 (6)
Hemoglobin (g/dl)	13.4±.24 (4)	13.2±.42 (5)	12.5±.41 (5)
Blood Volume Index (ml/kg)	79.7±18 (5)	88.4±17 (3)	96.6±20 (6)

( ) indicate the number of values for each determination.

Bibliography Resulting from Contract

1. Habib MP, Dickerson F, Mooradian AD (1990). Ethane production rate is reduced with dietary restriction. J Appl Physiol 68:2588-2590.
2. Habib MP, Eskelson CD, Katz MA (1988). Ethane production rates in rats exposed to high oxygen concentrations. Am Rev Resp Dis 137:341-344.
3. Habib MP, Katz MA (1989). Ethane production rates and minute ventilation. J Appl Physiol 66(3):1264-1267.
4. Habib MP, Katz MA (1989). Source of ethane in expirate of rats ventilated with 100% oxygen. J Appl Physiol 66(3):1268-1272.
5. Katz MA, Schaeffer RC Jr (1991). Convection of macromolecules is the dominant mode of transport across horizontal .4 and 3 μ filters in diffusion chambers: Significance for biologic monolayer permeability assessment Microvasc Res, In Press.
6. Katz MA, Starr JF (1990). Pinchindé virus infection in strain 13 guinea pigs reduces intestinal protein reflection coefficient with compensation. J Infec Dis 162:1304-1308.
7. Katz MA, Starr JF (1991). The influence of volume expansion on capillary transport in the gut of Pichindé virus infected strain 13 guinea pigs. Submitted, J Medical Virology.
8. McCuskey RS, Eguchi H, McCuskey PA (1991). Microvascular alterations elicited by arenaviral infection in the liver, mesenter and intestinal villi of guinea pigs. Submitted, Microcirc Endothel and Lymph.
9. Saari JT, Dickerson FD, Habib MP (1990). Ethane production in copper deficient rats, Proc Soc Exp Biol Med 195:30-33.

Meeting Abstracts

1. Katz MA, Starr, JF (1990). Pichindé virus infection in Strain 13 guinea pigs reduces intestinal protein reflection coefficient (σ) with compensation. Clin Res 38:144A. Presented at WSCI meeting, Carmel, CA, Feb 6-9, 1990.
2. Schaeffer RC Jr, Bitrick MS Jr (1990). Effects of lethal Pichindé virus infection in strain 13 guinea pigs on organ permeability index. FASEB J 4:A287. Presented at APS-FASEB annual meeting, Washington, DC, Apr 1-5, 1990.
3. Habib MP, Paquin M and Katz MA (1987). Time course of expired ethane in rats exposed to high F102. Clinical Research 35:170A. Presented at AFCR meeting, Carmel, CA, Feb 1987.
4. Habib MP, Dickerson F, Katz MA (1988). 100% oxygen increases ethane production from lungs of exsanguinated ventilated rats and in vitro. The Physiologist 31:A125. Presented at APS meeting, Montreal, Canada, October 1988.
5. Habib MP, Katz MA, Eskelson CD, Repine JE (1989). PEG-SOD and PEG-CAT decrease exhaled ethane (E) production in rats exposed to 100% oxygen. Am Rev Respir Dis 139:A45. Presented at the American Thoracic Society meeting in Cincinnati, OH, May 1989.
6. Saari JT, Habib MP. Copper deficiency enhances breath ethane production in rats. Presented at the FASEB Summer Research Conference on Micronutrients: Trace Elements, Copper Mountain, CO, July 23-28, 1989.
7. Saari JT, Habib MP (1989). Breath ethane production in copper deficient rats. The Physiologist 32:171. Presented to 1989 APS/ATS fall meeting, Rochester, MN, Oct 15-19, 1989.
8. Habib MP, Dickerson FD, Mooradian AD (1990). Ethane (E) production rates in diabetic (DM) rats. Am Rev Respir Dis 141:A544. Presented at American Thoracic Society meeting, Boston, MA, May 1990.
9. Lackey DL, Habib MP, Lantz RC, Grad R et al (1990). Vitamin A attenuates bleomycin induced rat lung injury. FASEB Journal 4(4):A1139. Presented at FASEB meeting, Washington, DC, April 1990.
10. Mooradian AD, Habib MP, Dickerson FD. The effect of age and food restriction on thyroid hormone-induced lipid peroxidation. The Endocrine Society Abstracts, P151, abstract #506, presented at the 72nd annual meeting of the Endocrine Society meeting, Atlanta, GA, June 20-23, 1990.

List of all Personnel Receiving Pay from Contract Support

Technician	Study
Starr, James F.	a
Dorosheff, Paul	b & e
Eguchi, Heroshi	b & e
Kidwell, Stella	b & e
Bitrick, Michael S., Jr.	c
Holberg, Walter	c
Hoerr, Lucia	c
Dickerson, Frank	d

Research Scientist	Study
Cilento, Eugene, Ph.D.	b & e